

## ABSTRACT

Title of Thesis: EVALUATION OF ACETATE THRESHOLDS UNDER VARIOUS TERMINAL ELECTRON-ACCEPTING CONDITIONS: APPLICATION TO BIOREMEDIATION MONITORING

Xiaomin Su, Master of Science, 2004

Thesis directed by: Assistant Professor Jennifer G. Becker

Department of Biological Resources Engineering

A major challenge associated with intrinsic bioremediation is demonstrating its success. The consumption of electron acceptors during bioremediation of hydrocarbons and other contaminants can result in shifts in the predominant terminal electron-accepting processes (TEAPs), which may be useful for monitoring. Because traditional assessment tools have disadvantages, an accurate indicator of TEAPs is still needed.

Acetate thresholds were evaluated to test the hypothesis that characteristic ranges of acetate thresholds may exist for different TEAPs and be useful as a bioremediation monitoring tool. Acetate thresholds established by pure microbial batch cultures using different TEAPs were measured experimentally. Furthermore, the factors controlling acetate thresholds were investigated using a microbial respiration model.

Acetate thresholds increased in the order: Fe(III) < Mn(IV) ≈ nitrate < sulfate < CO<sub>2</sub>. Modeling results indicated that acetate thresholds were controlled by kinetics under Mn(IV)-, nitrate- and sulfate-reducing conditions and by thermodynamics under

methanogenic conditions. The results suggested that acetate thresholds could be a potentially useful bioremediation indicator.

EVALUATION OF ACETATE THRESHOLDS UNDER VARIOUS  
TERMINAL ELECTRON-ACCEPTING CONDITIONS:  
APPLICATION TO BIOREMEDIATION MONITORING

By

Xiaomin Su

Thesis submitted to the Faculty of the Graduate School of the  
University of Maryland, College Park in partial fulfillment  
of the requirements for the degree of  
Master of Science,  
2004

Advisory Committee:

Dr. Jennifer G. Becker, Chair  
Dr. Hubert J. Montas  
Dr. Eric A. Seagren

©Copyright by  
Xiaomin Su  
2004

## TABLE OF CONTENTS

CHAPTER 1: Introduction.....	1
1.1 Concept of bioremediation.....	1
1.2 Lines of evidence for bioremediation assessment.....	2
1.3 Using consumption of electron acceptors as a bioremediation “footprint”.....	3
1.4 Framework of the thesis.....	6
CHAPTER 2: Literature Review.....	8
2.1 Traditional approaches for determining the dominant TEAPs in complex anaerobic systems.....	8
2.2 Substrate thresholds as an indicator of predominant TEAPs.....	11
CHAPTER 3: Hypothesis and Objectives.....	18
3.1 Hypothesis.....	18
3.2 Research objectives.....	20
CHAPTER 4: Materials and Methods.....	21
4.1 Microbial Cultures.....	21
4.1.1 Organisms, media, and growth conditions	21
4.1.2 Media preparation and culture technique	24
4.2 Analytical methods.....	28
4.2.1 Measurement of acetate	28
4.2.2 Measurement of Ferrous iron with the phenanthroline method	30

4.2.3 Measurement of methane	32
4.2.4 Measurement of protein	35
4.3 Threshold experiment.....	37
 CHAPTER 5: A Microbial Respiration Model for Predictions of Substrate Threshold....	43
5.1 Limitation of conventional Monod kinetics.....	43
5.2 Summary of microbial growth models incorporating thermodynamic and kinetic controls.....	44
5.3 Description of a new kinetically and thermodynamically consistent rate model for microbial respiration.....	50
5.4 Application of the new rate model to predict and interpret acetate thresholds under various TEA conditions.....	55
5.5 Determination of respiration rate law expressions for acetate oxidation under various TEA conditions.....	56
 CHAPTER 6: Results and Discussion.....	68
6.1 Introduction.....	68
6.2 Threshold experimental results.....	68
6.2.1 Results obtained with <i>Geobacter metallireducens</i> growing on Fe(III)	68
6.2.2 Results obtained with <i>Geobacter metallireducens</i> growing on Mn(IV)	75
6.2.3 Results obtained with <i>Geobacter metallireducens</i> growing on nitrate	77
6.2.4 Results obtained with <i>Desulfotomaculum acetoxidans</i> growing on sulfate	79

6.2.5 Results obtained with <i>Methanosarcina barkeri</i> growing via acetotrophic methanogenesis	82
6.2.6 Comparison and discussion of the acetate thresholds	84
6.3 Simulation of the experimental results using the microbial respiration model....	88
6.3.1 Calibration of the microbial respiration model	88
6.3.3 Controlling effects of $F_D$ and $F_T$ on acetate thresholds	101
CHAPTER 7: Conclusions.....	111
Reference.....	112
Appendix.....	121

# CHAPTER 1

## Introduction

In this chapter, first, the concept of bioremediation is introduced, and potential lines of evidence that can be used for bioremediation assessment are presented. In particular, the consumption of electron acceptors as a potentially useful bioremediation “footprint” is discussed in detail, because of its direct relevance to this project. Lastly, the framework of this thesis is outlined.

### 1.1 Concept of bioremediation

Significant amounts of a wide variety of industrial organic chemicals have been deliberately or accidentally released into the environment in the past few decades. Many of these contaminated sites are unlined. As a result, no barrier between the waste and groundwater exists, which can seriously threaten the quality of potential sources of drinking water for human beings (Dua et al., 2002). Conventional physical or chemical cleanup technologies, such as adsorption onto activated carbon, venting, incineration or secure landfilling, are expensive and energy-intensive (Eweis et al., 1998). The limitations of conventional cleanup technologies have spurred investigations into an effective alternative, bioremediation. Bioremediation is a managed or spontaneous treatment approach in which microbiological processes are used to degrade or transform contaminants to less toxic or nontoxic forms, thereby mitigating or eliminating environmental contamination (Crawford and Crawford, 1996).

Bioremediation approaches can be divided into three main classes: engineered *in situ*, intrinsic *in situ*, and engineered *ex situ* technologies. *In situ* and *ex situ* approaches

differ in that contaminated water and solids remain in place during *in situ* bioremediation, whereas groundwater is pumped out and soil is excavated for aboveground treatment when *ex situ* technologies are used. Engineered bioremediation refers to employing engineering tools to greatly increase contaminant transformation rates. On the other hand, intrinsic bioremediation, which is also referred to as “natural attenuation”, relies on intrinsic (or naturally-occurring) processes, including biological activity, to limit the migration of contaminants away from the source. The primary advantage of intrinsic bioremediation over other bioremediation approaches is that of cost. Compared to other technologies, intrinsic bioremediation can also minimize site disruption, volatile compound emission, and health risks to neighboring residents or site occupants (Crawford and Crawford, 1996). Thus, if applicable, intrinsic bioremediation has great appeal for attenuating a wide range of pollutants for the purpose of groundwater cleanup and protection. However, intrinsic bioremediation is not without its obstacles. For example, the effectiveness of intrinsic bioremediation depends on many factors, including the physical and chemical properties of the individual pollutants and the activities of the indigenous microorganisms. Another challenge associated with intrinsic bioremediation is that it is carried out in the subsurface, which is inherently complex and difficult to observe (Madsen, 1991). Thus, one of the factors that limit its widespread application is that it is difficult to evaluate the success of intrinsic bioremediation in the field.

## **1.2 Lines of evidence for bioremediation assessment**

To demonstrate that intrinsic attenuation processes can effectively limit contaminant migration, a monitoring plan that correlates microbial activity to the

observed loss of contaminant is needed. The National Research Council (NRC) (1993) identified three lines of evidence that are needed to demonstrate the occurrence of intrinsic or engineered bioremediation in the field:

1. Recorded decrease of contaminant levels at the site
2. Laboratory assays indicating that microorganisms at the site have the potential to degrade the contaminants
3. Evidence showing that biodegradation potential is actually realized in the field.

The first and second types of evidence are relatively simple to obtain by sampling the groundwater over time as the cleanup progresses and using common chemical or microbial analytical techniques. The most difficult evidence to obtain is that which falls into the third category. This evidence is critical for demonstrating that natural attenuation or biodegradation is occurring and at rates that are protective of human health. Therefore, it is also the key to convincing people that bioremediation is effective at a contaminated site. Rittmann et al. (1994) put forward three principal types of evidence, which are equally capable of demonstrating that bioremediation potential is actually realized in the field. They are “stoichiometric consumption of electron acceptors, formation of inorganic carbon that originated in organic carbon, and increases in degradation rates over time.” This research focuses on the development of an assessment tool that can be used to obtain evidence of consumption of electron acceptors, which may serve as a very useful “footprint” of bioremediation, especially in petroleum hydrocarbon-contaminated areas.

### **1.3 Using consumption of electron acceptors as a bioremediation “footprint”**

Generally, in petroleum hydrocarbon-contaminated sites, pollutants are initially

degraded under aerobic conditions. Indigenous aerobic bacteria use the hydrocarbons as electron donors and oxygen as an electron acceptor so that the maximum free energy can be gained from hydrocarbon metabolism. If the stoichiometric amount of hydrocarbons introduced by spills is far in excess of the amount of the dissolved oxygen needed to support degradation of the hydrocarbons, aerobic organisms will deplete all of the available oxygen and transform the aquifer environment from an aerobic to anaerobic condition (Zwolinski et al., 2000). Under anaerobic conditions, ideally, bacteria sequentially deplete other terminal electron acceptors (TEAs), such as nitrate, manganese (IV), iron (III), sulfate and/or carbon dioxide, in the order of decreasing standard free energy yield (Seagren and Becker, 2002). As a result, the sequential depletion of TEAs in a contaminated plume should, theoretically, resulting in characteristic spatial or temporal separation of redox zone in which different TEAs dominate (Ludvigsen et al., 1998). Figure 1.1 illustrates the temporal development of redox zones in a hypothetical contaminant plume emanating from a point source. Following the introduction of organic pollutants into the aquifer, the plume is primarily aerobic (panel a). Over time, strongly reduced redox zones are completely developed throughout the plume (panel c). Eventually less-reduced redox zones are slowly established in the contaminant plume as the strength of the point source declines (panel e). It should be noted that in some cases redox zones are not restrictively separated and some overlaps can be found in the temporal sequence of TEA-consuming processes (Watson et al., 2003)

The consumption of TEAs in groundwater impacted by petroleum hydrocarbons provides evidence that microbially-mediated destruction of the contaminants is occurring. Furthermore, knowing the spatial or temporal distribution of redox zones in groundwater

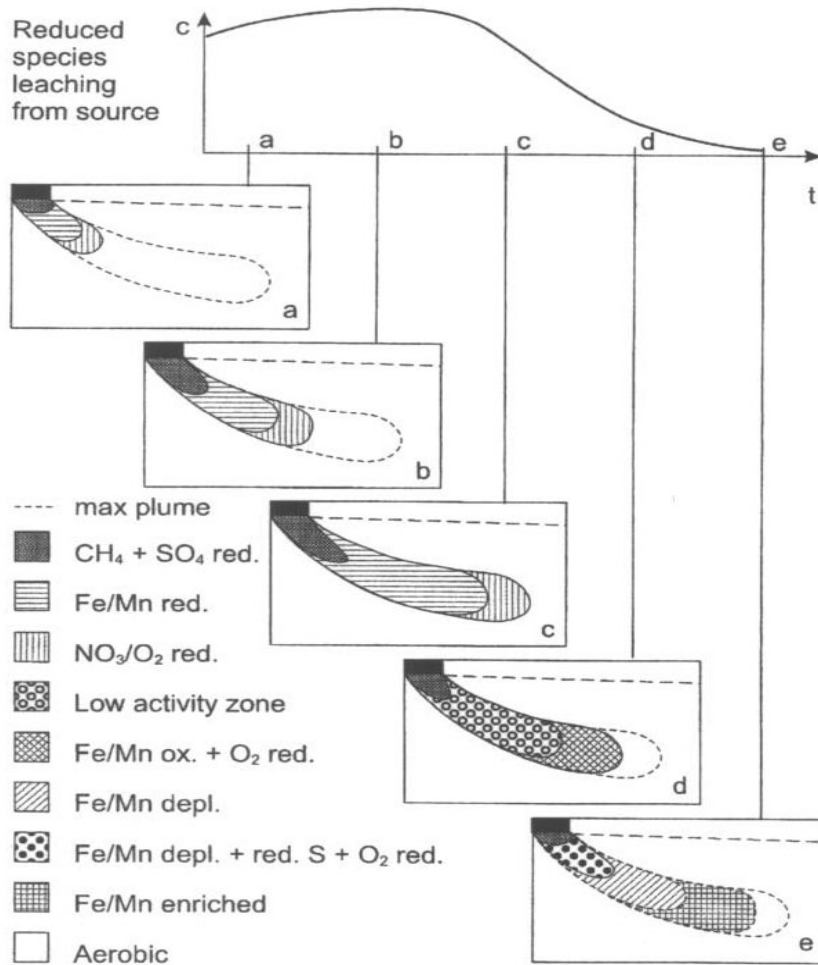


Figure 1.1 Illustration of development of redox zones in a contaminant plume emanating from a point source over time (from Christensen, et al. 2000).

is key to predicting the fate and transport of contaminants in groundwater systems because redox potential affects the rate and extent of the biodegradation of organic contaminants and the speciation and solubility of metals (Chapelle, et al., 1996).

However, interpretation of electron acceptor consumption as a bioremediation “footprint” is complicated by several factors (Lovley and Goodwin, 1988). First, a number of different electron acceptors may be present at a given site. Second, some electron acceptors will not be utilized at a given site if the appropriate microorganisms are not present or active. Third, measuring the removal of some electron acceptors in subsurface samples is technically difficult. Fourth, migration of electron acceptors away from active zones will affect the correct identification of the redox state at a given site. Thus, this research focuses on the development of a bioremediation assessment tool that can be used to obtain evidence of consumption of electron acceptors, without the complications associated with direct measurement of electron acceptors *in situ*. It is anticipated that this tool will be particularly useful in applications where monitoring natural attenuation of petroleum-contaminated sites is required.

#### **1.4 Framework of the thesis**

The following chapters describe this research project in detail. Chapter 2 provides a review of background information available in the literature necessary to understand the importance of, and the approach used in this project. Subsequently Chapter 3 puts forward the hypothesis and research objectives of the project. The experimental materials and methods used in this project are described in Chapter 4. Then, in Chapter 5, the selection and application of a microbial respiration model to test the hypothesis, as well

as to predict and interpret the experimental results is described. Next, in Chapter 6, the experimental and modeling results are presented and discussed. Finally, in Chapter 7, conclusions are drawn based on the experimental and the modeling results.

## CHAPTER 2

### Literature Review

The aim of this chapter is to review the available background information pertinent to bioremediation assessment tools used to obtain evidence of consumption of electron acceptors. The first major topic in this chapter is a brief review of traditional assessment tools for determining the predominant terminal electron-accepting processes (TEAPs) in complex anaerobic systems. The second topic is an assessment of an alternative approach, acetate thresholds measurements, for determining TEAPs.

#### **2.1 Traditional approaches for determining the dominant TEAPs in complex anaerobic systems**

Each electron acceptor redox couple, i.e., the oxidized and reduced forms of an electron acceptor, has a characteristic standard reduction potential ( $E_o'$ ), as shown in Table 2.1. The classic geochemical indicator of redox processes is platinum electrode measurement of reduction potential ( $E_o'$ ). Although the conceptual basis for measuring  $E_o'$  with a platinum electrode is relatively straightforward, there are many factors limiting its interpretation in environmental systems. First, multiple redox couples may be present. As a result, the electrode might respond to multiple redox couples in the system resulting in a mixed redox potential. In such a case, the meaning of the measured  $E_o'$  value is not clear. Second, the liquid junction potential might be significant in a system that contains many chemical species other than the redox couple of interest. In such a system, some of these species might bind to (absorb to) the electrode surface and change its catalytic properties.

Table 2.1 Standard reduction potentials at 25° C and pH 7 for selected environmentally important redox couples (adapted from Eweis, 1998).

Half reaction	$E_o'$ [V]
$\text{CO}_2 + \text{HCO}_3^- + \text{H}^+ + \text{e}^- = \text{CH}_3\text{COO}^- + 3\text{H}_2\text{O}$	-0.29
$\text{CO}_2(\text{g}) + 8\text{H}^+ + 8\text{e}^- = \text{CH}_4(\text{g}) + 2\text{H}_2\text{O}$	-0.25
$\text{SO}_4^{2-} + 9\text{H}^+ + 8\text{e}^- = \text{HS}^- + 4\text{H}_2\text{O}$	-0.22
$\text{FeOOH}(\text{s}) + \text{HCO}_3^- + 2\text{H}^+ + \text{e}^- = \text{FeCO}_3(\text{s}) + 2\text{H}_2\text{O}$	-0.05 <sup>a</sup>
$\text{NO}_3^- + 10\text{H}^+ + 8\text{e}^- = \text{NH}_4^+ + 3\text{H}_2\text{O}$	0.36
$\text{MnO}_2(\text{s}) + \text{HCO}_3^- + 3\text{H}^+ + 2\text{e}^- = \text{MnCO}_3(\text{s}) + 2\text{H}_2\text{O}$	0.52 <sup>a</sup>
$\text{Fe}^{3+} + \text{e}^- = \text{Fe}^{2+}$	0.76
$\text{O}_2(\text{g}) + 4\text{H}^+ + 4\text{e}^- = 2\text{H}_2\text{O}$	0.82

<sup>a</sup>Based on  $[\text{HCO}_3^-] = 10^{-3} \text{ M}$ .

As a result, the measured value of  $E_o'$  might not correctly reflect the properties of the system (Benjamin, 2002). Other factors, such as irreversible reactions, slow electrode kinetics, small exchange currents, and inert redox couples, may also affect the measurement of  $E_o'$ . Consequently, when measured with a platinum electrode, the  $E_o'$  of an environmental system cannot be accurately correlated to a single specific redox couple (Chapelle et al., 1996), and is usually of little value in quantifying the dominant redox process.

In addition to redox potential measurement with platinum electrodes, measurement of hydrogen concentrations was introduced by Lovley and Goodwin (1988) as an alternative indicator of the predominant redox process in an environmental system. Hydrogen is a key intermediate in the catabolism of organic matter under anaerobic conditions. Both theoretical analyses and field data suggest that a characteristic range of hydrogen concentrations exists for each predominant anaerobic redox process. These characteristic hydrogen concentrations may reflect the threshold concentrations below which hydrogen cannot be further metabolized for each anaerobic terminal electron acceptor process. The theoretical bases of substrate thresholds in general are discussed below, along with a summary of studies in which hydrogen thresholds were determined. However, in general, it appears that the lower the free energy yield from oxidation of hydrogen coupled to the reduction of a given terminal electron acceptor respiration is, the higher the threshold concentration of hydrogen will be (Cord-Ruwisch et al., 1988; Lovley and Goodwin, 1988; Chapelle et al., 1996; Hoehler et al., 1998). The major advantage of the hydrogen concentration as a redox process indicator is its timely response to redox processes (Lovley and Goodwin, 1988). Specifically, anaerobic

microorganisms in groundwater systems typically metabolize hydrogen very quickly. As a result, the hydrogen pool is very small and its residence time ranges from just a few seconds to minutes. Further, hydrogen transport in groundwater systems is extremely limited (Postma and Jacobsen, 1996). Therefore, hydrogen thresholds can reflect ongoing, local redox processes. However, measurement of hydrogen thresholds can be affected by solute concentrations, temperature, and other non-redox factors in certain groundwater systems. Moreover, because of the gaseous property of hydrogen, its measurement can also be affected by several factors related to the procedures used in procuring samples from the subsurface, including the sampling and pumping methods and the sample-well casing material (Chapelle et al., 1997). Furthermore, quantification of the low hydrogen levels present in contaminant plumes via gas chromatography (GC) requires a highly sensitive and specialized reduction gas detector. Clearly, a sensitive, meaningful, and readily quantifiable indicator of TEAPs in complex groundwater systems is still needed in order to make accurate predictions about the fate of environmental contaminants and evaluate the success of *in situ* bioremediation projects.

## **2.2 Substrate thresholds as an indicator of predominant TEAPs**

Using hydrogen concentrations to characterize the redox processes under anaerobic conditions, as described above, implies that substrate thresholds may be used as an indicator of predominant TEAPs. Substrate thresholds refer to the concentrations below which the substrates cannot be further metabolized (Lovley and Goodwin, 1988).

Determination of substrate threshold values for different anaerobic bacteria and TEAPs has primarily focused on hydrogen and organic acid such as acetate. For example,

hydrogen thresholds were found to be associated with specific predominant TEAPs in bottom sediments in a variety of surface water environments (Lovley and Goodwin, 1988). The characteristic hydrogen ranges were 7-10 nM for methanogenesis; 1-1.5 nM for sulfate-reduction; 0.2 nM for Fe(III)-reduction; and less than 0.05 nM for Mn(IV) or nitrate-reduction. Hydrogen thresholds also were observed in pure monoculture and cocultures (Cord-Ruwisch et al., 1988). For example, a comparatively high hydrogen threshold value was measured in methanogenic culture, while a lower value was associated with sulfate reduction and the lowest hydrogen threshold value was observed in nitrate reducing cultures. A recent field study provided the following data set of comparable steady-state hydrogen concentration ranges for several different TEAPs: nitrate-reduction (<0.1 nM), Fe(III)-reduction (0.2-0.8 nM), sulfate-reduction (1-4 nM), and methanogenesis (5-30 nM) (Chapelle, 1997; Chapelle et al., 1997). A similar trend in hydrogen thresholds was also obtained in both field and experimental studies for a wide range of TEAPs (Hoehler et al., 1998). In all of these studies, the relative magnitude of the hydrogen concentration decreased as the redox potential of the TEA couple increased.

In addition to hydrogen thresholds, threshold values for acetate degradation by different physiological groups, especially acetoclastic methanogens, have been measured. For example, the following acetate thresholds were determined for a acetoclastic methanogens: 1.180 mM (*Methanosarcina barkeri* 227), 0.396 mM (*Methanosarcina mazei* S-6), and 0.069 mM (*Methanothermobacter* sp.) (Westermann et al., 1989). Lower acetate threshold values were observed in sulfate-reducing environments (2-50  $\mu$ M) (McMahon and Chapelle, 1991; Chapelle and Lovley, 1992) and in Fe(III)-reducing environments (0.5-3  $\mu$ M) (Chapelle and Lovley, 1992).

Threshold values of formate have also been observed, and ranged from 5 to 60  $\mu\text{M}$  in sulfate-reducing environments (McMahon and Chapelle, 1991; Chapelle and Lovley, 1992) and from 0 to 6  $\mu\text{M}$  in Fe(III)-reducing environments (Chapelle and Lovley, 1992). In addition, a threshold value below which benzoate was not degraded in a coculture after extended incubation times was observed and ranged from 214 nM to 6.5  $\mu\text{M}$  (Hopkins et al., 1995). In this case, the magnitude of the threshold appeared to be related to the concentration of acetate, an end-product of benzoate degradation in the coculture.

Both thermodynamic and kinetic factors probably play a role in determining the substrate thresholds in growing cells. First, thermodynamics represents the ultimate control on any chemical transformation. A reaction that is not thermodynamically feasible cannot occur spontaneously. In addition, conservation of energy in the form of ATP, which is the goal of catabolic (respiration) processes, cannot occur without at least a minimum input of energy. Thus, the substrate threshold of a microbially-mediated redox process may represent the point below which the free energy change of the overall reaction is not sufficient to support any level of microbial metabolism (Hopkins et al., 1995; Warikoo et al., 1996; Hoehler et al., 1998).

It should be noted that a difference exists in the amount of energy needed to support microbial metabolism in resting and growing cells. In a resting cell, where no growth is occurring, the minimum substrate concentrations needed to support microbial metabolism might reflect the energy needed to conserve ATP and/or in inducing specific enzymes to facilitate substrate transport across the cell membrane as well as cellular maintenance. For a growing cell, additional energy may be needed to sustain growth,

which probably would increase the substrate threshold level (Alexander, 1999).

It is also important to note that at non-standard conditions, the free energy change of a reaction is influenced by several factors. For example, in a hydrocarbon-contaminated pool, the following factors would affect the free energy change of a redox reaction: temperature, pH, the nature of the TEA, concentrations of the TEA, and other reactants and products (Hoehler et al., 1998). If a constant environmental temperature and pH are assumed, then the nature of the TEA and the reactant and product concentrations would predominantly determine the free-energy that is available to conserve energy and support microbial metabolism.

As noted above, kinetics also may play an important role in controlling the substrate threshold. For example, even if an overall redox reaction is energetically favorable, under a very low substrate concentration condition, certain microorganisms may not be able to take up the substrates effectively. This may cause substrate uptake to stop or occur at a very low rate. Therefore, given a zero or very low consumption rate, the substrate concentrations may remain relatively constant for a long time, reflecting a superficial substrate threshold. One measure of the affinity of microorganisms for substrates at low concentrations is the half saturation constant  $K$  in the Monod equation. Thus, an organism's substrate affinity or  $K$  value may be relevant to the control of substrate thresholds (Fukuzaki et al., 1990). In fact, organisms with lower  $K$  values appear to have lower threshold concentrations.

In continuous-flow systems, thermodynamic and kinetic controls on threshold concentrations can be incorporated in the concept of  $S_{\min}$  [ $\text{Ms L}^{-3}$ ], the substrate concentration below which biomass cannot be maintained at steady-state. Although  $S_{\min}$

is a steady-state concept, we can derive the definition of  $S_{\min}$  based on a batch system. In discussing  $S_{\min}$ , it is assumed that microbial growth kinetics can be described by the Monod equation. The Monod equation predicts that the specific growth rate of bacteria is a function of the concentration of a rate-limiting substrate,

$$\mu = \frac{1}{X} \frac{dX}{dt} = \mu_{\max} \frac{S}{K + S} \quad (2.1)$$

where  $\mu$  is the specific growth rate constant [ $T^{-1}$ ];  $X$  is the concentration of biomass [ $M L^{-3}$ ];  $t$  is time [ $T$ ];  $S$  is the concentration of the rate-limiting substrate [ $M L^{-3}$ ];  $\mu_{\max}$  is the maximum specific growth rate constant [ $T^{-1}$ ]; and  $K$  is the half saturation constant [ $M L^{-3}$ ], which characterizes the affinity of microbial cells for the substrate and is equal to the substrate concentration at which  $\mu = \frac{1}{2} \mu_{\max}$ .

$\mu_{\max}$  is related to  $q_{\max}$  [ $T^{-1}$ ], the maximum specific substrate utilization rate according to:

$$\mu_{\max} = q_{\max} Y \quad (2.2)$$

where  $Y$  is the true yield coefficient [ $M_x M_s^{-1}$ ]. The net rate of change in biomass concentration in a continuous-flow system is also a function of the decay constant,  $b$  [ $T^{-1}$ ], according to:

$$\frac{dX}{dt} = \mu X - bX \quad (2.3)$$

Substituting equation 2.1 and 2.2 into equation 2.3 and solving for  $S$  at steady-state gives the substrate concentration at which microbial growth is just balanced by decay, i.e.,  $S_{\min}$ :

$$S = S_{\min} = \frac{bK}{aY - b} \quad (2.4)$$

As discussed by McCarty (1972),  $Y$  is a function of the free-energy change of the electron donor oxidation and electron acceptor reduction half-reactions. Thus, the free yield ( $Y$ ) resulting from the oxidation of a given electron donor such as acetate will increase as the free energy of the electron acceptor reduction half reaction increases. An increase in the free energy change of the electron acceptor half- reaction corresponds to an increase in the standard reaction potential ( $E_o'$ ) of the redox couple (Table 2.1). Thus, from equation 2.4, it can be seen that  $S_{\min}$  is a function of thermodynamic factors, which are captured by  $Y$ , and by kinetic factors, including  $K$  (Seagren and Becker, 1999; Lovley and Goodwin, 1988). Specifically, as  $K$  decreases and the free energy change (and  $E_o'$ ) for the electron acceptor reduction half reaction increases,  $S_{\min}$  decreases. Unfortunately, the  $S_{\min}$  concept cannot be applied to non-steady state continuous-flow systems or batch systems, because under these conditions, the substrate concentration may fall below  $S_{\min}$  (Rittmann et al., 1994).

To sum up, substrate threshold phenomena are common, especially in anaerobic systems, and the levels of substrate thresholds appear to be related to the predominant

specific TEAP. Although hydrogen thresholds measurement is a very useful tool to indicate the predominant TEAPs, it is not simple to obtain accurate hydrogen concentration measurements. Therefore, it may be worthwhile to obtain other substrate thresholds measurement that relies on simple and straightforward procedures as indicators of the predominant TEAPs in complex anaerobic systems. The theoretical evaluation of the roles of thermodynamics and kinetics in determining substrate thresholds and the utilization of substrate thresholds as an indicator of different TEAPs is discussed further in Chapter 5.

## CHAPTER 3

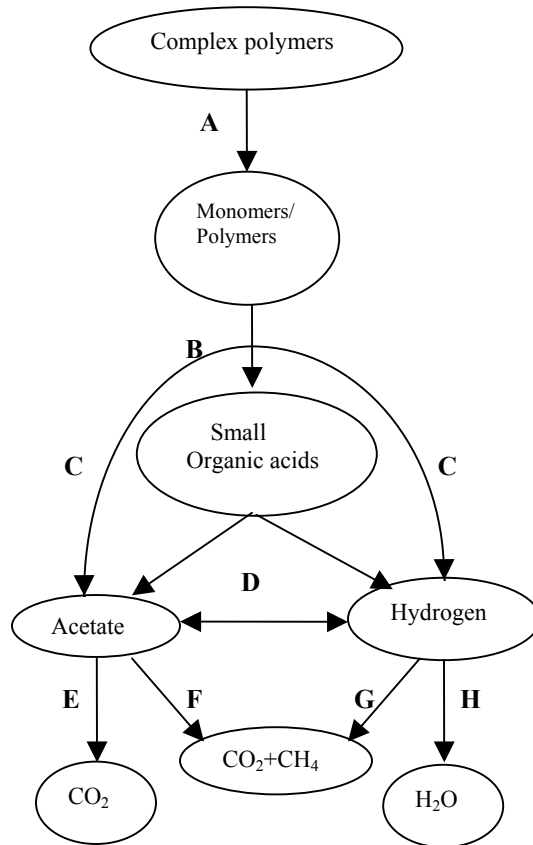
### Hypothesis and Objectives

In this chapter, the hypothesis of this project is put forward. In addition, the objectives of the project, along with the approaches to achieve them, are outlined.

#### 3.1 Hypothesis

In Chapter 2, it was mentioned that measurement of hydrogen could be used as an indicator of the predominant TEAP. In addition to hydrogen, acetate is another key intermediate in the anaerobic biotransformation of organic compounds, and it is frequently detected at petroleum-contaminated sites undergoing *in situ* bioremediation (e.g. Chapelle et al., 1996; Chapelle et al., 1997). Figure 3.1 clearly indicates that acetate and hydrogen play similar roles in the biodegradation pathways of complex organic compounds. During the degradation of complex polymers to simple mineral molecules, hydrogen and acetate are produced as intermediates. Hydrogen and acetate can be intertransformed via acetogenesis, operating in the forward and reverse directions (Process D). In addition, hydrogen and acetate can both serve as electron donors in anaerobic TEAPs (Processes E and H). Furthermore, both hydrogen and acetate can be consumed in methanogenesis (Processes F and G). This suggests that acetate thresholds, like hydrogen thresholds, may be related to the dominant electron acceptor-consuming processes in complex anaerobic environments (Seagren and Becker, 1999).

Thus, the overall hypothesis of this research is that in complex anaerobic systems,



- A** enzyme hydrolysis
- B** facultative reduction
- C** obligate anaerobic reduction
- D** autotrophic acetogenesis/acetotrophy
- E, H** anaerobic terminal electron acceptor-consuming process
- F** acetotrophic methanogenesis
- G** hydrogenotrophic methanogenesis

Figure 3.1 Biodegradation pathway of complex organic compounds (adapted from Hoehler et al., 1998).

characteristic ranges of acetate threshold concentrations may exist for different predominant TEAPs and, thus, may be useful as bioremediation “footprints”. Compared to measuring hydrogen, characterization of acetate levels in groundwater is relatively simple, largely because it is soluble in water and does not form a gas at ambient temperatures.

### **3.2 Research objectives**

The overall goal of the project is to experimentally and mathematically evaluate the hypothesis that each TEAP establishes a characteristic range of acetate threshold concentrations. Specifically, the objectives are to:

1. Experimentally evaluate the hypothesis by measuring the threshold concentration of acetate established during growth of pure microbial batch cultures that couple the oxidation of acetate to different terminal electron acceptors.
2. Mathematically evaluate the hypothesis using a microbial respiration model that incorporates growth kinetics and thermodynamic terms.

## CHAPTER 4

### Materials and Methods

The aim of chapter 4 is to present the materials and methods used in the project. First, the microbial cultures used in the threshold experiments are listed, followed by the description of their culture medium, growth conditions and the anaerobic techniques applied to inoculate and maintain the cultures. Second, the analytical methods used to obtain all the data in the threshold experiments are described. Lastly, the process for performing the threshold experiments is presented.

#### 4.1 Microbial Cultures

##### 4.1.1 Organisms, media, and growth conditions

A summary of the pure cultures that were used in the acetate threshold experiments is presented in Table 4.1, along with the terminal electron acceptors used by each organism for the oxidation of acetate, and the standard redox potential of the electron acceptor couples. The electron acceptor couples and microorganisms are listed in order of highest to lowest predicted acetate threshold.

*Methanosarcina barkeri* (type strain) and *Desulfotomaculum acetoxidans* (type strain) were obtained from the Oregon Collection of Methanogens (OCM, Portland, OR). The medium used to grow *M. barkeri* consisted of the following components (per liter) (Bryant and Boone, 1987): NaCl, 0.46 g; MgCl<sub>2</sub> × 6H<sub>2</sub>O, 0.09 g; NiCl<sub>2</sub> × 6H<sub>2</sub>O, 0.002 g; CaCl<sub>2</sub> × 2H<sub>2</sub>O, 0.06 g; (NH<sub>4</sub>)<sub>2</sub>SO<sub>4</sub>, 0.23 g; KH<sub>2</sub>PO<sub>4</sub>, 0.23 g; K<sub>2</sub>HPO<sub>4</sub>, 0.23 g; NaHCO<sub>3</sub>, 2.50 g; yeast extract, 0.2 g; Na<sub>2</sub>S × 9H<sub>2</sub>O, 0.50 g; Cysteine, 0.25 g; Na-acetate × 3H<sub>2</sub>O, 1.36 g; 10 ml each of Wolfe's trace element solution (Ferguson and Mah, 1983) and

Table 4.1 Summary of the microorganisms and terminal electron acceptors that will be used in the proposed research

Terminal electron acceptor couple	Standard redox potential, pH=7, ( $E_o'$ ), V	Organism	Relative magnitude of acetate threshold
CO <sub>2</sub> /CH <sub>4</sub>	-0.25	<i>Methanosarcina barkeri</i>	Highest  Lowest
SO <sub>4</sub> <sup>2-</sup> /HS <sup>-</sup>	-0.22	<i>Desulfotomaculum acetoxidans</i>	
NO <sub>3</sub> <sup>-</sup> /NH <sub>4</sub> <sup>-</sup>	0.36	Geobacter metallireducens	
MnO <sub>2</sub> /Mn <sup>2+</sup>	0.52		
Fe <sup>3+</sup> /Fe <sup>2+</sup>	0.76		

vitamin solution (Wolin et al., 1963); and resazurin, 0.50 mg (added as a redox indicator). The pH of the complete medium was 7. The medium used to culture *D. acetoxidans* consisted of the following components (per liter) (Widdel and Pfennig, 1981): NaCl, 1.17 g; MgCl<sub>2</sub>×6H<sub>2</sub>O, 0.40 g; KCl, 0.30 g; CaCl<sub>2</sub>×2H<sub>2</sub>O, 0.15 g; NH<sub>4</sub>Cl, 0.27 g; KH<sub>2</sub>PO<sub>4</sub>, 0.20 g; Na<sub>2</sub>SO<sub>4</sub>, 2.84 g; NaHCO<sub>3</sub>, 4.50 g; Na<sub>2</sub>S×9H<sub>2</sub>O, 0.50 g; 10 ml each of Wolfe's trace element and vitamin solutions; and resazurin, 0.5 mg (added as a redox indicator). 20 mM Na-acetate×3H<sub>2</sub>O (1.420 g/l) and 20 mM sodium sulfate (2.841 g/l) were provided as the electron donor and acceptor, respectively. The pH of the complete medium was 7.

*Geobacter metallireducens* was provided by Dr. Derek R. Lovley of the Department of Microbiology at the University of Massachusetts. The medium used to grow *G. metallireducens* contained the following components (per liter) (Lovley and Phillips, 1988): NaHCO<sub>3</sub>, 2.50 g; NH<sub>4</sub>Cl, 0.25 g; KCl, 0.1 g; Na-acetate×3H<sub>2</sub>O, 2.72 g; NaH<sub>2</sub>PO<sub>4</sub>×H<sub>2</sub>O, 0.6 g; and 10 ml each of Wolfe's trace element and vitamin solutions. 10 mM Na-acetate×3H<sub>2</sub>O (0.820 g/l) was added as the electron donor. In addition, Mn(IV), Fe(III), or NO<sub>3</sub><sup>-</sup> was provided as the electron acceptor. For growth of *G. metallireducens* under manganese-reducing conditions, approximately 50 mM Mn(IV) was provided as poorly crystalline MnO<sub>2</sub>. A stock solution of poorly crystalline MnO<sub>2</sub> was prepared by first dissolving 20 mmol of KMnO<sub>4</sub> (3.16 g) and 3.2 g of NaOH in 1 liter of distilled water, which was stirred with a magnetic stir bar in a 2-l glass beaker. 1 liter of a 30 mM MnCl<sub>2</sub>×4H<sub>2</sub>O solution (5.94 g/l) was slowly added to the solution of KMnO<sub>4</sub>. The MnO<sub>2</sub> that formed settled to the bottom of the beaker. The precipitate was collected by centrifuging at 5000 rpm for 20 min. The supernatant was carefully poured

out and the precipitate was washed with distilled water. The washing step was repeated two more times. The precipitate was resuspended in 500 ml of distilled water in a plastic bottle. The concentration of this MnO<sub>2</sub> solution was 111 mM, determined by atomic absorption spectrophotometry. The MnO<sub>2</sub> stock solution was stored at ambient temperature for several months. The pH of the complete medium was 7. The nitrate-reducing medium used to culture *G. metallireducens* was similar to the manganese-reducing medium, except that 20 mM of Na-acetate×3H<sub>2</sub>O (1.700 g/l) served as the electron acceptor in place of manganese dioxide. The pH of the complete medium was 7. Similarly, in the iron-reducing medium used to culture *G. metallireducens*, 50 mM of Fe(III) (12.245 g/l) replaced manganese as the electron acceptor. Soluble iron was added to the medium in the form of an Fe(III)-citrate complex, which was prepared as follows: ferric citrate was added to water that had been heated until almost boiling, allowed to dissolve, and then the solution was cooled to room temperature. The pH was adjusted to 6.0 using 10 N NaOH. The pH of complete medium was 7.0.

All microorganisms were incubated in a dark incubator at 35°C without shaking.

#### **4.1.2 Media preparation and culture technique**

All media were prepared using the serum bottle variation (Miller and Wolin, 1974) of the Hungate technique (e.g., Balch and Wolfe, 1976; Hungate, 1950; Bryant, 1972). After being deoxygenated, solutions without the reducing reagents and vitamin were transferred by a pipette flushed with O<sub>2</sub>-free N<sub>2</sub>:CO<sub>2</sub> (80:20) mixture (certified standard; Airgas, Inc.; Radnor, PA) into culture tubes or serum bottles that were also flushed with the gas before and during the addition of medium. The tubes and bottles were sealed with

thick butyl rubber stoppers (Geo-Microbial Technologies, Inc.; Ochelata, OK) and aluminum crimp caps. The culture vessels were sterilized by autoclaving at 210 °C for 30 min. The reducing reagent solutions, such sodium sulfide and cysteine solutions, were made and autoclaved separately and mixed with the other solutions 24 hours before inoculation. The 100X vitamin stock solution was also made and sterilized with 0.2 µm syringe filter separately and added to the rest of medium right before inoculation.

All inoculations, transfers, and additions were done using sterile disposable syringes (Fisher Scientific; Fair Lawn, NJ) and 22 gauge hypodermic needles (Fisher Scientific; Fair Lawn, NJ). The surface of each stopper was flame sterilized prior to insertion of the syringe needle. Syringes and needles were flushed with sterile O<sub>2</sub>-free N<sub>2</sub> or N<sub>2</sub>:CO<sub>2</sub> gas for a few seconds before removing material from a culture vessel.

The above operations were accomplished using a high-pressure anaerobic gassing manifold system. The gassing manifold was previously constructed for cultivation of anaerobic cultures under elevated pressures in stoppered culture vessels. A schematic of the gassing manifold system is shown in Figure 4.1. Compressed gas cylinders (A) were connected to a copper catalyst vessel (B) that contained reduced copper filings (Spectrum Chemical Mfg, Corp.; Gardena, CA) used for removing trace amounts of oxygen in the gas. The gas passed over the heated reduced copper filings to the manifold. The copper filings were regularly re-reduced by passing a H<sub>2</sub>:N<sub>2</sub> (10:90) mixture (Certified standard; Airgas, Inc.; Radnor, PA) through the catalyst vessel. During catalyst regeneration, the gas was vented to a hood via a three-way valve (C1). The manifold consisted of another three-way valve (C2) connected to the catalyst outlet, a vacuum source, and six two-way valves (E). Four of the two-way valves were connected to rigid polyethylene tubing (F).

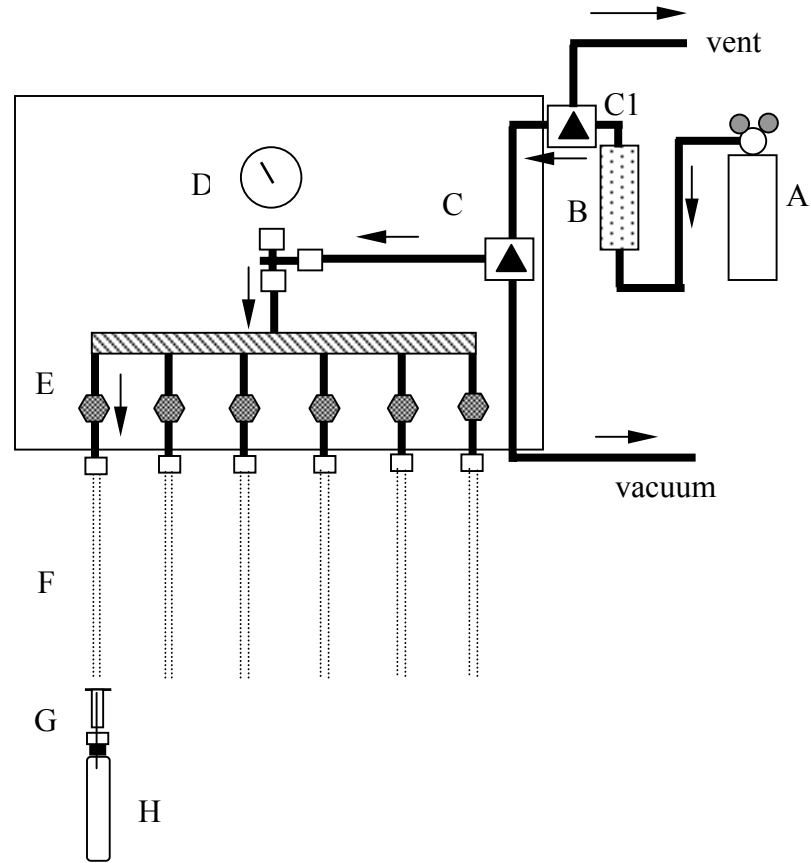


Figure.4.1 Gassing manifold with apparatus for supply of oxygen-free gas. (A) Gas mixture tank; (B) copper catalyst vessel (oxygen scrubber) with heater; (C.1-2) three-way valve; (D) pressure-vacuum gauge; (E) two-way valve; (F) polyethylene tubing; (G) needle; (H) culture tube.

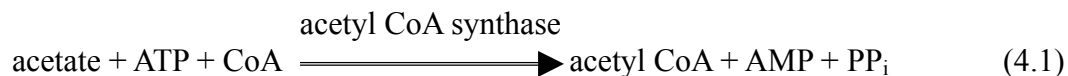
At the end of each length of tubing was a hose barb luer fitting to which a luer needle (G) can be attached. For aseptic work, the gas can be sterilized by attaching 0.2- $\mu\text{m}$  sterile, disposable syringe filters (Millex®-FG, PTFE; Millipore; Carrigtwohill, Co.; Cork, Ireland). The rest of the two-way valves were connected to thick tubing (not shown). The thick flexible tubing was attached to either a cotton-packed glass syringe with a luer-lock hub, to which a cannula was attached, or a glass dispersion tube. The rigid tubing and luer needles were used for manipulation of culture tubes and serum bottles, while the flexible tubing and cannula or dispersion tube configurations were used for gassing larger volumes of solutions or media. Pressure in the manifold was regulated with a two-stage regulator on the gas cylinder. Direct readout of pressure was made with a pressure-vacuum gauge (Ashcroft; Halliburton Company; Berea, KY) (D) in the manifold assembly.

All cultures were transferred every three to six weeks using an inoculum of 10% (v/v). The purity of the cultures was checked periodically and at the conclusion of each threshold experiment using phase-contrast microscopy. The purity of all cultures at the conclusion of the threshold experiments was further checked by inoculating thioglycollate medium with Hemin, Vit K without indicator (Anaerobe Systems; Morgan Hill, CA) in 7-ml tubes. The strict anaerobes used in this work typically have a restricted substrate range and should not grow in the complex, rich thioglycollate medium, whereas growth of contaminating organisms in the medium would be expected. All cultures underwent at least three serial transfers before an acetate threshold experiment was initiated. The inocula used for threshold experiments were harvested during the mid-exponential growth phase.

## 4.2 Analytical methods

### 4.2.1 Measurement of acetate

Acetate was quantified using an enzymatic technique in which acetate and acetyl coenzyme A (CoA) reacted with adenosine triphosphate (ATP) to form adenosine monophosphate (AMP) and pyrophosphate (PP<sub>i</sub>) according to (King, 1991):



For each enzyme reaction, an approximately 1.2-ml sample of acetate-oxidizing culture was removed anaerobically and aseptically, and filtered with a syringe filter (13-mm diameter; 0.2- $\mu\text{m}$  pore size; polysulfone filter media with polypropylene housing; Whatman Inc.; Lifton, NJ) into a 10-ml beaker. 1000  $\mu\text{l}$  of the filtrate was transferred to a 7-ml screw-cap polypropylene vial (Wheaton Scientific; Millville, N.J.), which contained 10  $\mu\text{l}$  each of CoA (10 mM) (Sigma-Aldrich; Louis, MO), CoA synthase (20 U  $\text{ml}^{-1}$ ) (Sigma-Aldrich; Louis, MO), bovine serum albumin (BSA) (200  $\mu\text{g ml}^{-1}$ ) (Fisher Scientific; Fairlawn, NJ), and disodium ATP (10 mM) (CalBiochem Bioscience Inc.; La Joalla, CA). The solutions were well mixed by hand shaking and incubated at 35 °C for 12 h to allow the reaction to occur. Following the reaction period, each vial was immersed into a 100°C water bath for 2 min, cooled down at room temperature for approximately one hour and shaken by hand for several seconds. The resulting AMP was assayed using high-performance liquid chromatography (HPLC), as described below. The enzymatic method was selected for analysis of acetate in the threshold experiments, in which very low concentrations were expected in some cases, because the reported detection limit of the method (0.1  $\mu\text{M}$ ; King, 1991) was much lower compared to the detection limits (about 1-10  $\mu\text{M}$ ) of other approaches commonly used to quantify acetate

directly in aqueous solutions (e.g., gas chromatography (Wu and Scranton, 1994; Ho et al., 2002), ion chromatography (Min and Zinder, 1989), and capillary electrophoresis (Bondoux et al., 1992)). The reaction products were filtered with syringe filters (4-mm diameter; 0.45- $\mu\text{m}$  pore size; cellulose acetate; Nalge Nunc International Corp.; Rochester, NY) and transferred to 1-ml HPLC sample vials (Waters Corp.; Milford, MA) for quantification of AMP via reverse-phase HPLC. A WATERS Carbamate Analysis HPLC System was controlled with Millennium 2.10 software (WATERS). Loop injections (200  $\mu\text{l}$ ) were made with an autosampler (717 plus; WATERS) and pumped using two 100-ml constant volume pumps (WATERS). Separations were performed using a mobile phase of potassium phosphate (50 mM; pH 4.5; Fisher Scientific; Fairlawn, NJ.) (pH=4.5) with 10% HPLC-grade methanol (Fisher Scientific; Fairlawn, NJ.) operating under the isocratic condition and ambient temperature at a flow rate of 0.4 ml min<sup>-1</sup> and a Supelcosil<sup>TM</sup> LC-18 column (25 cm  $\times$  4.6 mm ID, 5- $\mu\text{m}$  packing; Supelco; Bellefonte, PA) connected with a Brownlee RP18 SPHERI-5 guard column (30  $\times$  4.6 mm; Alltech Associates Inc.; Deerfield, IL). The mobile phase was prepared using HPLC grade water (Fisher Scientific; Fairlawn, NJ.), filtered (GN-6 Metrical<sup>®</sup> membrane filter; 0.45  $\mu\text{m}$  pore size; Pall Gelman Laboratory; East Hill, NY), and degassed in-line using a helium sparge. Detection was accomplished by UV absorbance with a photodiode array detector (WATERS, 996) operated at 260 nm wavelength. Two injections of each sample were made. The injector was automatically purged every six injections.

The acetate concentrations of unknown samples were determined by comparison with a series of external sodium acetate (Fisher Scientific; Fairlawn, NJ) standards that were made in glass flasks and stored in a refrigerator (4°C) for several months. A typical

standard curve is shown in Figure 4.2.

All solutions, with the exception of the mobile phase, were prepared with 18-m $\Omega$  distilled deionized water. Stock solutions of CoA, CoA synthase, BSA and ATP were frozen (-20°C) in 2-ml plastic centrifuge tubes after initial preparation and stored for several months.

#### **4.2.2 Measurement of Ferrous iron with the phenanthroline method**

Fe(II) was produced by the reduction of Fe(III) as an electron acceptor during growth of *G. metallireducens* in the Fe(III)-citrate microbial medium, and was quantified using the Hach Ferrous Iron 1,10-phenanthroline method (Method 8146; Hach Company; Loveland, CO), which was adapted from the standard method for quantification of Fe(II). The basis of this method is 1,10-phenanthroline indicator in Ferrous Iron Reagent (Hach Company; Loveland, CO), which reacts with ferrous iron in the sample to form an orange color with an intensity that is directly proportioned to the Fe(II) concentration. Ferric iron does not react with the reagent. The following procedure was used in Fe(II) determinations:

A 1-ml syringe was used to aseptically withdraw a 200  $\mu$ l sample from an anaerobic culture serum bottle containing ferric citrate medium and transfer it to a 10-ml glass beaker. A 200- $\mu$ l range pipette (Rainin; Woburn, MA) was used to transfer 100  $\mu$ l sample to a 7-ml screw-cap polypropylene vial (Wheaton Scientific; Millville, NJ), which contained 2 ml of 0.5 N HCl to acidify the sample. After 15 min, 1 ml of acidified sample was transferred to a 25-ml volumetric flask, in which the sample was diluted with 18 m $\Omega$  distilled deionized water to 25 ml. The diluted sample was transferred to a clean 25-ml

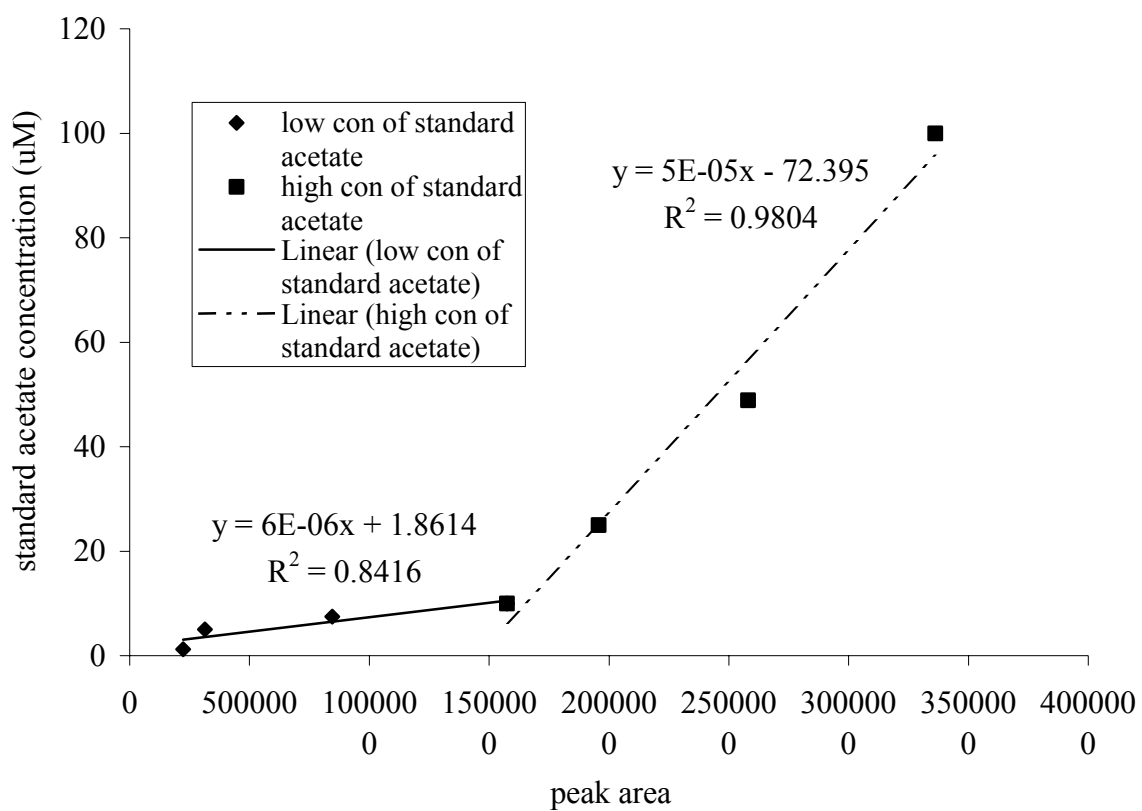


Figure 4.2 A typical standard curve of acetate measurement.

glass sample cell (Hach Company; Loveland, CO). A DR/4000 spectrophotometer (Hach Company; Loveland, CO) was powered on, and program number 2150 was chosen for Fe(II) measurement. The wavelength dial was rotated to set the wavelength at 510 nm. The sample cell was wiped with a Kimwipe (Kimberly-Clark Inc.; Mississauga, Ontario) and placed into the cell holder of the spectrophotometer as the reference cell. With the cover closed, the instrument was zeroed. The sample cell was taken out, and the contents of one Ferrous Iron Reagent Powder Pillow were added to the sample cell. The sample cell was swirled to mix for several seconds and put back into the cell holder. After a 3 min reaction time, the results (in mg/l Fe(II)) was read.

The accuracy of the Fe(II) measurement was checked by measuring the concentration of a standard solution. To prepare the standard solution, 0.7022 g of ferrous ammonium sulfate, hexahydrate (Fisher Scientific; Fairlawn, NJ) was dissolved in 18 mΩ distilled deionized water in a 1-liter volumetric glass flask. 0.25 ml of this solution was further diluted in a 25-ml volumetric glass flask, which contained 1 ml of 0.5 N HCl, with 18 mΩ distilled deionized water to make a 1.0-mg/l standard solution. The 1.0-mg/l standard solution was immediately measured following the above procedure. The measurement result was 0.995 mg/l.

#### **4.2.3 Measurement of methane**

Production of methane over time by *M. barkeri* was measured using a gas chromatograph (GC) (Hewlett Packard Model 5890 Series II plus; Hewlett Packard Company; Wilmington, DE) equipped with a flame-ionization detector (FID) and 3.2 mm by 2.4-meter stainless-steel GC column packed with 1% SP-100 on 60/80 Carbopack-B

(Supelco, Inc.; Bellefonte, PA). Helium was used as the carrier gas at flow rate of 40 ml/min, and the FID was fueled by hydrogen and air provided at flow rate of 40 ml/min and 400 ml/min, respectively. The injector and detector temperatures were set at 200°C and 250°C, respectively. The oven temperature was maintained according to the following sequence: 60°C for two minutes, followed by a 20°C/min ramp to 150°C and a 10°C/min ramp to 200°C.

The sampling procedure used to obtain aqueous samples during the threshold experiments involved flushing a portion of the contents of the headspaces, including methane, from the bottles. The loss of methane was accounted for by measuring methane in each sample bottle before and after obtaining aqueous samples. 0.5 ml headspace samples were withdrawn using a 1-ml gas-tight syringe equipped with an on-off push-button valve (Dynatech A-Z; Supelco Inc.; Bellefonte, PA) and manually injected into the GC.

Methane concentrations of unknown samples were determined by comparison with standard methane gas (Scotty Specialty Gases; Bellefonte, PA). The methane standard curve was obtained through use of the following set-up: latex tubing was used to connect a methane gas cylinder to the atmosphere; when the gas cylinder was open, a 100- $\mu$ l gas-tight syringe equipped with an on-off push-button valve (Dynatech A-Z; Supelco Inc.; Bellefonte, PA) was inserted into the tubing, slowly flushed with methane and then filled to the desired volume; the syringe was drawn out and injected onto GC. 0, 5, 10, 25, 50 and 75  $\mu$ l standard methane samples were measured to obtain a linear standard curve (Figure 4.3).

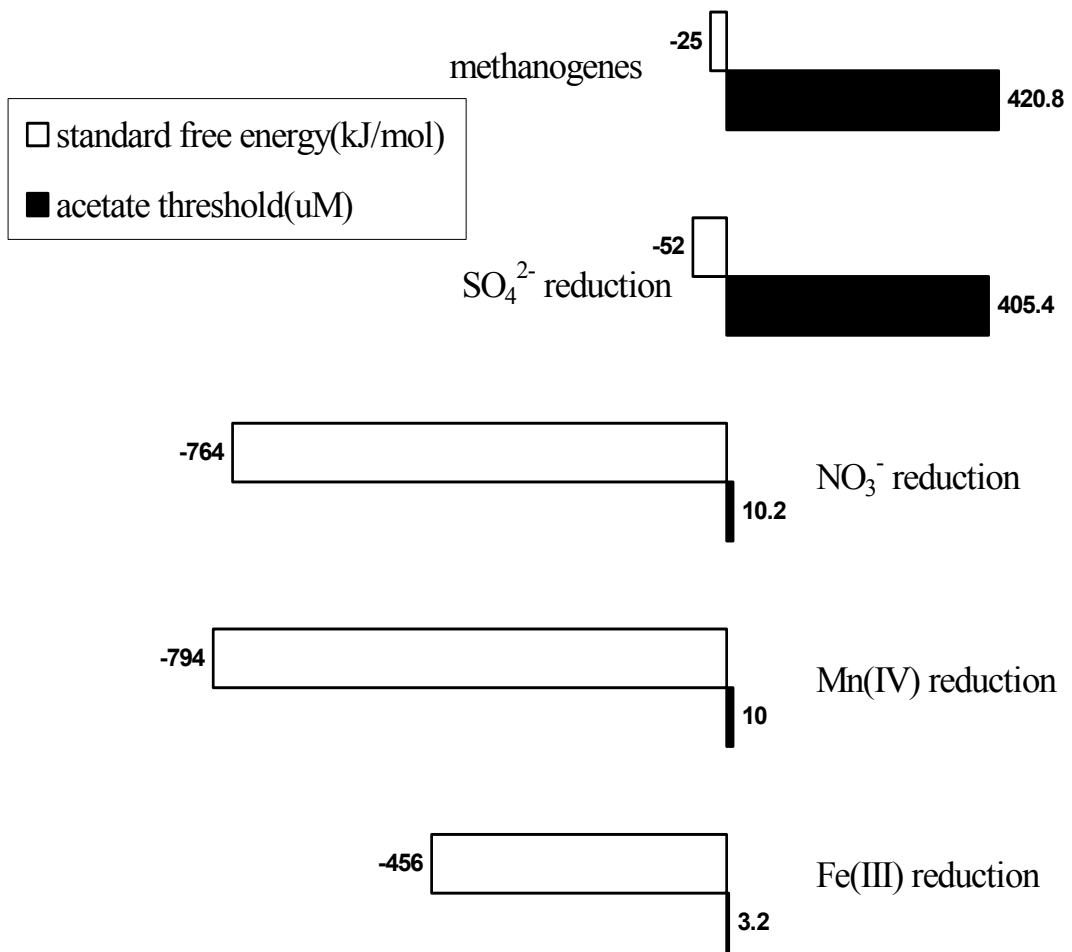


Figure 4.3 A typical standard curve of methane measurement

#### 4.2.4 Measurement of protein

In order to determine the physiological state of the acetate-oxidizing cultures before transfers and during threshold experiments, and compare the results of acetate threshold experiment with modeling predictions, biomass must be measured. Two different approaches to measuring biomass were used in this research. One method involves turbidimetric measurement with a Spectronic 20 spectrophotometer (Bausch&Lomb, Inc.; Rochester, NY). This approach was used to measure the relatively high cell densities that occurred during maintenance of nitrate- and sulfate-reducing cultures. However, in some cases, measurement of biomass using the turbidimetric approach was not possible due to low cell densities (methanogenic cultures) or interference caused by reduced form of the electron acceptors (Fe(III)- and Mn(IV)-reducing cultures). In order to quantify biomass in those cases where meaningful measurements of biomass cannot be obtained using turbidimetric measurements, protein concentrations in the acetate-oxidizing cultures were measured instead. Protein concentration should be directly related to biomass activity because the mineral medium itself contained no protein, except for the medium of *M. barkeri* that contained yeast extract. In this study, protein was measured using the Quanti Pro Bicinchoninic Acid (BCA) Protein Assay Kit (Sigma-Aldrich, Inc.; Saint Louis, MI). The reported protein detection limit using this kit is 0.5 µg/ml. The principle of the BCA protein assay is similar to the Lowry method (Lowry, et al., 1951). Both rely on the formation of a  $\text{Cu}^{2+}$ -protein complex under basic conditions, which is reduced to  $\text{Cu}^+$  by cysteine, cystine, tryptophan, tyrosine, and the peptide bond (Wiechelman et al., 1988). Thus, the concentration of  $\text{Cu}^+$  is proportional to the amount of protein present.  $\text{Cu}^+$  reacts with

BCA to form a purple-blue complex under alkaline conditions, which is quantified spectrophotometrically (Smith et. al., 1985).

To measure cell protein, the cells were first harvested from the cultures with a method adapted from Gälli and McCarty (1989). 500 µl of culture was withdrawn and precipitated with 100 µl of 3.0 M trichloroacetic acid (0.5 M final concentration) in a 2-ml plastic centrifuge tube. The sample was centrifuged at 8000 rpm for 20 min. The supernatant was removed with a Pasteur pipette. 0.5 ml of 0.66 N NaOH was added to the pellet to solubilize the protein over a two-day period at 35°C. This provides the sample for assay with the Quanti Pro BCA kit (QP-BCA), which was carried out as described below.

The required amount of QP-BCA working reagent needed for the protein assay was prepared by mixing together 25 parts of QuantiPro Buffer QA (a solution of sodium carbonate, sodium tartate, and sodium bicarbonate in 0.2 M NaOH, pH 11.25; Sigma-Aldrich Inc.; Saint Louis, MI), 25 parts of Quanti Pro BCA QB (4% (w/v) bicinchoninic acid solution, pH 8.5; Sigma-Aldrich, Inc.; Saint Louis, MI) and 1 part of reagent QC (copper(II) sulfate, Pentahydrate 4% solution; Sigma-Aldrich, Inc.; Saint Louis, MI.) The total volume of QP-BCA working reagent prepared depended upon the number of blanks, standards, and unknown samples to be assayed. The QP-BCA working reagent was mixed with magnetic stir bar until it was a uniform, light green color.

0.4 ml of protein extract obtained from a given sample using the above procedure was transferred to a 7-ml screw-cap polypropylene vial (Wheaton Scientific; Millville, NJ) which contained 0.6 ml of 18-mΩ distilled deionized water to make a 1-ml diluted sample. 1 ml of the QP-BCA reagent was added to 1 ml each of BSA protein standard,

blank (18-m $\Omega$  distilled deionized water), and unknown diluted samples and thoroughly mixed through gentle vortexing. The vials were incubated at 60°C for 1 hour, and then the reaction solutions were transferred to 1-ml disposable plastic cuvettes (Sigma-Aldrich, Inc.; Saint Louis, MO). The absorbance of each solution was measured at 562 nm with a DR/4000 spectrophotometer (Hach Company; Loveland, CO).

The concentration of protein in samples was determined by comparison with standards containing known concentrations of bovine serum albumin (BSA). The BSA protein standards were prepared by diluting a 1 mg/ml BSA protein standard (included in the kit) with 18-m $\Omega$  distilled deionized water to a concentration of 50  $\mu$ g/ml in a 7-ml screw-cap polypropylene vial (Wheaton Scientific; Millville, NJ). The 50  $\mu$ g/ml standard was stored at 4°C for up to a week. 0.5, 5, 10, 20, and 30  $\mu$ g/ml protein standards were made volumetrically by diluting 50  $\mu$ g/ml BSA standard with 18-m $\Omega$  distilled deionized water. Fresh protein standards were prepared every time samples were analyzed. A typical protein standard curve is shown in Figure 4.4.

### **4.3 Threshold experiment**

Threshold experiments were conducted in triplicate. The initial growth conditions used in the threshold experiment are summarized in Table 4.2. The inocula were obtained during the approximately mid-exponential growth phase from batch cultures. The growth curves of *G. metallireducens* cultures growing under Fe(III) and nitrate-reducing conditions were determined by measuring Fe(II) production and turbidity, respectively. The growth of *G. metallireducens* under the Mn(IV)-reducing condition was estimated based on the color change of the medium (from colorless to light green). The growth

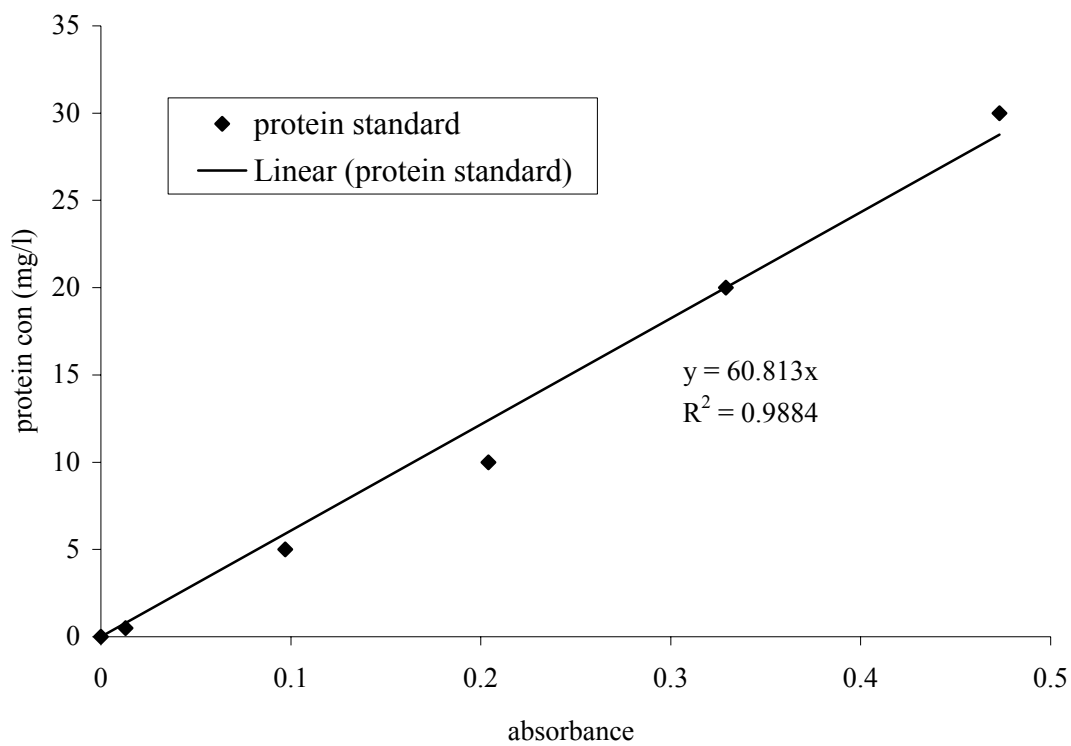


Figure 4.4 A typical standard curve of protein measurement.

Table 4.2 A summary of the initial growth conditions used in the threshold experiments.

Different TEAP or methanogenesis	Initial concentration of electron acceptor (mM)	Initial concentration of Na-acetate (mM)	Organism
Fe(III)-reduction	50 and 80	10	<i>Geobacter metallireducens</i>
MnO <sub>2</sub> -reduction	50	10	
NO <sub>3</sub> <sup>-</sup> -reduction	20	10	
SO <sub>4</sub> <sup>2-</sup> -reduction	20	10	<i>Desulfotomaculum acetoxidans</i>
methanogenesis	N/A	10	<i>Methanosarcina barkeri</i>

curve of *D. acetoxidans* culture growing on sulfate-reduction medium was determined by turbidimetric measurement. The growth curve of *M. barkeri* was determined by measurement of methane production.

To initiate a threshold experiment, 5 ml of a mid-log growth phase suspended culture was transferred to each 160-ml serum bottle containing 45 ml of an appropriate medium and a N<sub>2</sub>:CO<sub>2</sub> (80:20,v/v) headspace. The serum bottles were gently mixed by inverting, and an aqueous sample (2 ml) was withdrawn to a 10-ml glass beaker using a 3-ml syringe so that time zero measurements of acetate, protein, and, in some cases, electron acceptor concentrations could be obtained. According to the time zero measurements of acetate and protein concentrations, the initial ratio of acetate concentration (mg/l) to biomass concentration (mg/l) was more than 20 on a Chemical Oxygen Demand (COD) basis for all cultures. Provision of a large amount of growth substrate to a relatively small amount of biomass ensured that the cultures grew during the threshold experiments, and, thus, the results defined in these experiments reflected the intrinsic growth kinetics of the organisms (Grady et al., 1996). 0.01 to 1 ml sample was transferred from the beaker to a 7-ml screw-cap polypropylene vial (Wheaton Scientific; Millville, NJ) which contained 0.99 to 0-ml of 18-mΩ distilled deionized water to attain a final volume of 1-ml and an appropriate concentration of acetate for analysis using the enzymatic method, as previously described. The amount a sample was diluted for acetate analysis depended on the aqueous acetate concentration and thus varied over the course of each threshold experiment. Specifically, at the beginning of a threshold experiment, 0.01 ml of sample was diluted to 1 ml so that the final concentration was less than 0.1 mM, which was the upper detection limit for acetate measurement using the enzymatic

method as described above. During early to late exponential growth of the acetate oxidizing cultures, 0.02, 0.05, 0.1 or 0.5 ml of sample was diluted to a final volume of 1 ml, reflecting the decreasing acetate concentrations during this period. During stationary growth, when the lowest (threshold) acetate concentrations occurred, 1-ml aqueous samples were not diluted and were analyzed directly for acetate concentrations. 0.5 ml of each culture sample was analyzed for protein concentration measurement. 0.1 ml of the Fe(III)-reducing culture samples was analyzed for the reduced electron acceptor level. 0.5 ml of headspace gas samples of the methanogen culture was analyzed for the production of methane. These analyses were repeated on samples taken at regular intervals, the length of which was determined by the amount of time required for acetate to reach a threshold concentration.

All serum bottles were incubated at 35°C in the dark without shaking. This temperature was selected based on the optimal growth temperature for the cultures used in this study: 30-35°C for *G. metallireducens* (Lovley and Phillips, 1988); 36°C for *D. acetoxidans* (Widdel and Pfennig, 1977); and 37°C for *M. barkeri* (Bryant and Boone, 1987).

Acetate concentrations were monitored until the last two measurements were not significantly different, demonstrating that a threshold concentration had occurred. For *G. metallireducens* under Fe(III)-, Mn(IV)- and Nitrate-reducing conditions, when the thresholds were reached, 0.2 ml of a 40 mM Na-acetate × 3H<sub>2</sub>O solution was reinjected to the serum bottle, resulting in a final acetate of approximately 0.6 mM. After reinjection, the analyses of acetate, protein and reduced electron acceptor concentrations continued until the measurement of acetate concentrations again satisfied the statistical criterion that

the last two measurements were not significant different. The purpose of reinjection was to make sure that electron acceptors were not limiting, and the acetate threshold levels were consistent before and after reinjection of acetate, i.e., that the levels were true thresholds.

## CHAPTER 5

### **A Microbial Respiration Model for Predictions of Substrate Threshold**

In this chapter, a general mathematical model of microbial growth is developed to predict threshold concentrations and evaluate the importance of kinetic and thermodynamic effects in determining substrate thresholds during growth under a wide variety of bacterial models of metabolism.

#### **5.1 Limitation of conventional Monod kinetics**

The empirical Monod equation (Equation (2.1)) is the most commonly used model for describing bacterial growth kinetics (Rittmann and McCarty, 2001). Monod kinetics is useful for predicting the dynamics of batch and continuous cultures during balanced growth under a wide range of conditions. However, Hoh and Cord-Ruwisch (1996) noted that in order for the Michaelis-Menten model of enzyme reaction kinetics, which like the Monod equation is a saturation model, to be applicable, the limiting substrate cannot be self-inhibitory and the concentrations of end products must remain relatively constant. The same restrictions apply to the use of the Monod equation to model microbial growth. However, with respect to this study, it is the prediction of a reaction rate that approaches zero only when the rate-limiting substrate concentration drops to zero that makes the Monod equation unacceptable for the prediction and evaluation of substrate threshold phenomena. Predictions made by the Monod equation conflict with experimental and field observations of the presence of finite amounts of substrate, even though microbial metabolism has ceased (Lovley, 1985; Cord-Ruwisch et

al., 1988; Giraldo-Gomez et al., 1992; Conrad, 1996). In other words, the Monod kinetics incorrectly predicts the reaction rate under very low substrate concentration conditions and is unable to predict threshold phenomena. This shortcoming is likely due, at least in part, to the failure of the Monod equation, like other empirical rate laws, to take into account the fact that as the substrate concentration becomes very low, the amount of energy available in the cellular environment balances the amount of energy that can be conserved as ATP (Jin and Bethke, 2003). At a thermodynamic equilibrium, microbial metabolism ceases because of lack of driving force or Gibbs free energy change. Thus, as previously discussed, in growing cells, the threshold phenomena may reflect a thermodynamic equilibrium between the amount of energy available from respiratory redox reactions and that conserved through ATP production, which is used for microbial metabolism, maintenance, and other cellular needs.

## **5.2 Summary of microbial growth models incorporating thermodynamic and kinetic controls**

Because of the inability of Monod kinetics to predict substrate thresholds, the literature was reviewed to identify microbial growth models that incorporate thermodynamic, as well as kinetic, controls on growth. Several key features of these models are summarized below.

For example, in order to incorporate the effects of end-product inhibition in anaerobic digestion processes, Hoh and Cord-Ruwisch (1996) developed an equilibrium-based Model for a reversible reaction,  $E+S \Leftrightarrow ES \Leftrightarrow E+P$ , in which  $E$ ,  $S$ , and  $P$  are enzyme, substrate, and product concentrations, respectively. This model accounts for

differences in the amount of reaction driving force during the course of a reaction according to:

$$\mu = \frac{\mu_{\max} \cdot S (1 - Q/K_e)}{K + S (1 + Q/K_e)} \quad (5.1)$$

where  $Q$  is the mass-action ratio (actual ratio of [products] over [substrates]), and  $K_e$  is the equilibrium constant (ratio of [products] over [substrates] at dynamic equilibrium).

The thermodynamic term ( $Q/K_e$ ) in Equation (5.1) reflects the free energy change for the reaction according to

$$\Delta G' = RT \ln(Q/K_e) \quad (5.2)$$

where  $\Delta G'$  is Gibbs free energy change of the reaction at pH 7 (kJ/mol),  $R$  is the universal gas constant (0.00834 kJ/mol·K), and  $T$  is the absolute temperature (K). Thus, the dimensionless ratio  $Q/K_e$  ranges from approximately 0 to 1 and measures the displacement of the current reaction from its thermodynamic equilibrium. At the beginning of a reaction,  $Q/K_e$  is close to 0 and  $\Delta G'$  is very negative, which drives the forward reaction at a rapid rate; as the reaction proceeds to thermodynamic equilibrium,  $Q/K_e$  approaches 1, and  $\Delta G'$  approaches 0, and the reaction ceases.

Equation (5.1) can be further rearranged to,

$$\mu = \frac{\mu_{\max} \cdot (S - P / K_e)}{K + (S + P / K_e)} \quad (5.3)$$

where  $P$  is the product of  $S$  and  $Q$ . In this form, the model suggests the reaction will cease when  $S$  equals a threshold concentration of  $P / K_e$  results and complete consumption of the substrate will not necessarily occur when the metabolism ceases.

According to the equilibrium-based model, the rate-limiting substrate reaches a threshold value when the free energy change of the reaction  $\Delta G'$  is equal to zero. However, later studies pointed out that substrates reach thresholds before  $\Delta G'$  approaches zero.

Kleerebezem and Stams (2000) modified the equilibrium-based model of Hoh and Cord-Ruwisch (1996) to account for the consumption of a portion of the free energy change of a catabolic reaction for ATP synthesis and cellular growth. Rearranging Equation (5.2) and (5.3) and replacing  $\Delta G'$  with the driving force ( $\Delta G_{DF}$ , kJ/mol) yields,

$$\mu = \frac{\mu_{\max} S (1 - \exp(\Delta G_{DF} / RT))}{K + S (1 - \exp(\Delta G_{DF} / RT))} \quad (5.4)$$

$\Delta G_{DF}$  accounts for the effects of the energy demands of cell synthesis and maintenance on the reaction driving force according to:

$$\Delta G_{DF} = \Delta G'_{CAT} - \Delta G_{\mu/m} \quad (5.5)$$

where  $\Delta G'_{CAT}$  is the Gibbs free energy change of the catabolic reaction (kJ/mol) and is equivalent to  $\Delta G'$  in Hoh and Cord-Ruwisch's model (1996), and  $\Delta G_{\mu/m}$  is the energy needed for cellular growth and maintenance purposes. According to this model, when  $\Delta G'_{CAT}$  approaches  $\Delta G_{\mu/m}$ , the reaction ceases, and the substrate reaches a threshold concentration.

Fennell and Gossett (1998) developed a model of production of, and competition for, hydrogen in a dechlorinating culture. Their model includes an expression for the specific growth rate constant for electron donor fermentation that is similar to Equation (5.4), except that the thermodynamic term in the denominator is excluded

$$\mu = \frac{\mu_{\max} S \left[ 1 - \exp\left(\frac{\Delta G' - \Delta G_{critical}}{RT}\right) \right]}{K + S} \quad (5.6)$$

Here,  $\Delta G_{critical}$  (kJ/mol) is “the marginally negative free energy that the organisms must have available to live and grow”. The  $\Delta G_{critical}$  value was determined experimentally for the fermentation of butyrate ethanol, lactate, and propionate by the dechlorinating culture and was found to be approximately equal to  $-19$  kJ/mol electron donor in each case (Fennell and Gossett, 1998).

Similarly, a kinetic model of the bacterial reduction of goethite with a thermodynamic term similar to the one in Fennell and Gossett's model described above was developed by Liu et al. (2001a):

$$\mu = \frac{\mu_{\max} S}{K + S} \left[ 1 - \exp\left(\frac{\Delta G_r - \Delta G_{\min}}{RT}\right) \right] \quad (5.7)$$

Here  $\Delta G_{\min}$  is the minimum energy required to drive ATP synthesis and was experimentally determined to be equal to  $-22.7$  kJ/mol lactate for oxidation of variable concentrations of lactate coupled to the reduction of FeOOH provided at a range of concentrations.

Finally, Noguera et al. (1998) developed a model of hydrogen and electron flow during growth of *Desulforibro vulgans* using different metabolic modes. Their model incorporated thermodynamic regulation of fermentative growth on lactate and respiration growth on sulfate plus hydrogen or lactate, by recognizing that energy reactions will only take place if:

$$\frac{Q}{\alpha K} < 1 \quad (5.8)$$

where  $Q$  is the reaction quotient (the ratio of product and reactant activities, with each product and reactant activity raised to its stoichiometric coefficient),  $K$  is the reaction equilibrium constant, and  $\alpha$  is a threshold factor defined as:

$$\alpha = \exp\left(\frac{\Delta G_{\min}}{RT}\right) \quad (5.9)$$

where  $\Delta G_{\min}$  is a minimum amount of useful energy that cells can derive from catabolic

reactions and prevents electron flow through a biochemical pathway from reaching thermodynamic equilibrium. Thus, it was assumed that a reaction would not take place for  $\frac{Q}{\alpha K} \geq 1$ . For  $\frac{Q}{\alpha K} < 1$ , the factor  $1 - \frac{Q}{\alpha K}$  was included in rate expressions to represent the decrease in reaction rate that occurs when the free energy change of a reaction approaches  $\Delta G_{\min}$  ( $\frac{Q}{\alpha K} \rightarrow 1$ ). Similarly, when the reaction free energy change is large ( $Q \ll \alpha K$ ),  $1 - \frac{Q}{\alpha K}$  approaches unity and the reaction rate is affected only by kinetics, not thermodynamics.

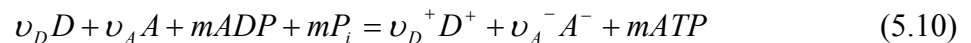
In summary, a term containing a  $\frac{Q}{K}$  and/or  $\Delta G_{\min}$  (or  $\Delta G_{critical}$ ) factor was incorporated in several kinetic models to reflect thermodynamic controls on microbial growth. However, these models have several limitations that make them difficult to apply in this research. First, in some of these models, the minimum free energy required to sustain metabolism ( $\Delta G_{\min}$ ) is assumed to be fixed and reflect the energy associated with translocation of one  $H^+$  across the cell membrane for the synthesis of 1/3 ATP (Liu et al, 2001b). However, variable  $H^+$ /ATP stoichiometries have been reported for bacteria (Kleerebezem and Stams, 2000) and Jackson and McInerney (2002) demonstrated that  $\Delta G_{\min}$  is variable and depends on microbial physiology. Second, the models described above were developed for the description of specific physiologic systems (i.e., geothite-reduction, dehalogenation, fermentation and/or sulfate-reduction). In this study, a variety of systems in which the oxidation of acetate is coupled to various terminal electron-accepting processes must be described. The systems that have to be modeled have in common that they are anaerobic respiratory processes ( $NO_3^-$ , Fe(III)-, Mn(IV)-,  $SO_4^{2-}$ -

reduction ) or at least have a chemiosmotic component (CO<sub>2</sub>). A new model that can be used to describe respiratory processes in general was recently reported by Jin and Bethke (2003). It incorporates both kinetics and thermodynamic controls on growth. Because of its flexibility and inclusion of a thermodynamic term, it was used in this research to test the hypothesis that in complex anaerobic systems, characteristic ranges of acetate concentrations may be associated with different TEAPs.

### **5.3 Description of a new kinetically and thermodynamically consistent rate model for microbial respiration**

In order to reflect the thermodynamic and kinetic controls on microbial growth, the new rate model developed by Jin and Bethke (2003) consists of three key components: 1) a thermodynamic factor; 2) a kinetic factors for an electron donor; 3) a kinetic factor for an electron acceptor. These components and their derivation are briefly described below.

Based on chemiosmotic theory (Mitchell, 1961), microbial respiration involves the transfer of electron from an electron donor to an electron acceptor that is associated with the translocation of protons across the cell membrane in order to synthesize ATP from ADP and phosphate P<sub>i</sub>. Combining the redox reaction and ATP synthesis gives,



where  $D$  is the concentration of electron donor and carbon source [M L<sup>-3</sup>];  $A$  is the concentration of electron acceptor [M L<sup>-3</sup>];  $D^+$  and  $A^-$  are the oxidized and reduced

forms of  $D$  and  $A$ , respectively;  $\nu_D$ ,  $\nu_D^+$ ,  $\nu_A$  and  $\nu_A^-$  are reaction coefficients; and  $m$  is the number of ATP molecules synthesized per  $\nu_D$  moles of  $D$  oxidized.

The net thermodynamic driving force,  $f$ , for the above overall reaction is given as

$$f = -\Delta G - m\Delta G_p \quad (5.11)$$

Here,  $\Delta G$  is the free energy change of the redox reaction (kJ/mol); and  $\Delta G_p$  is the free energy change associated with synthesis of one mole of ATP (kJ/mol). The value of  $\Delta G_p$  is assumed to be 50 kJ/mol, which is appropriate under typical physiological conditions (White, 1995).

The value of  $\Delta G$  can be calculated according to

$$\Delta G = \Delta G^0 + RT \ln \frac{[D^+]^{\nu_{D^+}} [A^-]^{\nu_{A^-}}}{[D]^{\nu_D} [A]^{\nu_A}} \quad (5.12)$$

where  $\Delta G^0$  is the standard Gibbs free energy change.

The thermodynamic factor  $F_T$  is expressed as

$$F_T = 1 - \exp\left(-\frac{f}{\chi RT}\right) = 1 - \exp\left(\frac{\Delta G + m\Delta G_p}{\chi RT}\right) \quad (5.13)$$

Here  $\chi$  is the average stoichiometric number, which is defined as “the ratio of the free

energy change of the overall reaction to the sum of the free energy change for each elementary step” (Jin and Bethke, 2002). Essentially,  $\chi$  reflects the number of times the rate-determining steps occurs during respiration (Equation (5.11)). For a forward respiratory process, the thermodynamic factor ( $F_T$ ) ranges from 0 to 1. When the driving force  $f$  drops to zero,  $F_T$  is equal to 0, which means that the microbial reaction ceases. Consequently, the limiting substrate will reach its threshold level.

The unitless kinetic factors for electron donor and acceptor,  $F_D$  and  $F_A$ , respectively, which reflect the effects of the concentrations of substrates and end product on the reaction rate, are given by

$$F_D = \frac{[D]^{\beta_D}}{[D]^{\beta_D} + K_D[D^+]^{\beta_{D^+}}} \quad (5.14)$$

and

$$F_A = \frac{[A]^{\beta_A}}{[A]^{\beta_A} + K_A[A^-]^{\beta_{A^-}}} \quad (5.15)$$

respectively, where  $\beta_D$ ,  $\beta_{D^+}$ ,  $\beta_A$ , and  $\beta_{A^-}$  are unitless exponents whose values are determined by “details of the mechanism of electron transport” and are assumed to be equal to unity (Jin and Bethke, 2003); and  $K_D$  and  $K_A$  are constants that represent “the standard free energy changes of the electron-donating and –accepting reactions” (Jin and Bethke, 2003). The units of  $K_D$  and  $K_A$  depend on the number of oxidized or reduced

products of the electron donor and acceptor that appear in the rate law for a given respiration process. The values of  $F_D$  and  $F_A$  vary from almost 0 to 1. When substrates are abundant and the concentrations of end products are low,  $F_D$  and  $F_A$  approach to 1, which means that substrates are “saturating” and do not limit the intrinsic growth rate. When substrates are very low and end products accumulate to a significant level,  $F_D$  and  $F_A$  are close to zero, and the microbial reaction rate becomes kinetically inhibited by the substrate concentrations and accumulation of end products. It should be noted that  $F_D$  and  $F_A$  cannot reach zero because of the thermodynamic control on  $[D]$  and  $[A]$  by  $F_T$ .

Under certain conditions, the kinetic factors  $F_D$  and  $F_A$  can be reduced to conventional Monod kinetic terms. An example of these conditions is when the concentrations of redox reaction end products, i.e., the oxidized forms of electron donor and reduced forms of electron acceptors, can be taken as constant, e.g., because they are insoluble, volatile or controlled by pH buffers. They can then be combined with  $K_D$  and  $K_A$  in Equation (5.14) and (5.15) to form the lumped parameters  $K'_D$  and  $K'_A$ , respectively. In this case, the kinetic factors  $F_D$  and  $F_A$  can be written in the format of conventional Monod kinetic terms and  $K'_D$  and  $K'_A$  are equivalent to Monod half-saturation constants.

Given sufficient energy, high substrate and low end product concentrations and other optimum conditions, the microbial reaction rate will reach the maximum intrinsic rate ( $v_{\max}$ ;  $\text{M L}^{-3} \text{T}^{-1}$ ), which is given by

$$v_{\max} = k[X] \quad (5.16)$$

where  $k$  is the intrinsic rate constant ( $T^{-1}$ ). However, in most cases, the reaction rate is unlikely to reach the maximum because of substrate limitations and the accumulation of end products. This can be reflected by incorporating the thermodynamic and kinetic factors described above into the intrinsic reaction rate Equation (5.16) to create a general rate law that is the product of the intrinsic reaction rate, the thermodynamic factor and the two kinetic factors,

$$v = k[X]F_T F_D F_A \quad (5.17)$$

Here  $v$  is the reaction rate ( $M L^{-3} T^{-1}$ ).

This new model of microbial respiration processes is fully general because it accounts for both kinetic and thermodynamic effects on microbial growth. The new rate model developed by Jin and Bethke shares some common features with the models described above. For example, all of the models incorporate a thermodynamic factor into the Monod or analogous kinetic models to reflect the role of thermodynamics in controlling the reaction rate, which is useful for predicting threshold phenomena in growing cultures. However, the new rate model differs from the previous ones in that it introduces a variable value term  $m\Delta G_p$  as an energy barrier in the thermodynamic factor, in place of fixed value terms such as  $\Delta G_{\min}$  or  $\Delta G_{critical}$  used in the other models. The value of the term  $m\Delta G_p$  depends on  $m$ , which is determined by the terminal electron-accepting process and other aspects of an organism's physiology (Van Spanning et al., 1995). The variability allowed by  $m\Delta G_p$  in the thermodynamic factor is in agreement with experimental observations that the amount of free energy remaining when bacterial

metabolism ceases was highly variable and depended on the substrate activation steps, as well as the terminal electron-accepting condition (Jackson and McInerney, 2002). Furthermore, the new rate model accounts for the inhibition effect of the buildup of end products on the reaction rate in the kinetic terms.

#### **5.4 Application of the new rate model to predict and interpret acetate thresholds under various TEA conditions**

In this research, acetate was used as the electron donor by pure anaerobic cultures under the following electron-accepting conditions:  $\text{NO}_3^-$ , Fe(III)-, Mn(IV)-, and  $\text{SO}_4^{2-}$  - reducing and methanogenesis. The acetate thresholds under different terminal electron-accepting conditions were compared to test the hypothesis. Simulation of these experiments using the previously-described respiration rate model can be used in a predictive manner to facilitate the design of successful experiments and interpret the experimental results at a mechanistic level. For example, experimental simulations made it possible to estimate the amount of time required before an acetate threshold would be reached, and thus, appropriate sampling schedules could be planned. Further, the predictions of substrate, product, and biomass concentrations were useful for refining the analytical methods used to quantify the levels of these species during the experiments. For example, information obtained from preliminary simulations was used to select analytical methods that had appropriate concentration ranges and to estimate sample dilution requirements. As mentioned above, after the threshold experiment data have been obtained, the respiration rate model can be used in a descriptive manner to interpret the experimental results. Specifically, the model can be used to evaluate the relative

importance of kinetics and thermodynamics in determining acetate concentrations, especially at the threshold level.

### **5.5 Determination of respiration rate law expressions for acetate oxidation under various TEA conditions**

In order to apply the respiration rate model to the prediction and determination of acetate oxidation in the study, appropriate rate law expressions for each TEA condition were needed. Development of these rate law expressions is described below.

The first step in obtaining a rate law expression is to write the overall reaction for acetate oxidation coupled to reduction of the TEA and synthesis of ATP (Equation (5.10)).

In order to write the balanced redox/ATP synthesis reactions, an estimate of  $m$  is needed for each TEA condition evaluated. In general, detailed information on the biochemistry and physiology of acetate oxidation and electron transport in the organisms studied (*Geobacter metallireducens*, *Desulfotomaculum acetoxidans*, and *Methanosarcina barkeri*) is not available in the literature. This made obtaining good estimates of  $m$  (and  $\chi$ ) challenging. The rationale used to estimate  $m$  and  $\chi$  values for each of the experimental systems is outlined below.

As suggested above, the electron transport system(s) used by *G. metallireducens* for growth using Fe(III), Mn(IV), or  $\text{NO}_3^-$  as an electron acceptor has not been thoroughly characterized. However, Champine et al. (2000) predicted that the theoretical energy yield for *G. metallireducens* growing on acetate plus ferric iron would be in the range of 0.3 to 0.6 mol ATP per mole acetate oxidized. This estimate was based on a

comparison of cellular yields of *G. metallireducens* and the Gram-negative organism *Desulfuromonas acetoxidans* during growth on acetate. Therefore, the average value in this range (0.45 mol ATP per mole acetate) was assumed for Fe(III)-reducing conditions. Because the free energy changes for acetate oxidation coupled to the reduction of Fe(III) or Mn(IV) are similar, it is unlikely that the ATP yield for *G. metallireducens* growing on Mn(IV) will be significantly different compared to growth of this strain on Fe(III). Therefore, an  $m$  of 0.45 mol ATP per mole acetate oxidized was also assumed for the Mn(IV)-reducing condition.

An upper bound for  $m$  during growth of *G. metallireducens* on nitrate (via dissimilatory nitrite ammonification) was determined based on the electrochemical potential ( $\Delta p$ ) created across the cell membrane during this mode of respiration. According to Simon et al. (2000),  $\Delta p$  during growth of *Wolinella succinogenes* via dissimilatory nitrite ammonification was  $\sim 0.17\text{V}$ . The maximum number of protons translocated per electron transferred,  $(n_{\text{H}^+}/n_e)_{\text{max}}$ , can be calculated according to (Simon, 2002):

$$(n_{\text{H}^+}/n_e)_{\text{max}} = \Delta E_o' / \Delta p \quad (5.18)$$

where  $\Delta E_o'$  is the standard redox potential change (pH=7) for the redox reaction.  $\Delta E_o' = 0.63\text{ V}$  for oxidation of acetate coupled to reduction of nitrite to ammonia). The theoretical maximum ratio of ATP synthesized per electron transferred  $(n_{\text{ATP}}/n_e)_{\text{max}}$  is found according to:

$$(n_{\text{ATP}}/n_e)_{\text{max}} = \Delta E_o' \cdot F / \Delta G_p \quad (5.19)$$

Thus,  $(n_{\text{ATP}}/n_e)_{\text{max}}$  is approximately 1.22 mol ATP per e- transferred. Reduction of nitrite to ammonia is a 6 e- reduction and thus could theoretically result in an ATP yield of over 7 ATP per mol nitrite reduced (or mol acetate oxidized). However, this is a maximum value and does not take into account any costs associated with transporting nitrate across the cell membrane or other respiratory processes. Further, the energy yield from dissimilatory ammonification (even beginning at the level of nitrate) is lower than that Fe(III)- or Mn(IV)-reduction. For example,  $\Delta G^{\circ}$  for acetate oxidation coupled to the reduction of nitrate to ammonium is  $-506.2$  kJ/mol acetate, compared to  $-821.71$  kJ/mol acetate for acetate oxidation coupled to Fe(III) reduction. Therefore, it is more likely that the ATP yield for the nitrate-reducing condition is similar to, or less than, the ATP yield for Fe(III) reduction, and  $m$  is assumed to be 0.45 mol ATP per mol acetate oxidized for nitrate reduction.

A different approach was used to estimate  $m$  for acetotrophic sulfate reduction. In this case, the number of ATPs that are consumed in acetate oxidation and sulfate reduction were compared to the number of ATPs that could be generated via substrate level and electron transport phosphorylation. *Desulfotomaculum acetoxidans* oxidizes acetate via the carbon monoxide dehydrogenase or reverse acetyl-CoA pathway (Thauer et al., 1989). The first step in this reaction consumes one ATP in the activation of acetate to acetyl phosphate, and only one ATP is produced through substrate level phosphorylation. Therefore, there is no net ATP synthesis due to substrate level phosphorylation. The dissimilatory reduction of sulfate occurs intracellularly after it is

activated to adenosine-phosphosulfate (APS), which consumes the equivalent of 2 ATP (Hansen, 1994). The number of ATP that could potentially be synthesized via electron transport phosphorylation was calculated as follows: The number of  $H^+$  translocated per  $e^-$  transferred by NADH dehydrogenase in sulfate-reducing is expected to be  $2H^+/2e^-$ , at best. If it is assumed that synthesis of 1 mol ATP is coupled to the ingress of  $3H^+$  across the cellular membrane, then, at most, 2.67 mol ATP per mol acetate converted to  $CO_2$  in an  $8e^-$  oxidation can be synthesized. This would result in a maximum yield of 0.67 mol ATP. Allowing for some inefficiencies, an  $m$  value of 0.33 mol ATP per mol acetate oxidized was assumed for the sulfate-reducing condition. This value is similar to the ATP yields reported for sulfate reduction involving other electron donors (Thauer et al., 1989).

Regarding  $m$  for aceticlastic methanogenesis, Thauer et al. (1989) noted that the growth yield of *Methanosarcina barkeri* is low (2 g/mol  $Ac^-$ ) due to the small free energy change associated with the aceticlastic reaction, which they suggested is at most sufficient to drive synthesis of 0.5 mol ATP. Therefore, an  $m$  value of 0.33 mol ATP per mol acetate oxidized was also assumed for the methanogenic condition.

In order to calculate the thermodynamic factor,  $F_T$ , in the respiration rate model, an estimate of  $\chi$  is needed, in addition to  $m$ . The value of  $\chi$  depends on the number of times the respiration rate-determining step occurs, which, in many electron transport chains frequently involves proton translocation across a redox enzyme (Jin and Bethke, 2003). However, one case in which proton translocation is not the rate-limiting step is when the electron acceptor is reduced extracellularly. In this case, the passage of electrons to the extracellular electron acceptor may be rate-limiting. Solid phase electron acceptors such as  $MnO_2$  are clearly extracellular. However, ferric citrate was also

assumed to be external to the outer membrane during growth of *G. metallireducens* via Fe(III) reduction (Champine et al., 2000). Therefore, for both Fe(III) and Mn(IV) reduction, transfer of electrons to the terminal electron acceptor was assumed to be the rate-limiting step. Reduction of Mn(IV) and Fe(III) is presumably mediated by a terminal oxidase that receives electrons in one electron transfers from a cytochrome such as cytochrome  $c_7$ . Thus, transfer of electrons derived from acetate presumably occurs eight times, or  $\chi = 8/\text{mol acetate}$  for Fe(III)- and Mn(IV)-reduction.

A value of 8/mol acetate was also assumed for  $\chi$  for growth of *G. metallireducens* on nitrate. In this case, proton translocation was assumed to be the rate-limiting step, rather than transfer of electrons to an external electron acceptor. Simon (2002) noted that other  $\delta$ -*Proteobacteria* that mediate dissimilatory nitrite reduction exhibit a  $\text{H}^+/\text{e}^-$  ratio of one, and all organisms that carry out this form of metabolism probably possess menaquinones. In addition, he noted that proton translocation by menaquinones at a  $1\text{H}^+/\text{e}^-$  ratio is probably important in the reduction of nitrate by *G. metallireducens*. Therefore, it was assumed the proton translocation by menaquinone is the rate-limiting step during respiratory growth of *G. metallireducens* on nitrate. Because oxidation of acetate releases eight electrons, this translates into  $\chi=8/\text{mol acetate}$ .

Jin and Bethke (2003) noted that if transport of electron donors or acceptors across the cell membrane is required for respiration, the transport step may be rate-limiting, especially if considerable amounts of energy have to be expended to facilitate this transport. The terminal reductases involved in sulfate reduction are cytoplasmic; therefore, transport of sulfate across the cell membrane is required in dissimilatory sulfate reduction and, in this study, is assumed to be the rate-limiting step. Sulfate and acetate

are consumed in this respiratory process in equimolar amounts; therefore  $\chi=1/\text{mol}$  acetate. It should be noted that when sulfate is available at mM concentrations, it is symported across the membrane with 2 H<sup>+</sup> (Hansen, 1994); however, this does not result in a net energy requirement because the sulfide generated from sulfate reduction can potentially leave the cell with 2H<sup>+</sup> (as H<sub>2</sub>S). On the other hand, activation of sulfate to APS requires a significant energy investment. If activation of sulfate is rate-limiting, a  $\chi$  value of unity would again result. If proton translocation, rather than sulfate transport or activation, were rate-limiting,  $\chi$  would probably equal 8/mol acetate because, based on studies conducted with *Desulfovibrio* strains, proton translocation during dissimilatory sulfate reduction probably is mediated by NADH dehydrogenase at a maximum expected ratio of 2H<sup>+</sup>/2e<sup>-</sup>. However, as noted above, for the purposes of this study,  $\chi$  is assumed to be unity for the sulfate-reducing condition.

Finally, a  $\chi$  value for acetate fermentation is needed. A reduced ferredoxin:heterodisulfide oxidoreductase system is involved in electron transport in the final step of acetate fermentation by *Methanosarcina* strains (Deppenmeier, 2002). Proton translocation by the heterodisulfide reductase has been confirmed. Proton translocation in this electron transport chain by a type of NiFe hydrogenase known as an Ech hydrogenase is also likely but has not been confirmed. In either case, the stoichiometry of the electron transport chain cannot exceed 2H<sup>+</sup>/2e<sup>-</sup>. Thus, in this study, it is assumed that proton translocation by either enzyme system is rate-limiting and  $\chi=8/\text{mol}$  acetate transformed via acetate fermentation.

In order to develop a general rate law (Equation (5.17)), in addition to  $m$  and  $\chi$  values, balanced redox reactions must be written for the oxidation of acetate coupled to

the reduction of the appropriate electron acceptors. The balanced redox reactions are presented in Table 5.1, along with the electron donor (D), oxidized electron donor ( $D^+$ ), electron acceptor (A), and reduced electron acceptor ( $A^-$ ), for each TEA condition.

As shown in Equations 5.12 and 5.13, development of the general rate law also requires that the standard free energy change ( $\Delta G^\circ$ ) be calculated for each of the overall reactions in Table 5.1. As previously discussed, the acetate threshold experiments were conducted at 35°C. Thus, standard free-energy of formation values ( $\Delta G^\circ_{f25^\circ}$ ), which are used to calculate  $\Delta G^\circ$  values, must be calculated for 35°C. This can be done using the van't Hoff equation:

$$\ln\left(\frac{K_{25}}{K_{35}}\right) = \left[\frac{\Delta H^\circ_{f25^\circ}}{R}\right] \left(\frac{1}{T_{25}} - \frac{1}{T_{35}}\right) \quad (5.20)$$

where  $K_{25}$  and  $K_{35}$  are the equilibrium constants at 25°C and 35°C, respectively;  $\Delta H^\circ_{f25^\circ}$  is the standard enthalpy of formation;  $T_{25}$  is 298.15 K; and  $T_{35}$  is 308.15 K.  $K_{25}$  was calculated for each chemical species from  $\Delta G^\circ_f$  according to:

$$\Delta G^\circ_{f25^\circ} = -RT \ln K_{25} = \exp\left[\frac{-\Delta G^\circ_{f25^\circ}}{RT}\right] \quad (5.21)$$

$K_{35}$  values were obtained by rearranging Equation 5.20, and  $\Delta G^\circ_{f35^\circ}$  values were obtained by substituting  $\Delta G^\circ_{f35^\circ}$  and  $K_{35}$  for  $\Delta G^\circ_{f25^\circ}$  and  $K_{25}$ , respectively, in Equation 5.21. The calculated  $\Delta G^\circ_{f35^\circ}$  values are summarized in Table 5.2 along with the  $\Delta G^\circ_{f25^\circ}$  and  $\Delta H^\circ_{f25^\circ}$

Table 5.1 Overall redox reactions for acetate oxidation coupled to the reduction of various terminal electron acceptors.

TEAP	D	D <sup>+</sup>	A	A <sup>-</sup>	Overall Reaction
Fe(III)-reduction	CH <sub>3</sub> COO <sup>-</sup>	HCO <sub>3</sub> <sup>-</sup>	Fe(III)	Fe(II)	CH <sub>3</sub> COO <sup>-</sup> + 8Fe <sup>3+</sup> + 4H <sub>2</sub> O = 2HCO <sub>3</sub> <sup>-</sup> + Fe <sup>2+</sup> + 9H <sup>+</sup>
Mn(IV)-reduction	CH <sub>3</sub> COO <sup>-</sup>	HCO <sub>3</sub> <sup>-</sup>	Mn(IV)	Mn(II)	CH <sub>3</sub> COO <sup>-</sup> + 4MnO <sub>2</sub> + 7H <sup>+</sup> = 4Mn <sup>2+</sup> + 2HCO <sub>3</sub> <sup>-</sup> + 4H <sub>2</sub> O
Nitrate-reduction	CH <sub>3</sub> COO <sup>-</sup>	HCO <sub>3</sub> <sup>-</sup>	NO <sub>3</sub> <sup>-</sup>	NH <sub>4</sub> <sup>+</sup>	CH <sub>3</sub> COO <sup>-</sup> + NO <sub>3</sub> <sup>-</sup> + H <sup>+</sup> + H <sub>2</sub> O = NH <sub>4</sub> <sup>+</sup> + 2HCO <sub>3</sub> <sup>-</sup>
Sulfate-reduction	CH <sub>3</sub> COO <sup>-</sup>	HCO <sub>3</sub> <sup>-</sup>	SO <sub>4</sub> <sup>2-</sup>	HS <sup>-</sup>	CH <sub>3</sub> COO <sup>-</sup> + SO <sub>4</sub> <sup>2-</sup> = 2HCO <sub>3</sub> <sup>-</sup> + HS <sup>-</sup>
Methanogenesis	CH <sub>3</sub> COO <sup>-</sup>	HCO <sub>3</sub> <sup>-</sup>	Acetate	CH <sub>4</sub>	CH <sub>3</sub> COO <sup>-</sup> + H <sub>2</sub> O = HCO <sub>3</sub> <sup>-</sup> + CH <sub>4</sub>

Table 5.2 Thermodynamic values for respiration rate law species.

Compound	$\Delta G^\circ_f$ at 25°C (kJ/mol) <sup>1</sup>	$\Delta H^\circ_f$ at 25°C (kJ/mol) <sup>1</sup>	$\Delta G^\circ_f$ at 35°C (kJ/mol)
Fe(II)	-85.0	-21.0	-84.9
Fe(III)	-10.5	-11.4	-9.3
MnO <sub>2</sub>	-465.0	-124.2	-463.1
Mn(II)	-227.7	-53.3	-227.8
NO <sub>3</sub> <sup>-</sup>	-110.6	-49.4	-107.4
NH <sub>4</sub> <sup>+</sup>	-79.5	-31.7	-77.7
SO <sub>4</sub> <sup>2-</sup>	-742.2	-216.9	-735.6
HS <sup>-</sup>	12.6	-4.2	13.6
ATP	-2098.0 <sup>2</sup>	-2992.9 <sup>2</sup>	-2068.0
ADP	-1234.4 <sup>2</sup>	-2001.9 <sup>2</sup>	-1208.6
P <sub>i</sub>	-1058.6 <sup>2</sup>	-1301.2 <sup>2</sup>	-1050.4

<sup>1</sup>From Snoeyink and Jenkins, 1980, unless noted.

<sup>2</sup>From Alberty, 1998.

values used to determine them. In addition, the following  $\Delta G^\circ_{p35^\circ}$  values (kJ/mol) were obtained directly from Fennell (1998 ): acetate (aq), -373.2;  $H^+$  (aq), 0;  $HCO_3^-$  (aq), -583.3; and  $H_2O$  (l), -235.6.

Similarly  $\Delta G_p$ , the free energy change of the reaction of ATP synthesis from ADP and  $P_i$ , which is 50 kJ/mol at normal physiological conditions, had to be corrected for 35°C. Using the same approach outlined above and the  $\Delta G^\circ_{p25^\circ}$  and  $\Delta H^\circ_{p25^\circ}$  values for ATP, ADP, and  $P_i$  (Table 5.2),  $\Delta G_{p35}$  was found to be 41.3 kJ/mol.

Expressions for  $F_D$ ,  $F_A$ , and  $F_T$  for each TEA condition were determined from the information presented in Tables 5.1 and 5.2. In each case,  $F_D$  is equal to:

$$F_D = \frac{[CH_3COO^-]}{[CH_3COO^-] + K_D[HCO_3^-]} \quad (5.22)$$

The  $F_A$  and  $F_T$  terms are summarized in Table 5.3. Simulation of the three kinetic or thermodynamic terms is discussed in the following chapter.

To perform simulations using the respiration rate model, estimates of  $k$ ,  $K_D$ , and  $K_A$  are also needed. These values were obtained by fitting equation 5.17 to experimental data using a MATLAB fitting routine which applied the nonlinear least square algorithm *lsqnonlin* (MATLAB, version 6.1, The Mathworks, Inc). For biomass simulation, the true yield constant,  $Y$ , is needed to calculate the production of biomass according to:

$$dX/dt = Yv \quad (5.23)$$

Table 5.3  $F_D$ ,  $F_A$ , and  $F_T$  expressions for each TEA condition.

TEAP or methanogenesis	$F_D$	$F_A$	$F_T$
Fe(III)-reduction	$\frac{[CH_3COO^-]}{[CH_3COO^-] + K_D[HCO_3^-]}$	$\frac{[Fe^{3+}]}{[Fe^{3+}] + K_A[Fe^{2+}]}$	$1 - e^{\left( \frac{-455.6 + RT \ln \left( \frac{[HCO_3^-] [Fe^{2+}] [H^+]^p}{[CH_3COO^-] [Fe^{3+}]^p} \right) + 0.45 \Delta G_{P35}}{8RT} \right)}$
Mn(IV)-reduction	$\frac{[CH_3COO^-]}{[CH_3COO^-] + K_D[HCO_3^-]}$	$\frac{[MnO_2]}{[MnO_2] + K_A[Mn^{2+}]}$	$1 - e^{\left( \frac{-794.4 + RT \ln \left( \frac{[HCO_3^-] [Mn^{2+}]^4}{[CH_3COO^-] [MnO_2] [H^+]^7} \right) + 0.45 \Delta G_{P35}}{4RT} \right)}$
Nitrate-reduction	$\frac{[CH_3COO^-]}{[CH_3COO^-] + K_D[HCO_3^-]}$	$\frac{[NO_3^-]}{[NO_3^-] + K_A[NH_4^+]}$	$1 - e^{\left( \frac{-763.7 + RT \ln \left( \frac{[NH_4^+] [HCO_3^-]^2}{[CH_3COO^-] [NO_3^-] [H^+]} \right) + 0.45 \Delta G_{P35}}{8RT} \right)}$
Sulfate-reduction	$\frac{[CH_3COO^-]}{[CH_3COO^-] + K_D[HCO_3^-]}$	$\frac{[SO_4^{2-}]}{[SO_4^{2-}] + K_A[HS^-]}$	$1 - e^{\left( \frac{-43.2 + RT \ln \left( \frac{[HS^-] [HCO_3^-]^2}{[CH_3COO^-] [SO_4^{2-}]} \right) + 0.33 \Delta G_{P35}}{RT} \right)}$
Methanogenesis	$\frac{[CH_3COO^-]}{[CH_3COO^-] + K_D[HCO_3^-]}$	$\frac{[CH_3COO]}{[CH_3COO] + K_A[HCO_3^-]}$	$1 - e^{\left( \frac{-24.3 + RT \ln \left( \frac{[HCO_3^-] [CH_4]}{[CH_3COO]} \right) + 0.33 \Delta G_{P35}}{8RT} \right)}$

$Y$  was determined experimentally based on the changes in protein and acetate concentrations measured during the course of the acetate threshold experiments.

## CHAPTER 6

### Results and Discussion

#### 6.1 Introduction

To test the hypothesis that characteristic ranges of acetate threshold concentrations exist for different predominant TEAPs, the constant minimum acetate concentrations obtained in anaerobic batch cultures under different TEA-reducing conditions were evaluated. Furthermore, the experimental results were used to calibrate the microbial respiration model described in Chapter 5. The experimental and simulated results are presented, compared, and discussed below.

#### 6.2 Threshold experimental results

##### 6.2.1 Results obtained with *Geobacter metallireducens* growing on Fe(III)

The threshold experiment in which Fe(III) served as the sole electron acceptor was done with *Geobacter metallireducens* and an initial concentration of Fe(III)-citrate of 0.05 M. The trends of acetate consumption and biomass and Fe(II) production as a function of time are presented in Figure 6.1. For the first approximately 30 hours, Fe(II), acetate, and biomass levels did not change significantly, presumably due to a lag phase that *G. metallireducens* experienced. In the next 30 to 40 hours, Fe(II) and biomass production increased rapidly, accompanied by a quick drop of acetate concentration, indicating *G. metallireducens* was growing exponentially. After the acetate concentration reduced to a certain low level at around 100 hours, biomass ceased to increase and the Fe(II) and acetate concentrations remained relatively constant, suggesting that the threshold concentration of acetate had been reached and, consequently,

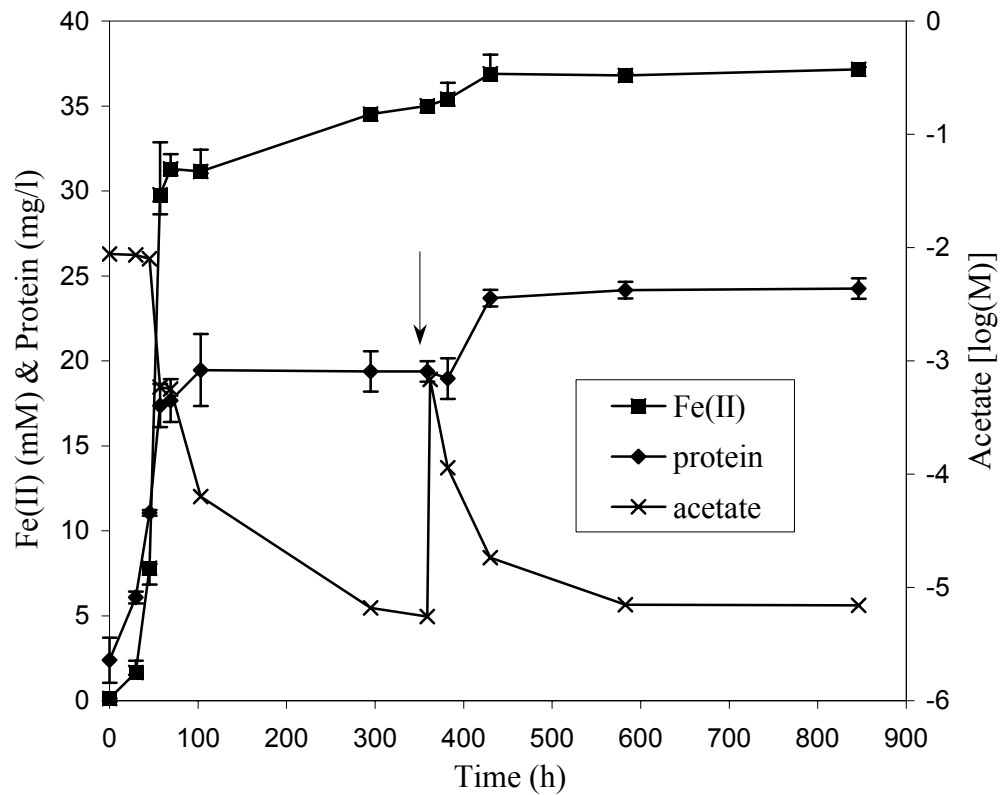


Fig. 6.1 Fe(II) and biomass production and acetate consumption (log transform) by strain *Geobacter metallireducens* with 0.05 M Fe(III)-citrate complex as electron acceptor and 0.01 M acetate as electron donor. The arrow indicated a second addition of acetate. Each data point represents the mean of duplicate cultures; error bars indicate one standard deviation.

entered the stationary phase. After 382 hours, 0.2 ml of a 0.04 M acetate stock solution was added to each of the replicated cultures to verify that the relatively constant acetate levels represented the threshold concentration (Löffler et al., 1999). Subsequently, Fe(II) and biomass concentrations increased and reached new plateaus, while the acetate concentration decreased and then remained at a relatively constant level that was comparable to that observed before acetate was resupplied.

The acetate concentrations in the Fe(III) reducing cultures were monitored until the last two measurements were statistically equivalent. The minimum acetate concentration measured in the culture medium was  $5.5 \times 10^{-6}$  M before respiking, and a P value of 0.5303 was obtained from analysis of the last two measurements using students' t test. Thus, the last two measurements of acetate concentrations were not significantly different ( $P > 0.05$ ). The minimum acetate concentration measured after respiking was  $6.9 \times 10^{-6}$  M and the P value obtained from analysis of the last two measurements (at 583 and 846 hours) using students' t test was 0.2929. The minimum acetate concentrations determined before and after acetate was resupplied were also not significantly different based on students' t test ( $df=3$ ;  $\alpha=0.05$ ). Based on these statistical analyses, it could be assumed that *G. metallireducens* did not take up any more acetate as an electron donor (using soluble Fe(III)-citrate as the only electron acceptor) after the acetate concentration dropped down to  $6.5 \times 10^{-6}$  M (the mean concentration of the last two measurements made for the two replicates before and after acetate was resupplied). Therefore, the minimum acetate concentrations ( $6.5 \times 10^{-6}$  M) can be considered as the electron donor thresholds for *G. metallireducens* growing on Fe(III)-citrate as the electron acceptor.

Determination of this and other threshold acetate concentrations should not have

been restricted by the acetate analytical detection limit, because the detection limit using the enzymatic/HPLC method used to measure acetate concentrations in this study was  $0.1 \times 10^{-6}$  M (King, 1991). Moreover, the measurement of the threshold acetate concentration apparently was not limited by the concentration of the electron acceptor [Fe(III)] either. Two observations support this assumption. First, a significant amount of the acceptor Fe(III) presumably remained in the medium before acetate was resupplied because the concentration of Fe(II) at this time was approximately  $35 \times 10^{-3}$  M. This should have left approximately  $15 \times 10^{-3}$  M Fe(III) in the medium, which would have been at least 15-fold times higher than the remaining acetate concentration. Thus, according to the stoichiometry of the appropriate rate law (Table 5.1), the concentration of Fe(III) should not have limited acetate metabolism. Secondly, after acetate was resupplied, reduction of Fe(III) to Fe(II) resumed without adding any more Fe(III). This confirmed that before respiking, the electron acceptor was not limiting oxidation of acetate by *G. metallireducens*.

The acetate threshold obtained in the experiment conducted under Fe(III)-reducing conditions was somewhat higher than the reported acetate concentration ( $0.5 \times 10^{-6}$  M) measured in sediment microcosm amended with clay that was coated with amorphous Fe(III) (Lovley and Phillips, 1987) or in the field measurements in Fe(III)-reducing aquifer sediments ( $\sim 1.0 \times 10^{-6}$  M) (Chapelle and Lovley, 1992) (Table 6.1). However, in general, one would not expect the threshold values obtained in laboratory studies conducted with pure cultures to be completely comparable with those obtained in the field or with environmental samples. First, microbial growth conditions such as pH and temperature may not be identical in the laboratory and in the field. Second, the

Table 6.1 Comparison of acetate thresholds under different predominant TEAPs obtained from the thresholds experiments and the literature.

TEAP	Microbial strain	Acetate threshold ( $\mu\text{M}$ )	
		Experimental value	Reported value
CO <sub>2</sub> -reducing	Methanosarcina barkeri	420.8	69-1000 <sup>a</sup>
SO <sub>4</sub> <sup>2-</sup> -reducing	Desulfotomaculum acetoxidans	405.4	2-50 <sup>b</sup>
NO <sub>3</sub> <sup>-</sup> -reducing	<i>Geobacter metallireducens</i>	10.2	N/A
MnO <sub>2</sub> -reducing		10.0	N/A
Fe <sup>3+</sup> -reducing		3.2	0.5-3 <sup>c</sup>

<sup>a</sup>. Westermann, 1989

<sup>b</sup>. McMahon and Chapelle, 1991; Chapelle and Lovley, 1992

<sup>c</sup>. Chapelle and Lovley, 1992

microbial characteristics of the experimental systems would be different. Pure cultures in the laboratory behave differently compared to mixed cultures in field samples. Lastly, a more important factor is probably that in complex environments where microorganisms are presented with multiple substrates at low concentrations, they are often able to utilize a given substrate (in a mixture) at a much lower concentration than if it is supplied as the sole substrate and at relatively high concentrations (e.g., Kovárová-Kovar and Egli, 1998).

An additional threshold experiment with *Geobacter metallireducens* growing on Fe(III) was done with an higher initial concentration ( $80 \times 10^{-3}$  M) of Fe(III)-citrate. The trends in acetate, Fe(II), and biomass concentrations are presented in Figure 6.2 and were similar to those observed for the threshold experiment conducted with an initial concentration of 0.05 M Fe(III)-citrate, as described above. The measured concentrations of Fe(II) in the two experiments were similar. Thus, the presumptive concentration of Fe(III) remaining at the conclusion of the experiment conducted with an initial Fe(III) concentration of 0.08 M was higher than the calculated Fe(III) concentration at the conclusion of the experiment conducted with a lower initial Fe(III) concentration. This makes sense, because, as noted above, Fe(III) was not limiting acetate metabolism in the previous experiment. Interestingly, compared to the acetate threshold obtained in the previous experiment, a slightly lower threshold value,  $3.5 \times 10^{-6}$  M, was obtained before resupplying acetate to the cultures amended with 0.08 M Fe(III). After acetate was added, the acetate threshold in the 0.08 M Fe(III) cultures was  $4 \times 10^{-6}$  M, again lower than that observed at the conclusion of the previous experiment. Again thresholds determined before and after respiking were not significantly different, based on comparison using

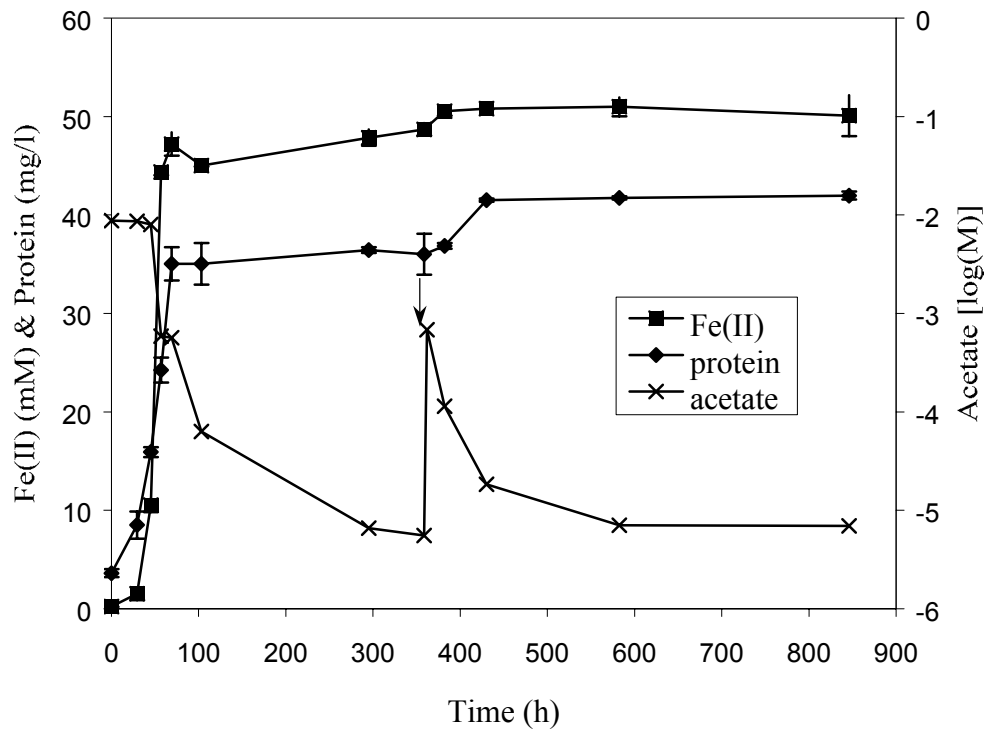


Figure. 6.2 Fe(II) and biomass production and acetate consumption (log transform) by strain *Geobacter metallireducens* with 0.08 M Fe(III)-citrate complex as electron acceptor and 0.01 M acetate as electron donor. The arrow indicated a second addition of acetate. Each data point represents the mean of duplicate cultures; error bars indicate one standard deviation.

students' t test (at 95% confident interval). Because Fe(III) was not limiting in either experiment, it is likely that the differences in the observed acetate thresholds were due to the relative biomass levels in the two experiments. In fact, examination of Figure 6.1 and 6.2 reveals that the initial biomass concentration in the 0.08 M Fe(III) was higher than that initially present in the 0.05 M experiment. Biomass concentrations remained higher throughout, and at the conclusion of, the 0.08 M Fe(III) experiment compared to the 0.05 M Fe(III) experiment. Higher biomass concentrations would be expected to achieve lower substrate concentrations. Thus, the observed trends in acetate thresholds were consistent with the biomass concentrations in the Fe(III) experiments.

### **6.2.2 Results obtained with *Geobacter metallireducens* growing on Mn(IV)**

A threshold experiment in which MnO<sub>2</sub> served as the terminal electron acceptor was also conducted with *Geobacter metallireducens*. The initial concentration of MnO<sub>2</sub> was 0.05 M. The trends of acetate consumption and biomass production for this experiment are shown in Figure 6.3. After a short lag phase, which was approximately 15 hours long, the cells entered the exponential phase, as revealed by a sharp increase in biomass levels and a quick drop in acetate concentration. Subsequently relatively constant levels of acetate were observed in the medium and *G. metallireducens* entered the stationary phase, as indicated by a plateau in biomass concentrations. At 341 hours, 0.2 ml of 0.04 M acetate solution was added into the medium, resulting in an acetate concentration of  $1 \times 10^{-5}$  M. Replenishment of the electron donor restored microbial growth, which triggered an increase in biomass production and acetate consumption, until the concentration of acetate decreased to a new apparent minimum concentration.

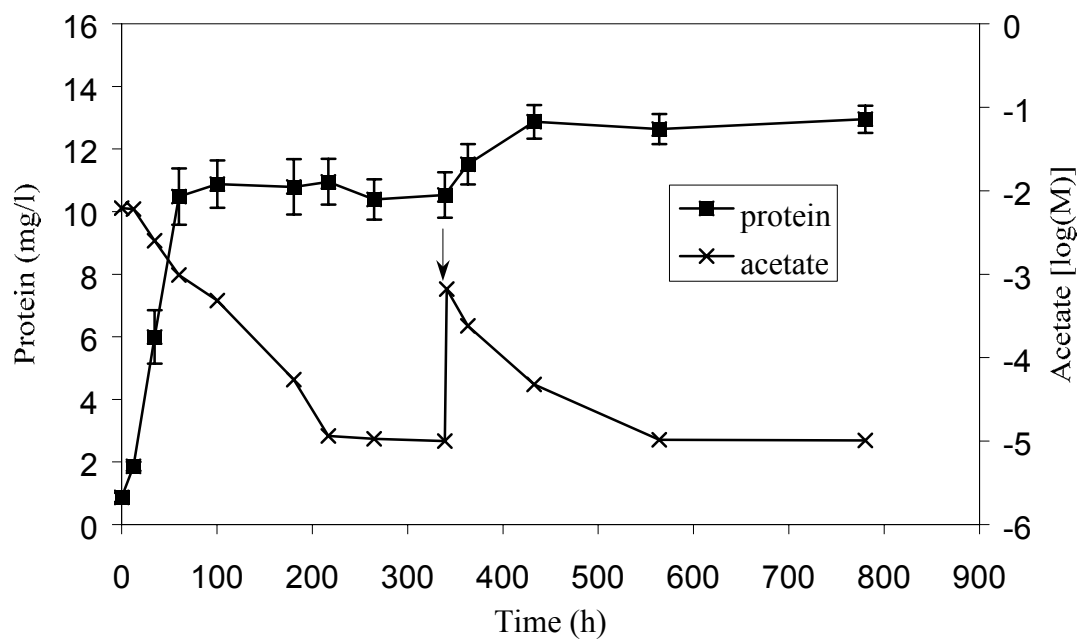


Figure 6.3 Biomass production and acetate consumption by strain *Geobacter metallireducens* with 0.05 M  $MnO_2$  as electron acceptor and 0.01 M acetate as electron donor. The arrow indicated a second addition of acetate. Each data point represents the mean of triplicate cultures; error bars indicate one standard deviation.

The minimum acetate concentrations were determined through periodic measurement of acetate concentrations until the last two measurements were statistically equivalent, based on evaluation using student's t test (P=0.3317 and 0.8982 before and after respiking, respectively). The mean minimum acetate value was  $1.0 \times 10^{-5}$  M before and after acetate was resupplied. The minimum acetate concentrations can be regarded as the acetate thresholds for growth of *G. metallireducens* under Mn(IV)-reducing conditions. Again, the acetate thresholds were not restricted by the detection limit. Likewise, the acetate thresholds were apparently not limited by the concentration of the electron acceptor because small black MnO<sub>2</sub> solids still could be observed for a long period of time after biomass concentrations leveled off. In addition, the fact that acetate metabolism resumed after it was resupplied provided further evidence that the electron acceptor was not limiting and there was enough MnO<sub>2</sub> remaining to support metabolism of available acetate.

### **6.2.3 Results obtained with *Geobacter metallireducens* growing on nitrate**

In the third threshold experiment conducted with *G. metallireducens*, NaNO<sub>3</sub> was provided as the sole electron acceptor at an initial concentration of 0.02 M. *G. metallireducens* did not experience a lag phase under the nitrate-reducing conditions (Figure 6.4). The strains grew exponentially for approximately 10 hours, as indicated by the accumulation of biomass and the consumption of acetate. Subsequently, biomass and acetate concentrations remained relatively constant, until more acetate was added to the medium at 303 h. After respiking with acetate, acetate metabolism was restored, resulting in an increase in biomass. As previously observed, after the concentration of acetate

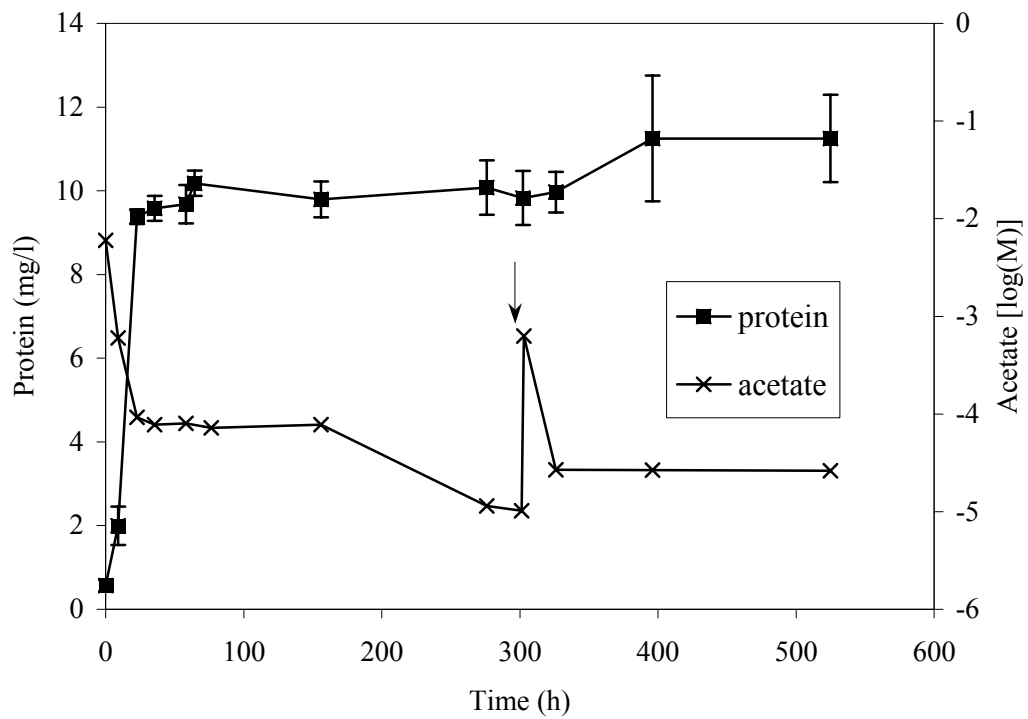


Figure 6.4 Biomass production and acetate consumption by strain *Geobacter metallireducens* with 0.02 M NaNO<sub>3</sub> as electron acceptor and 0.01 M acetate as electron donor. The arrow pointed out the time for acetate respire. The arrow indicated a second addition of acetate. Each data point represents the mean of duplicate cultures; error bars indicate one standard deviation.

decreased to a new minimum concentration, metabolism ceased and biomass concentrations leveled off again.

The acetate threshold values were obtained by periodically monitoring the acetate concentrations before and after acetate was resupplied. They were  $1.0 \times 10^{-5}$  M (P=0.6664 for student's t test evaluation of the last two measurements) before respiking with acetate and  $2.8 \times 10^{-5}$  M (P=0.8824 for student's t-test evaluation of the last two measurement) after respiking with acetate. The measurement of the acetate thresholds should not be restricted by the limit of the detection method, as mentioned above. Moreover, acetate metabolism should not have been limited by the concentration of the electron acceptor, because the initial concentration of NaNO<sub>3</sub> was 0.02 M, which was two-fold higher than the concentration of acetate at the beginning of the experiment. Therefore, approximately 0.01 M of NaNO<sub>3</sub> should have remained when biomass concentrations leveled off and the concentration of acetate fell below  $1 \times 10^{-3}$  M. The restoration of microbial metabolism after respiking with acetate further confirmed that the concentration of the electron acceptor was not limited.

Under the nitrate-reducing conditions, the acetate threshold value after respiking was approximately 2.5-fold higher than that before respiking. This difference was significant based on comparison using student's t test (df=6;  $\alpha=0.05$ )

#### **6.2.4 Results obtained with *Desulfotomaculum acetoxidans* growing on sulfate**

The threshold experiment using sulfate as the sole electron acceptor was conducted with *Desulfotomaculum acetoxidans* and an initial concentration of Na<sub>2</sub>SO<sub>4</sub> of 0.02 M. As shown in figure 6.5, compared to *G. metallireducens*, *D. acetoxidans*

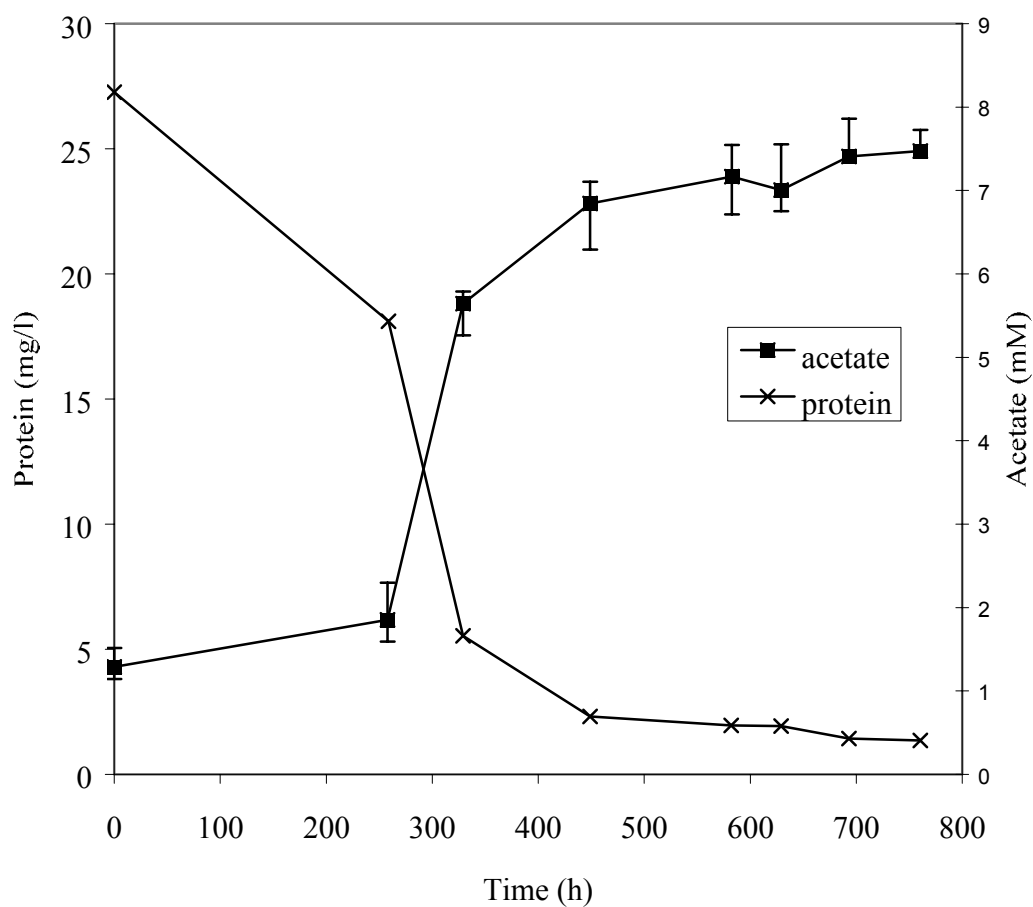


Figure 6.5 Biomass production and acetate consumption by *Desulfotomaculum acetoxidans* with 0.02 M  $\text{Na}_2\text{SO}_4$  as electron acceptor and 0.01 M acetate as electron donor. Each data point represents the mean of triplicate cultures; error bars indicate one standard deviation.

experienced a longer lag phase. By 250 h, the cells had entered the log phase, as shown by an exponential increase in biomass levels and a concomitant decrease in acetate concentrations. At about 450 h, relatively constant levels of biomass and acetate were observed in the medium and the cells apparently entered the stationary phase.

The acetate concentrations in the *D. acetoxidans* culture medium were periodically monitored until the last two measurements were not significantly different based on evaluation using student's t test. The acetate threshold was determined to be  $4 \times 10^{-4}$  M (P=0.086). The measured acetate threshold significantly exceeded the  $1 \times 10^{-6}$  M analytical detection limit. The acetate threshold should not have been affected by the concentration of the electron acceptor either because the initial concentration of sulfate was twice that of acetate, while according to the rate laws (Table 2.2), the theoretical stoichiometric ratio of sulfate to acetate was 1:1.

The acetate threshold value obtained for *D. acetoxidans* in a laboratory batch culture was nearly ten-fold higher than a reported value obtained from field measurements (Table 6.1). The potential explanations for the discrepancy in acetate thresholds determined using laboratory and field samples previously discussed for Fe(III)-reducing conditions also could apply here. In addition, the accumulation of the end product hydrogen sulfide has been shown to inhibit the growth kinetics of sulfate-reducing bacteria (e.g., Cooney et al., 1996). Although hydrogen sulfide production would have also occurred in the batch microcosms used by Lovley and Phillips (1987), it is likely that precipitation of sulfides by metals that were present in the sediment would have alleviated any toxicity effects in these systems.

### 6.2.5 Results obtained with *Methanosarcina barkeri* growing via acetotrophic methanogenesis

In the final acetate threshold experiment, *Methanosarcina barkeri* grew by converting acetate to methane and carbon dioxide. This metabolic process is known as acetotrophic or acetoclastic methanogenesis (Zeikus et al, 1985). Unlike the anaerobic respiratory processes used by *G. metallireducens* and *D. acetoxidans*, acetate utilization by *M. barkeri* did not involve a distinct terminal electron acceptor and this is reflected in the appropriate rate law (Table 5.1 ). However, in terms of chemiosmotic theory (Mitchell, 1961), the mechanism of energy conservation during the metabolism of acetate to methane and carbon dioxide is similar to that used to synthesize ATP during the oxidation of acetate coupled with the reduction of a terminal electron acceptor. In the process of acetotrophic methanogenesis, acetate is first cleaved to yield a carbonyl [CO] and a methyl group [CH<sub>3</sub>] (Figure 6.6). CO is internally oxidized to CO<sub>2</sub>. The electrons released by this oxidation are transferred to the methyl group via a series of electron and hydrogen atom carriers associated with the cell membrane to produce methane. Protons are translocated across the membrane during the electron transport process, and the resultant proton gradient is used to drive ingress of H<sup>+</sup> back across the membrane and ATP synthesis via electron transport phosphorylation. Donation of e<sup>-</sup> from the carbonyl group of acetate to the methyl group of acetate via an electron transport chain, translocation of H<sup>+</sup> across the cellular membrane, and ATP synthesis via e<sup>-</sup> transport phosphorylation are analogous to respiratory processes. Thus, it is reasonable to predict that the acetate threshold for acetotrophic methanogenesis might be subject to the same kinetic and thermodynamic controls that affect substrate thresholds for true anaerobic

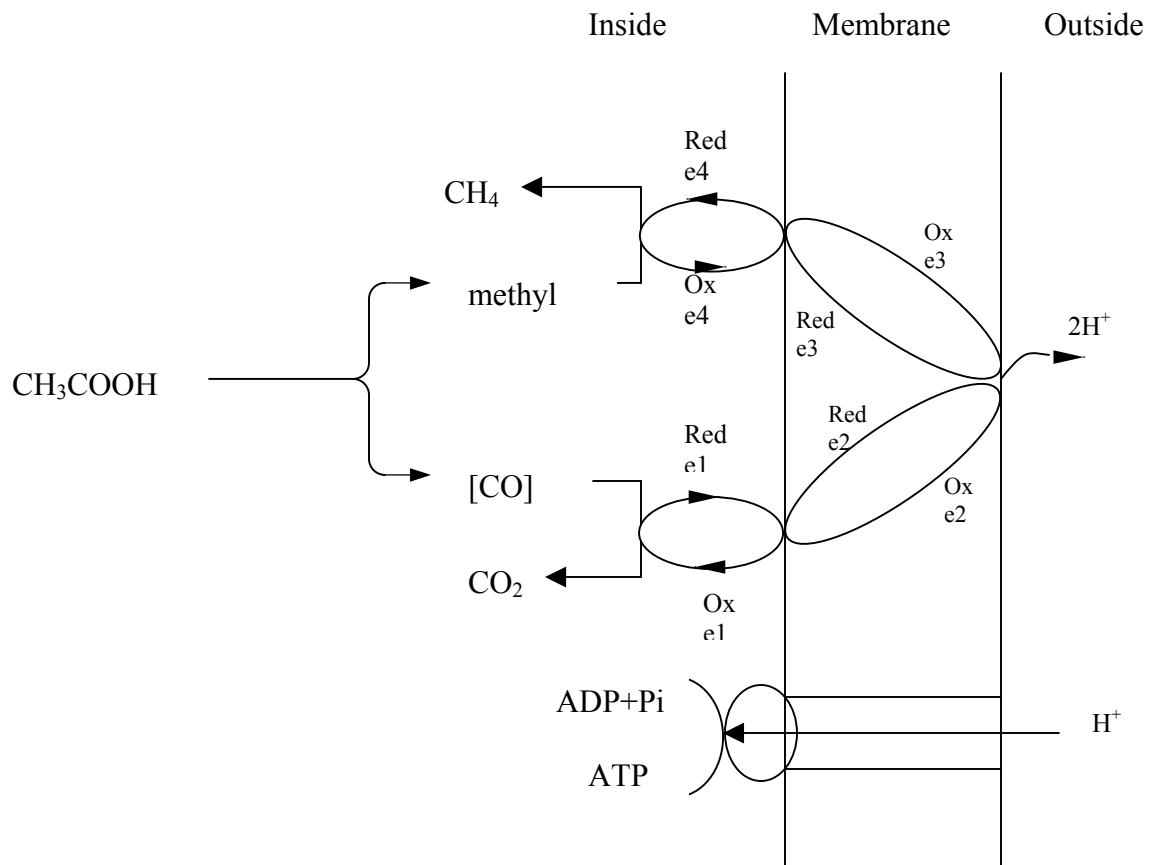


Figure 6.6 Model of acetotrophic methanogenesis. e1 to e4 are soluble electron and proton carriers. Red e is the reduced form of the carrier and Ox e is the oxidized form of the carrier. (adapted from Zeikus et al., 1985)

respiration. Therefore, measurement of the acetate threshold under methanogenic conditions was performed in order to gain insight into mechanisms that control acetate thresholds under anaerobic condition.

The growth curve of *M. barkeri* was qualitatively very similar to that of *D. acetoxidans* (Figure 6.7). Biomass concentrations remained fairly constant for at least 200 h; however, CH<sub>4</sub> production appeared to begin without any lag. The production of biomass and methane was accompanied by the consumption of acetate during exponential growth. After nearly 300 h, the acetate concentrations began to level off. As in previous experiments, the acetate threshold was determined by periodically measuring the acetate concentrations until the last two measurements were not significantly different based on evaluation using student's t test. Based on this analysis, the acetate threshold value was 420.8  $\mu\text{M}$  (P=0.8146). This acetate concentration significantly exceeded the analytical detection limit and, because acetate served as the sole growth substrate, limitation by an external terminal e<sup>-</sup> acceptor was not possible. The acetate threshold value obtained in this study was within the range of the reported acetate thresholds for pure cultures of acetoclastic methanogens (69 to over 1000  $\mu\text{M}$ , depending on the specific strains of methanogens; Westermann et al, 1989).

#### **6.2.6 Comparison and discussion of the acetate thresholds**

The acetate thresholds obtained under Fe(III)-, Mn(IV)-, nitrate-, and sulfate-reducing and methanogenic conditions, are summarized in Figure 6.8 along with the corresponding standard free energy ( $\Delta G^0$ ). Acetate thresholds for the different TEA increased in the order of:

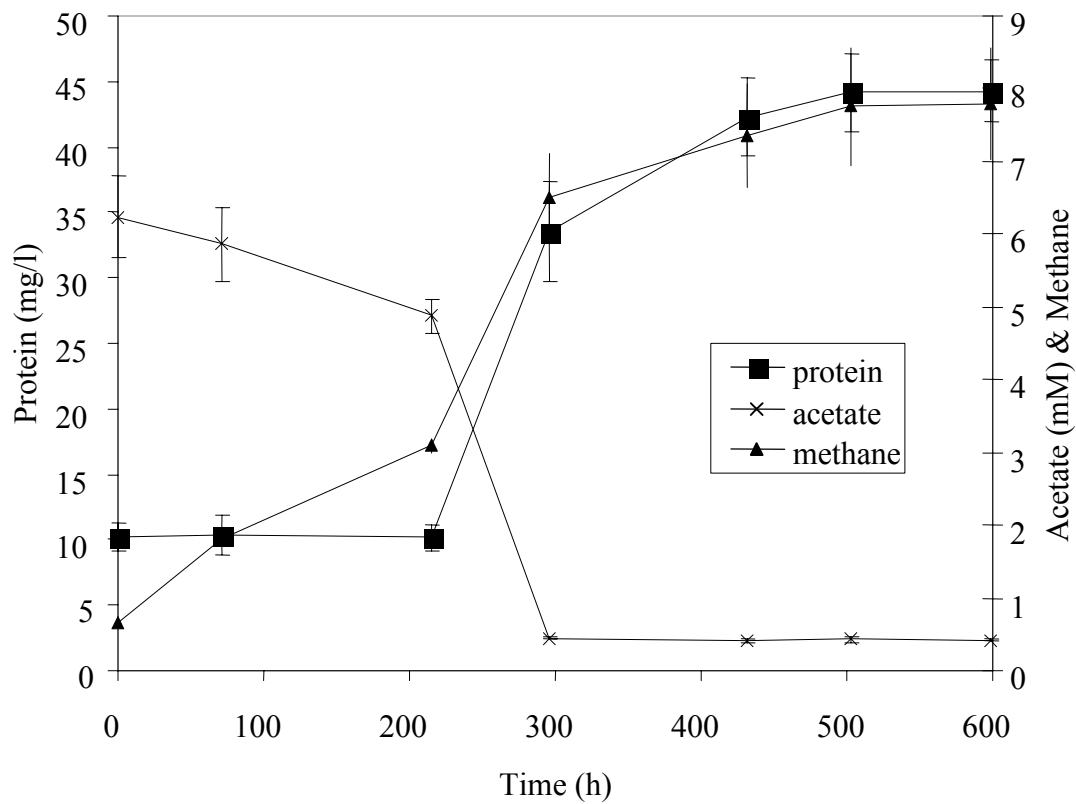


Figure 6.7 Biomass production and acetate consumption by strain *Methanosarcina barkeri* with 0.02 M acetate provided as the sole growth substrate. Each data point represents the mean of triplicate cultures; error bars indicate one standard deviation.

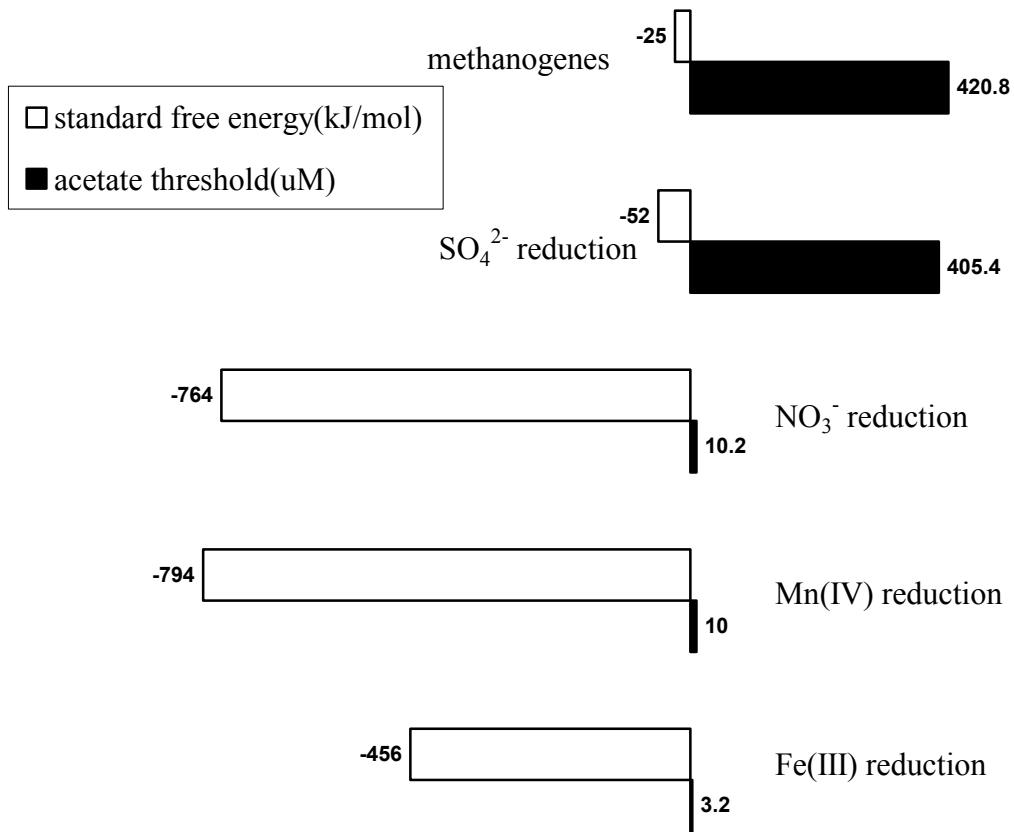
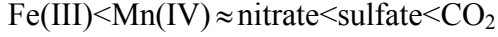


Figure. 6.8. Acetate thresholds obtained under Fe(III), Mn(IV), nitrate and sulfate reduction and acetotrophic methanogenesis conditions, along with their corresponding standard free energy  $\Delta G_{35}^{0'}$  released from the redox reactions



The results of the acetate threshold experiments suggest that acetate thresholds are very similar for TEA with relatively high redox potentials, i.e., Mn(IV), NO<sub>3</sub><sup>-</sup>, and Fe(III). However, acetate thresholds determined under Mn(IV)-, NO<sub>3</sub><sup>-</sup>, and Fe(III)-reducing conditions appear to be more than an order of magnitude lower than those determined for less favorable TEAP such as sulfate reduction or methanogenesis. These experimental observations are consistent with the theoretical evaluations made by Seagren and Becker (1999). They calculated the values of the non-dimensional parameter  $S_{\min}^*$  for acetate oxidation coupled to the reduction of several different TEAs, where

$$S_{\min}^* = S_{\min} / K \quad (6.1)$$

using the theoretical relationships between the stoichiometry and thermodynamics of the e<sup>-</sup> donor, e<sup>-</sup> acceptor and synthesis half-reactions with  $Y$  and  $q_{\max}$  (McCarty, 1972). They found that  $S_{\min}^*$  values were very similar for TEA with relatively high redox potentials (O<sub>2</sub>, Fe(III), and NO<sub>3</sub><sup>-</sup>).  $S_{\min}^*$  values calculated for sulfate-reducing and methanogenic conditions were much lower and were nearly an order of magnitude higher than the thresholds calculated for O<sub>2</sub>-, Fe(III)-, and NO<sub>3</sub><sup>-</sup>-reducing conditions. Thus, the experimental results and the evaluations by Seagren and Becker (1999) suggest that measurement of acetate concentrations may be most useful for distinguishing between relatively oxidized and relatively reduced conditions. Use of acetate concentrations in this manner would be similar to appropriate application of platinum electrode measurement of redox potentials in environmental samples.

## 6.3 Simulation of the experimental results using the microbial respiration model

### 6.3.1 Calibration of the microbial respiration model

In order to gain insight into the kinetic and thermodynamic factors that controlled the experimentally-determined acetate thresholds, simulation of  $F_D$ ,  $F_A$ , and  $F_T$  for each of the experimental systems studied was necessary. Thus, the microbial respiration model was calibrated with the experimental results and calculated data to identify the model parameters  $Y$ ,  $k$ ,  $K_D$ , and  $K_A$ . The model was calibrated by using the non-linear least squares optimization algorithm *lsqnonlin* (Matlab, version 6.1, The Mathworks, Inc) with a variable weight that is based on the reciprocal of the standard deviation of the measurements.

For each TEA condition, experimental data were available from two or three replicates. In general, there are two ways to fit data for the parameter estimation (Magbanua et al, 1998). The common approach uses arithmetic mean parameter values, which are obtained by averaging parameters estimated from data obtained from individual replicates. This approach is adequate when the variability among replicate parameter estimates is small. However, in this study, parameters estimated by different replicates were quite different (results are not shown), and so a simple arithmetic mean of individual parameter estimates is probably not appropriate. The alternative approach is to pool the data from the experimental replicates and perform parameter estimation based on the means of the data. This approach is practicable if the variations of the initial conditions are slight. Because the initial conditions of each replicate in this study are similar, indicated by relatively low standard deviations for initial biomass and substrates, this alternative approach was adopted for parameter estimation. Thus, the parameter

estimates were fit to data obtained by averaging the results obtained from individual replicates.

The concentrations of the oxidized and reduced forms of the donor  $D^+$  and  $D$ , respectively, and of the acceptor  $A$  and  $A^-$ , respectively, over time were highly intercorrelated. This is not surprising because  $[A^-]$ , and sometimes  $[A]$ , were calculated based on reaction stoichiometry (Table 5.1) and measured donor concentrations  $[D]$ . The concentration of the oxidized form of the electron donor  $[D^+]$  was calculated based on the amount of donor consumed, the initial total carbonate concentration, and the equilibrium equation for  $H_2CO_3/HCO_3^-$  (Snoeyink and Jenkins, 1980). The chemical species were also relatively well-correlated with  $[X]$ . This made it difficult to identify  $K_D$  and  $K_A$  uniquely using a single set of experimental data. Ideally, three sets of experiments should be used to estimate and evaluate electron donor and acceptor-related coefficients: one set in which the electron donor is always limiting, one in which the electron donor was provided in excess and e- acceptor is limiting, and one set in which both donor and acceptor are limiting, as done by Saez and Rittmann (1996) for estimation of dual Monod kinetic parameters. However, in this study, it was feasible only to perform electron donor-limited threshold experiments. That is, in general, the electron acceptor was provided in excess compared to the electron donor, based on the reaction stoichiometry presented in Table 5.1. Thus,  $K_A$  was set equal to zero for each TEA. As a result, only  $Y$ ,  $k$ , and  $K_D$  had to be fit to the data, and in each case, the electron acceptor term in the model was assumed to be zero-order with respect to substrate concentration and  $F_A=1$  for all TEA conditions at all times. Assuming  $K_A=0$  resulted in better fits, compared to fits obtained assuming  $K_D=0$  (data not shown).

However, it should be noted that the electron acceptor concentrations did decrease significantly during the course of the threshold experiments. Therefore, it is likely that  $F_A$  decreased below 1 and affected the respiration rate before the conclusion of at least some of the experiments. In addition, according to the reaction stoichiometry presented in Table 5.1, the amount of Fe(III) provided in the threshold experiment conducted under Fe(III)-reducing conditions with 0.05 M Fe(III) would not have been sufficient to support the oxidation of the added acetate. However, the redox reactions in Table 5.1 neglect the fact that not all of the electrons derived from a donor are directed to the electron acceptor (McCarty, 1972). Some electrons are consumed in biomass synthesis. This has the effect of reducing the amount of electron acceptor that is required to support oxidation of the electron donor. The significance of neglecting biomass synthesis on redox reaction stoichiometry and electron acceptor requirements decreases with decreasing free energy change, because as the energetics of microbial metabolism become less favorable, microorganisms have to divert an increasing fraction of the electrons derived from the donor to the electron acceptor for energy generation (Seagren and Becker, 2002). Fe(III) is a very favorable electron acceptor; therefore, if biomass synthesis is included in a balanced reaction of energy generation and biomass synthesis using the thermodynamic approach developed by McCarty (1972), an Fe(III)/acetate molar ratio of approximately 3.4:1 is calculated, compared to the ratio of 8:1 determined from Table 5.1. Thus, while not completely valid, the assumption that  $K_A=0$  offered the best solution for obtaining unique estimates of the other parameters.

The Matlab parameter estimation routine optimized the value of the protein concentrations at time zero ( $X_0$ ), even though initial biomass measurements were made.

Several considerations suggest that this is not unreasonable. In particular, accurate measurement of total protein concentrations is complicated by several factors. For example, different proteins often give different responses when quantified using a given method, and a wide variety of substances, including reducing agents and buffers, interfere with protein assays (Daniels et al., 1994). In fact, Brown et al. (1990) determined microbial growth kinetic parameters (such as  $\mu$ ) from oxygen uptake ( $O_u$ ) data using respirometry and found that "...the main term contributing to error in the computation of  $\mu$  at low  $O_u$  was  $X_0$ ". Even though the initial biomass concentration was a measured value, the investigators' often had a difficult time obtaining good fits to the experimental data because of error associated with the initial biomass measurements. Brown et al. obtained corrected  $X_0$  values by using a spreadsheet to visually examine the effects of slight changes in  $X_0$  on the curve fits. However, they limited adjustments to  $X_0$  to +/- 10% of the experimentally-determined values, to prevent these values from being arbitrarily chosen. In this study, all of the optimized  $X_0$  values generated by the parameter estimation routine were within 10% of the measured values.

The parameter estimates are presented in Table 6.2, and the simulations of the experimental data that were obtained by the microbial respiration model solved using Matlab function ODE23s and the parameter estimates are presented in Figures 6.9 to 6.14.

It should be noted that the Y values reported in Table 6.2 were obtained by linear regression using experimentally-determined  $X_0$  values, rather than optimized values. However, in some cases, electron donor and biomass concentrations used in the Y value determinations were measured before and/or after exponential growth occurred.

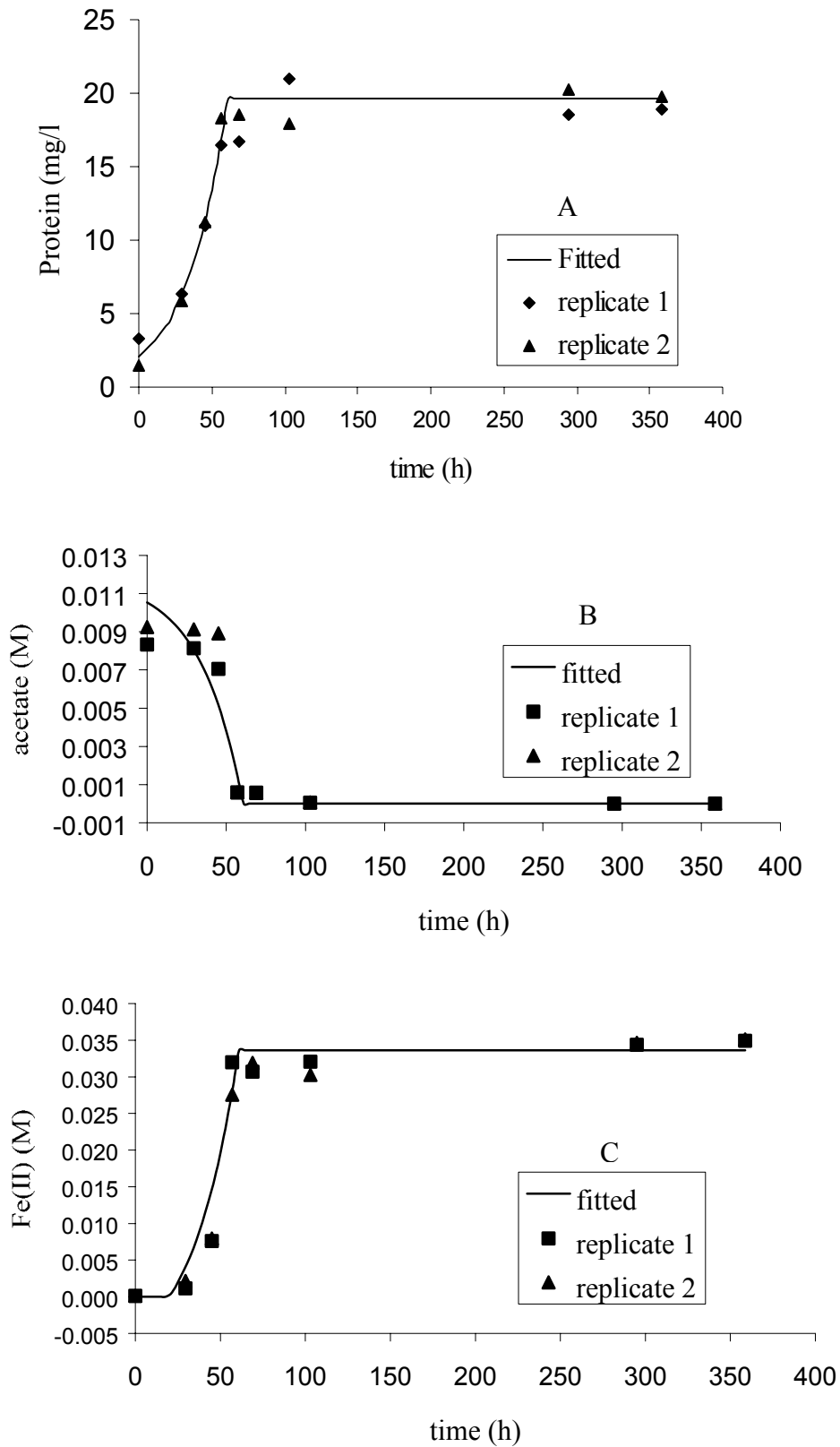


Figure 6.9 Fitted curve and experimental data under a  $5 \times 10^{-2}$  M Fe(III)-reducing condition. (A) protein vs time; (B) acetate vs time; (C) Fe(II) vs time.

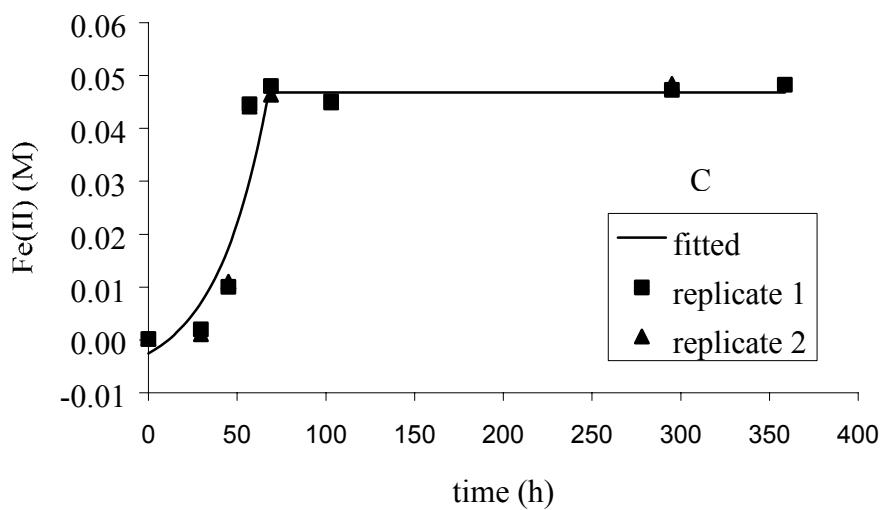
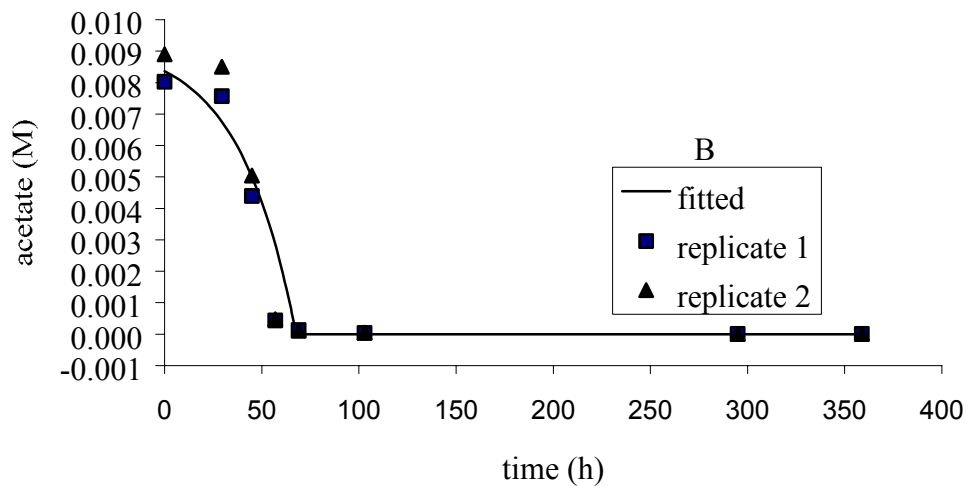
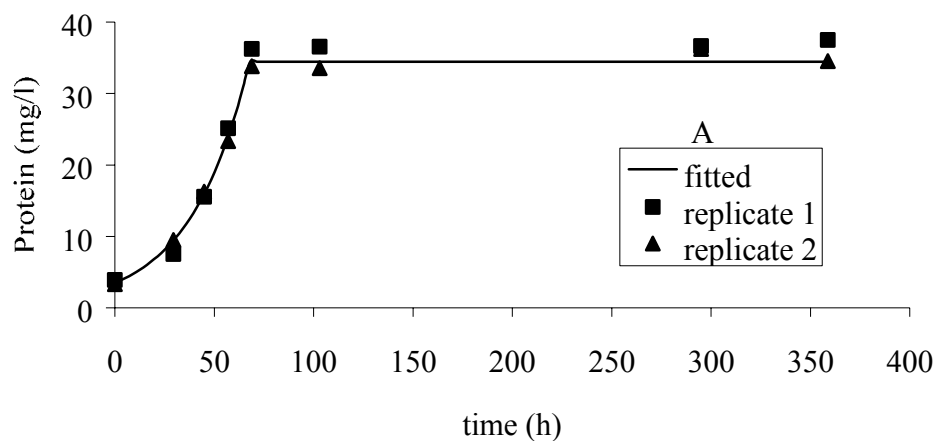


Figure 6.10 Fitted curve and experimental data under a 0.08 M Fe(III)-reducing condition. (A) protein vs time; (B) acetate vs time; (C) Fe(II) vs time.

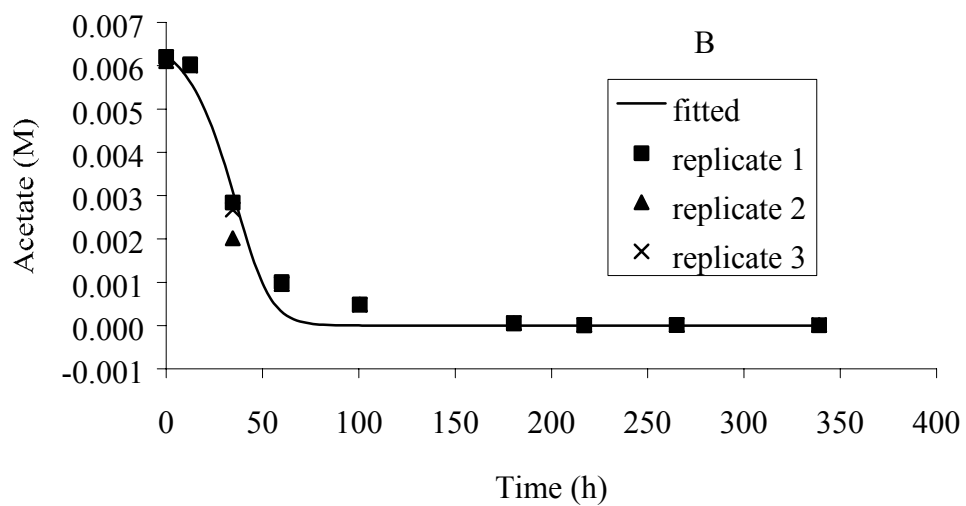
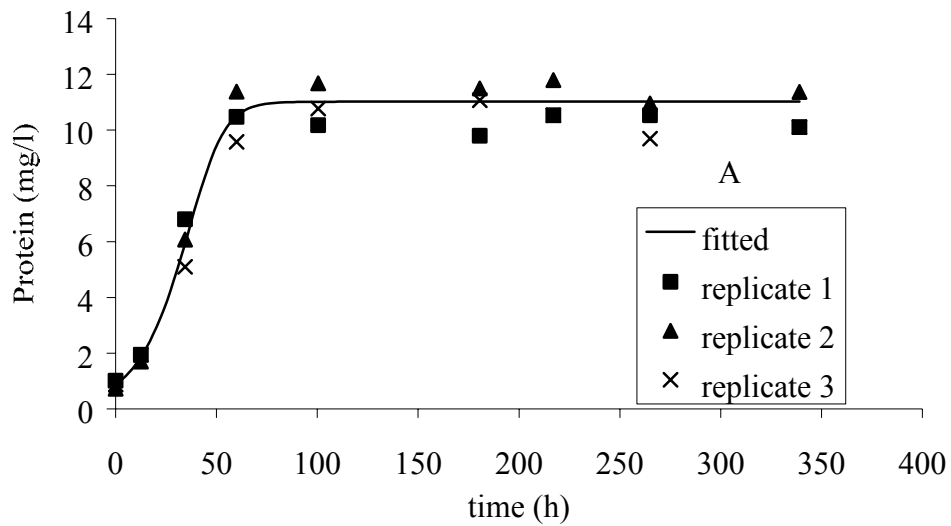


Figure 6.11 Fitted curve and experimental data under a 0.05 M Mn(IV)-reducing condition. (A) protein vs time; (B) acetate vs time.

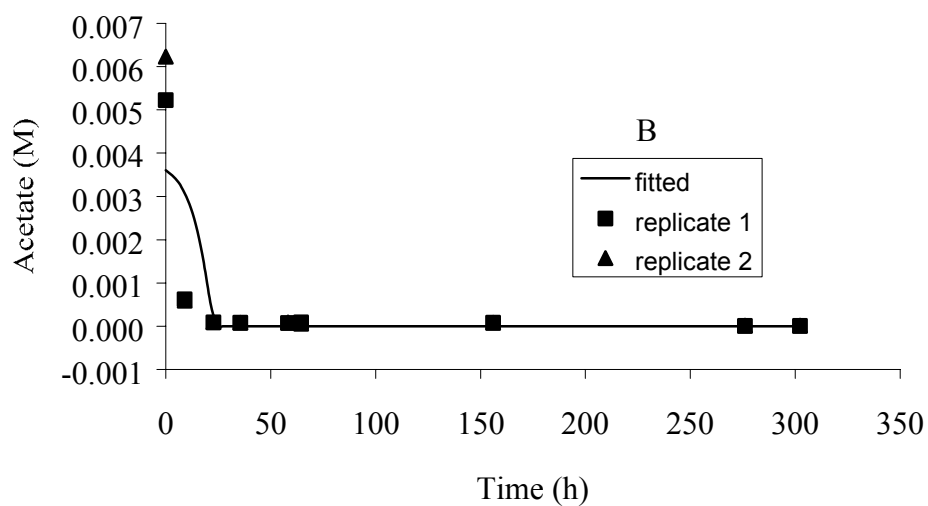
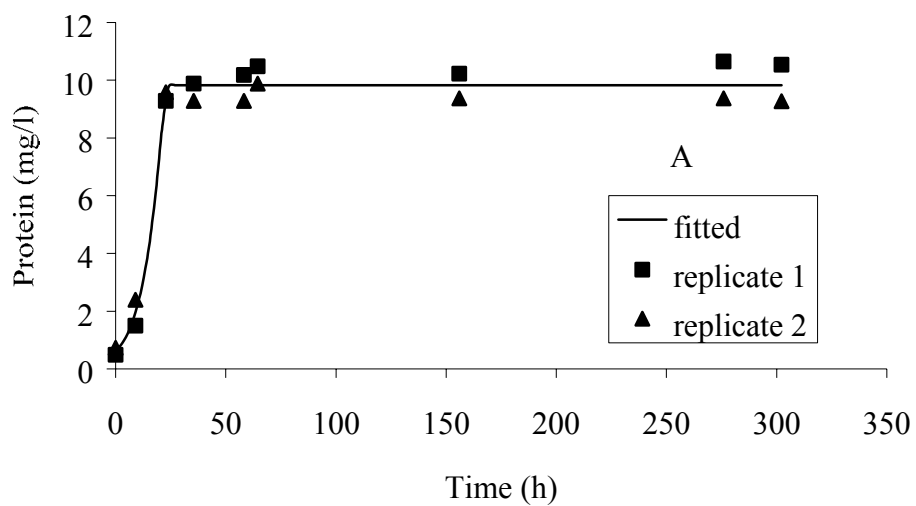


Figure 6.12 Fitted curve and experimental data under a 0.02 M nitrate-reducing condition. (A) protein vs time; (B) acetate vs time.

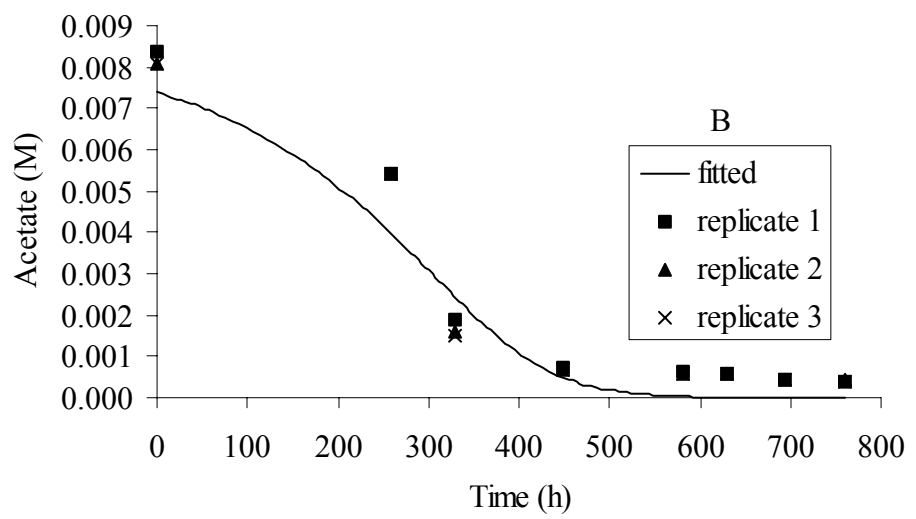
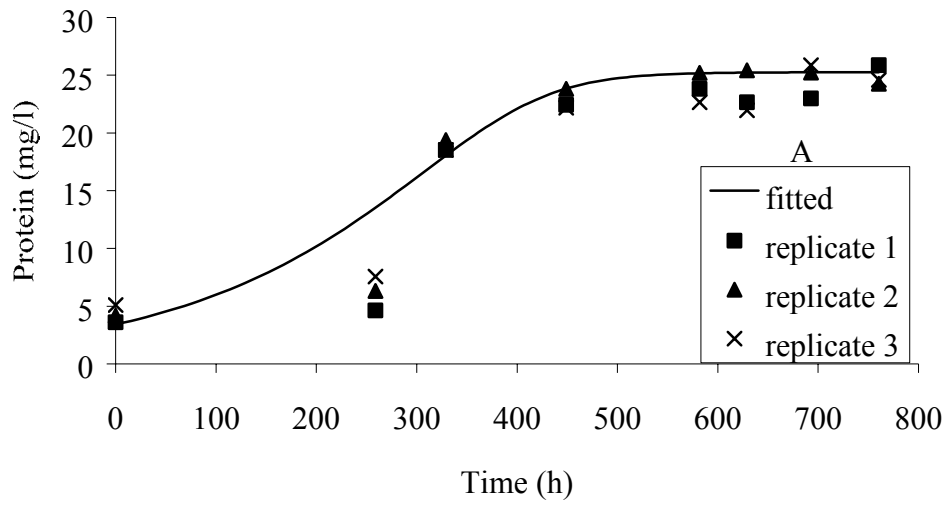


Figure 6.13 Fitted curve and experimental data under a 0.02 M sulfate-reducing condition. (A) protein vs time; (B) acetate vs time.

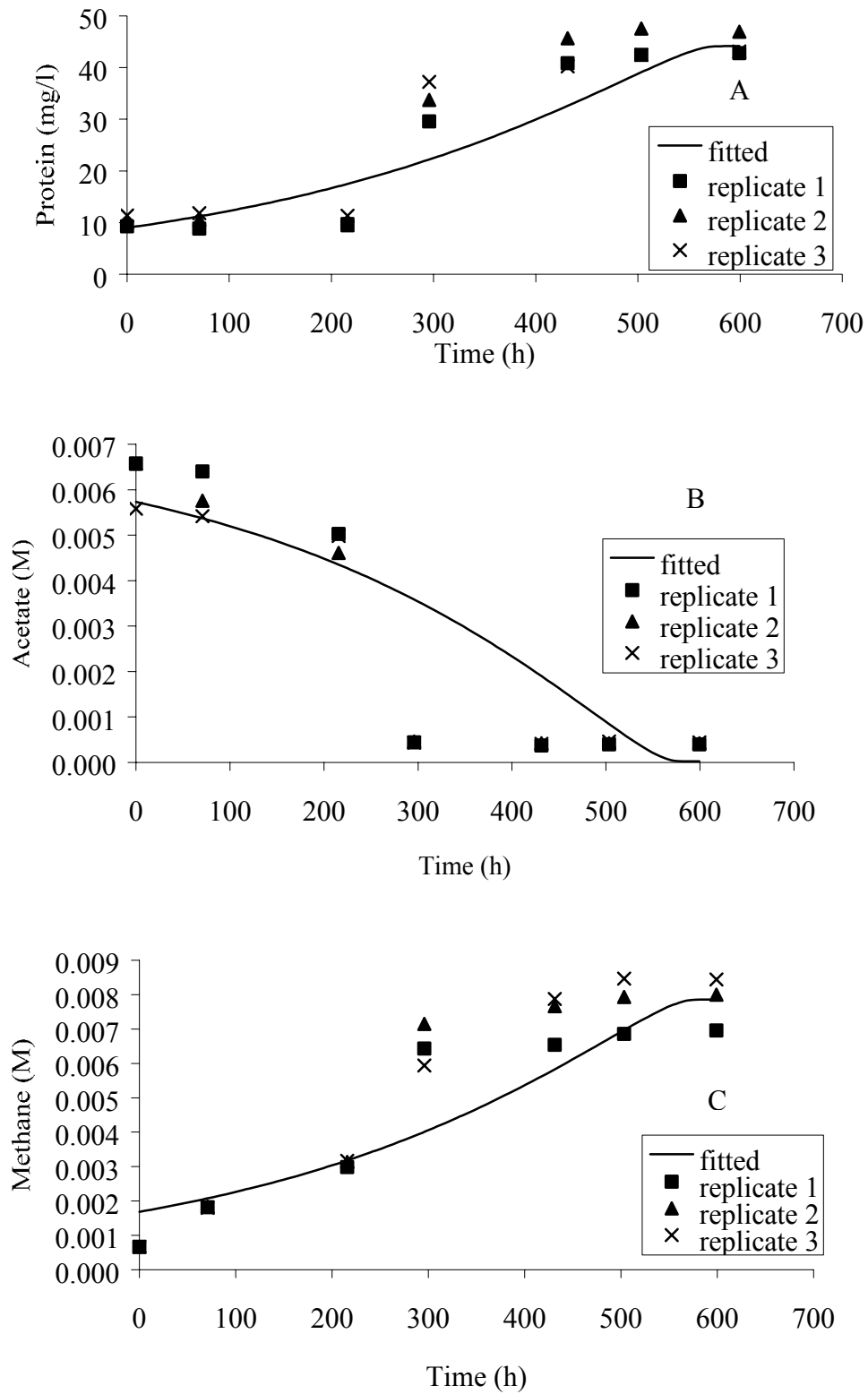


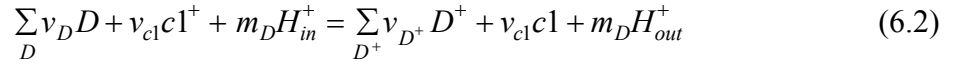
Figure 6.14 Fitted curve and experimental data under a methanogenesis condition. (A) protein vs time; (B) acetate vs time; (C) methane vs time.

Inclusion of measurements made before or after exponential growth could have introduced error into the estimated  $Y$  values. In fact, this might at least partially explain why the values of the growth yield  $Y$  under Fe(III) reduction conditions with 0.05 and 0.08 M as the initial Fe(III) concentrations, respectively, were not identical to each other, although the yields were obtained from two very similar batch culture systems with the same microorganism and anaerobic respiration process. Therefore, in the future, estimation of  $Y$  will be based on measurements made only while a culture was experiencing net growth. In addition, physiological differences in the cultures grown with 0.05 and 0.08 M Fe(III) could have conceivably contributed to the observed differences in  $Y$  values. For example, as discussed by Grady et al. (1996), pure cultures can replace low affinity/high capacity enzymes that are expressed under high substrate concentrations with high affinity/low capacity enzymes under nutrient-limited growth. Changes in enzyme expression and physiological adaptations associated with changes in substrate concentration could result in different yield values.

Growth yields reflect the amount of energy available in a redox reaction. Therefore, according to Figure 6.8, the measured yield values are expected to decrease according to Mn(IV)-reducing>nitrate-reducing>Fe(III)-reducing>sulfate-reducing>methanogenesis. As shown in Table 6.2, the trend in  $Y$  is opposite to that predicted by thermodynamics. Again, a likely explanation for this observation is that error was introduced into the  $Y$  determinations by including inappropriate data in these calculations.

The values of  $K_D$  under different TEAPs in Table 6.2 seem to be very variable.  $K_D$  is the constant that “reflect the standard free energy changes of the electron-donating reactions” (Jin and Bethke, 2002). A general reversible electron donating reaction

proceeds according to



Here  $c1^+$  and  $c1$  are the oxidized and reduced forms of the electron carriers.  $v_{c1}$  is the reaction coefficient for both  $c1^+$  and  $c1$ .  $K_D$  can be determined according to

$$K_D = \exp\left(-\frac{nF\Delta E_D^0 - m_D F\Delta p}{v_{c1} RT}\right) \quad (6.3)$$

where  $\Delta E_D^0$  is the standard redox potential difference of Reaction (6.2).  $\Delta p$  is the proton gradient. Therefore the value of  $K_D$  is related to the standard redox potential of the electron donor couple and the mechanism for translocation of electrons and protons, including the number of electrons and protons translocated per mole of electron donor. In this study, acetate is used as the electron donor under different TEAPs. This suggests that the variation in  $K_D$  values could be due, at least in part, to the different proton and electron translocation mechanisms mediated by different microorganisms and/or for different TEAPs. Based on the experimental results, it is not clear whether the standard redox potential of the electron donor couple and/or the translocation mechanism plays an important role in affecting the values of  $K_D$  determined in this study. However, if the former factor was predominant, the values of  $K_D$  should be equal or comparable for the experimental systems used in this study. On the other hand, if the latter factor played a

crucial role in determining  $K_D$ , the values of  $K_D$  would be determined case by case for different microorganisms and different TEAPs. The results qualitatively support the idea that the translocation mechanism affects  $K_D$  values. As previously noted,  $\chi$ , the number of times a rate-limiting step occurs in a respiratory chain is often associated with proton translocation. For Fe(III)- and nitrate-reducing and methanogenic conditions, a value of  $\chi=8$  was assumed and the lowest  $K_D$  values were associated with these TEAPs. In contrast,  $\chi$  values of four and one were assumed for Mn(IV)- and sulfate-reducing conditions, and higher  $K_D$  values were determined for these two TEAPs. In addition, the  $K_D$  term in the microbial respiration model is somewhat analogous to the half-saturation constant,  $K$ , in the Monod model. The Monod  $K$  term is not directly related to the thermodynamics of metabolic reactions, as previously suggested (Lovley and Goodwin, 1988). However, intuitively it makes sense that as the thermodynamics of the metabolic reaction become less favorable, the substrate affinity is likely to increase, because this would increase the likelihood that metabolism can occur for relatively unfavorable substrates present at low concentrations. If  $K_D$  in the microbial respiration model is also related to substrate affinity, then it might also be expected to decrease in the order predicted by thermodynamics, i.e., for this study: Mn(IV)-reducing  $\approx$  nitrate-reducing  $>$  Fe(III)-reducing  $>$  sulfate-reducing  $>$  methanogenesis. In general, this trend was observed for the  $K_D$  values determined in this study, except that the relative magnitudes of the  $K_D$  values for nitrate- and sulfate-reducing conditions were reversed relative to the predicted order. Finally, it should be recognized that at least some of the variation in  $K_D$  values can also probably be attributed to the apparently low sensitivity of the model to

this parameter.

Comparison of the experimental data to the model-simulated results demonstrates a good fit to the protein, electron donor and electron acceptor data under different TEAPs, except for methanogenesis (Figures 6.9—6.14). The simulated curves capture the main trends in the concentrations of protein, electron donor and electron acceptors. The simulated curves characterize a very short or non-obvious lag phase, followed by an exponential phase, and then present a stationary phase. In contrast, the simulated curve does not capture the trend in the protein, acetate, and methane concentrations under the methanogenic condition as well as under the other conditions. This can be observed by visually examining Figure 6.14 and from the relatively large weighted sum of the square error (Table 6.2). Setting a weighted error of 1 in the optimization technique improved the fit somewhat for the methanogenic conditions (results are not shown). However, the inability of the model to describe the methanogenic data is probably largely due to the lack of a term for modeling significant adaptation (or lag) periods, which were observed under methanogenic, and, to a lesser extent, under sulfate-reducing conditions.

### **6.3.3 Controlling effects of $F_D$ and $F_T$ on acetate thresholds**

To evaluate the factors controlling the acetate thresholds, the thermodynamic factor  $F_T$  and kinetic factor  $F_D$  were calculated using Equations (5.13) and (5.14).  $F_T$  and  $F_A$  were calculated from the experimental data and plotted in Figures 6.15 to 6.20, along with the experimentally-determined protein and acetate concentrations.

In the two Fe(III)-reducing threshold experiments, the thermodynamic factor  $F_T$  remained at a value of 1 throughout the experiment, and the kinetic factor  $F_D$  was also

very high ( $>0.99$ ) at the conclusion of the experiment (Figure 6.15). If  $F_T$  and  $F_D$  (and  $F_A$ ) were equal to 1, then Equations 5.16 and 5.17 indicate that the respiration rate was at its maximum value throughout the duration of the experiment and acetate should have been continuously consumed during this period. However, small but statistically consistent acetate thresholds were measured during both of these experiments. There are several possible explanations for the discrepancy between the trends in the thermodynamic and kinetic factors and the occurrence of acetate thresholds under Fe(III)-reducing conditions. First, it is possible that other factors contributed to the acetate thresholds. For example, at sufficiently low substrate concentrations, the necessary enzyme regulation may not occur (Rittmann et al., 1994). Alternatively, at very low substrate concentrations, the energy available for acetate uptake may be inadequate. This was recently observed for an organism that grows on acetate oxidations coupled to the reduction of various electron acceptors including chlorinated organic compounds (Sanford, personal communication). Second, it should be noted that the values of  $K_D$  for Fe(III)-reducing conditions, as determined using the optimization routine, were  $10^5$ - or  $10^6$ -fold lower than those determined under Mn(IV)-, nitrate-, and sulfate-reducing conditions. This means that the kinetic factor  $F_D$  had a very tiny effect on acetate thresholds under Fe(III)-reducing conditions, while, as discussed below, it had a big effect on acetate thresholds under Mn(IV)-, nitrate-, and sulfate-reducing conditions, as discussed below. Finally, in the optimization routine, it was assumed that the kinetic factor  $F_A$  is always one. Although this was a reasonable approach to solving a complicated model, it is possible that the assumption that  $K_A=0$  was not appropriate, and as a result,  $F_A$  had an unrecognized negative effect on the respiration rate. If  $F_A$

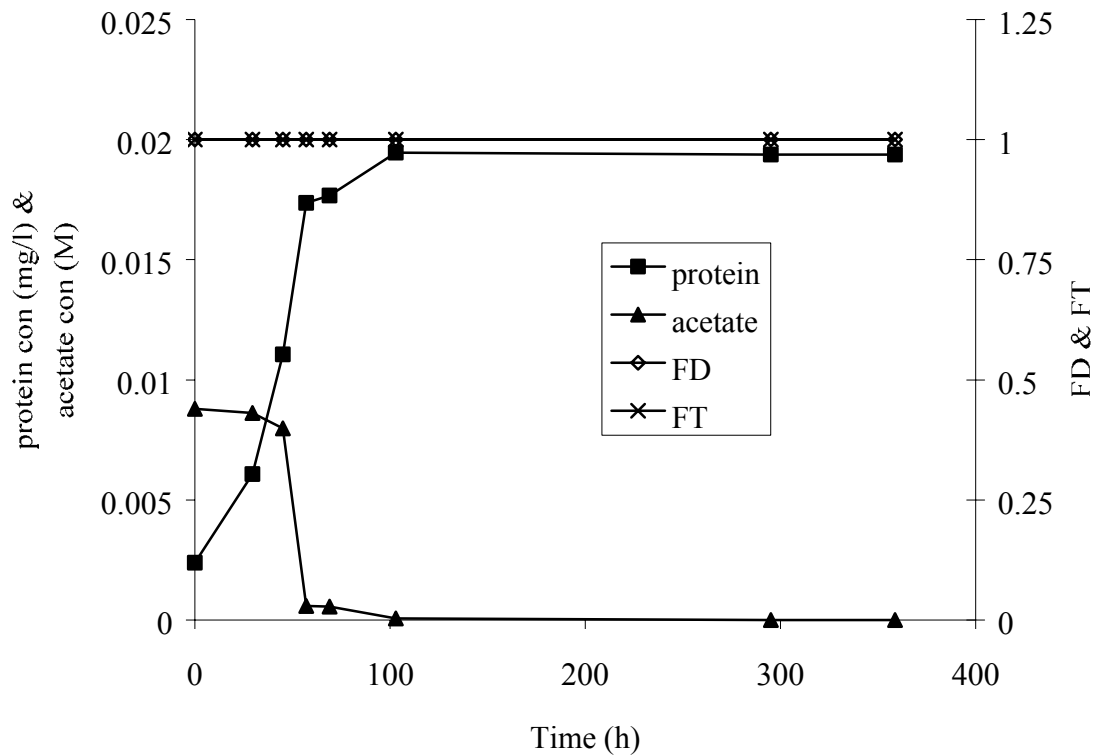


Figure 6.15  $F_D$ ,  $F_T$ , protein, and acetate concentrations under Fe(III)-reducing conditions. The initial concentration of Fe(III) added was 50 mM.

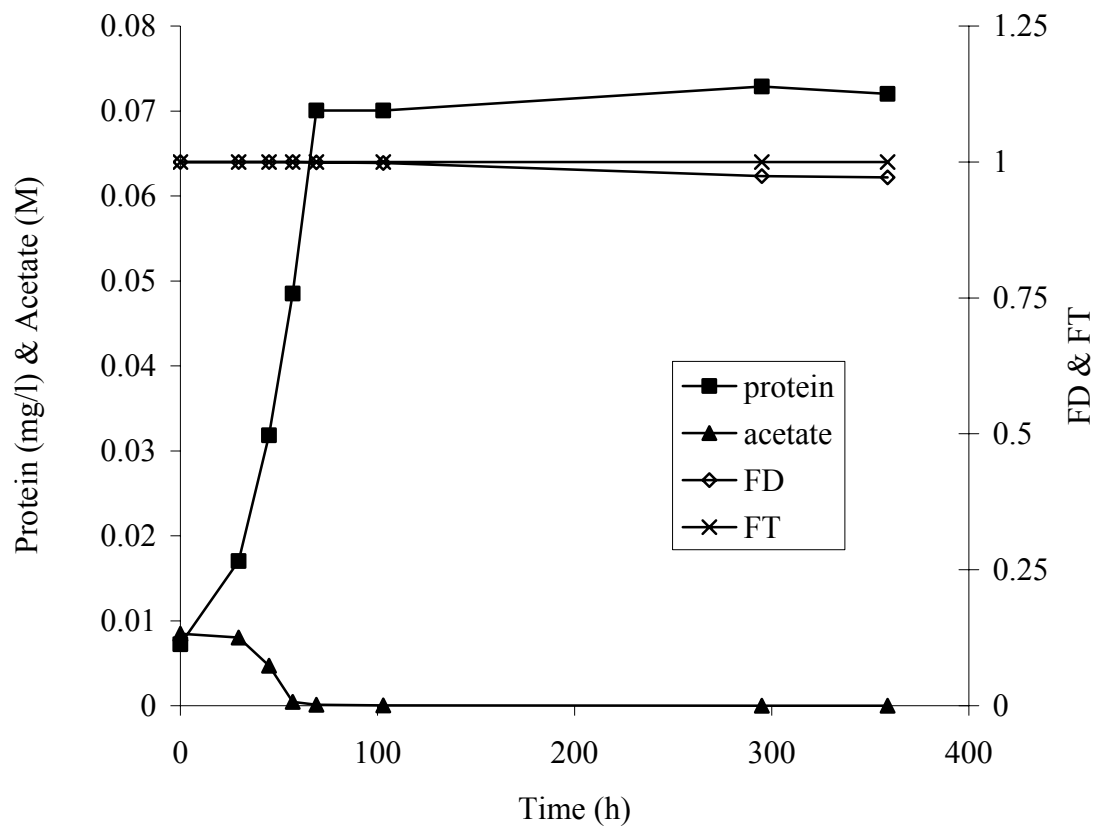


Figure 6.16  $F_D$ ,  $F_T$ , protein, and acetate concentrations under Fe(III)-reducing conditions. The initial concentration of Fe(III) added was 80 mM.

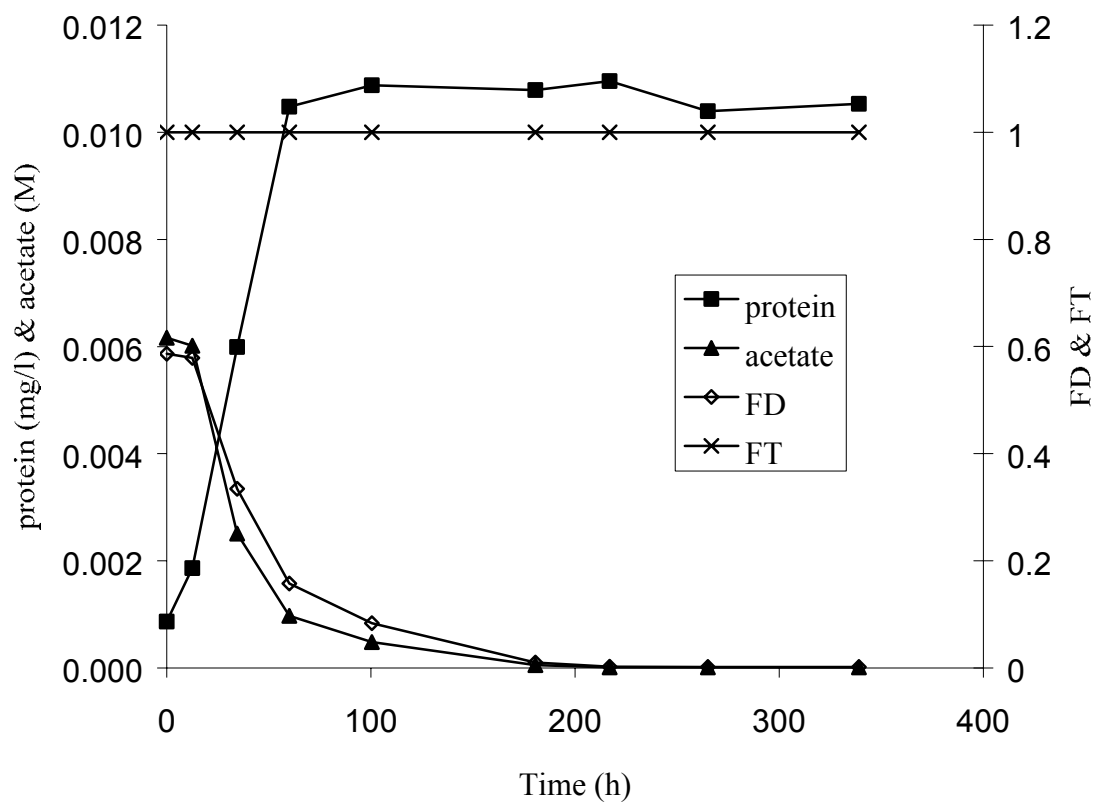


Figure 6.17  $F_D$ ,  $F_T$ , protein, and acetate concentrations under Mn(IV)-reducing conditions.

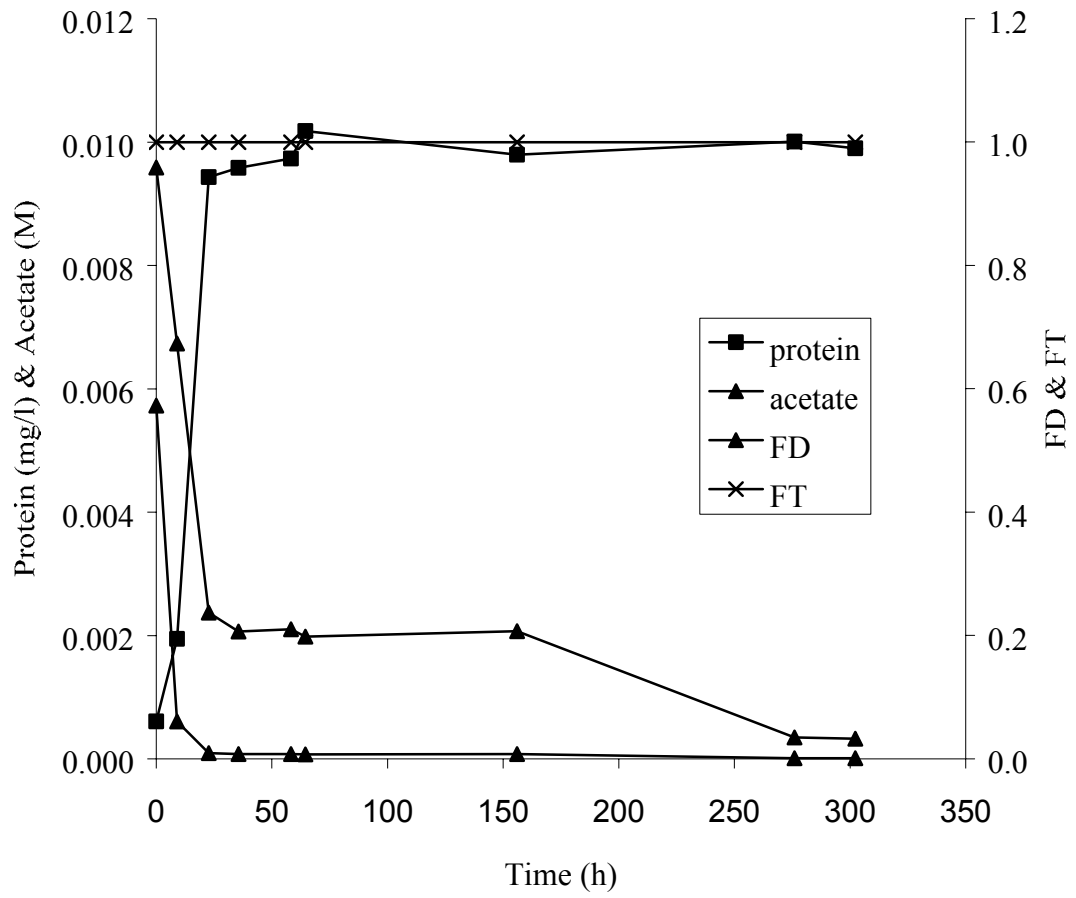


Figure 6.18  $F_D$ ,  $F_T$ , protein, and acetate concentrations under nitrate-reducing conditions.

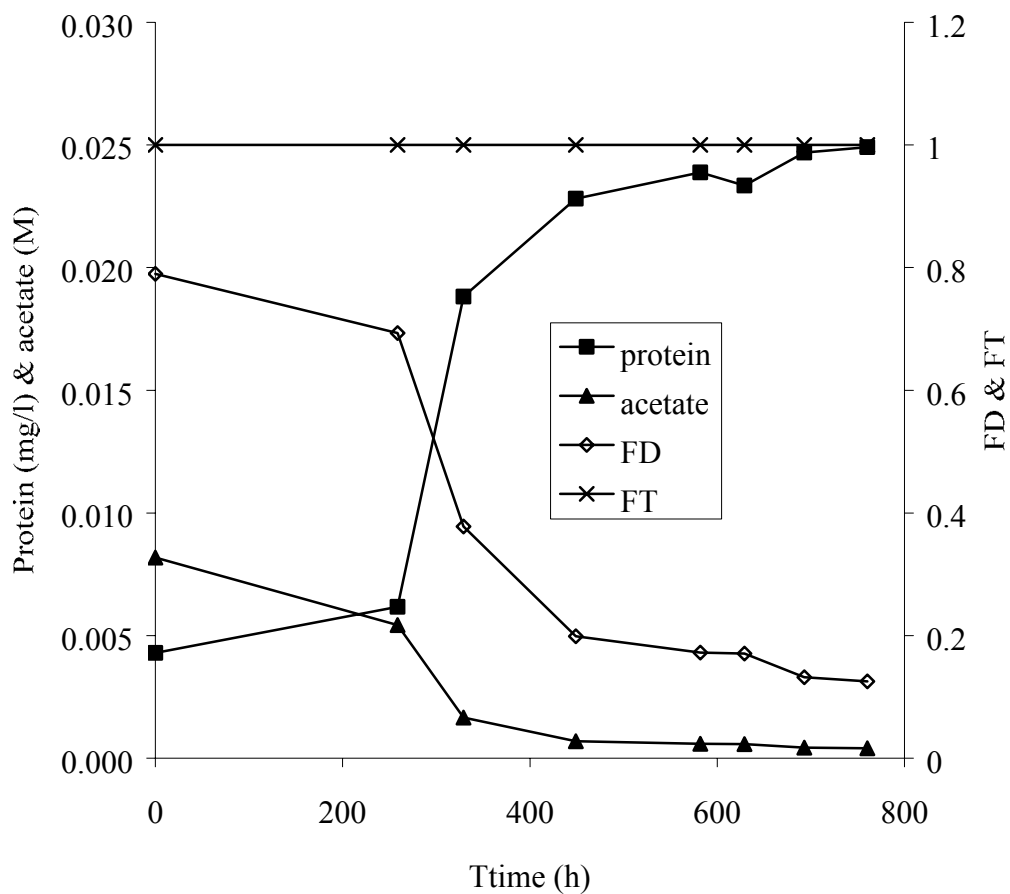


Figure 6.19  $F_D$ ,  $F_T$ , protein, and acetate concentrations under sulfate-reducing conditions.

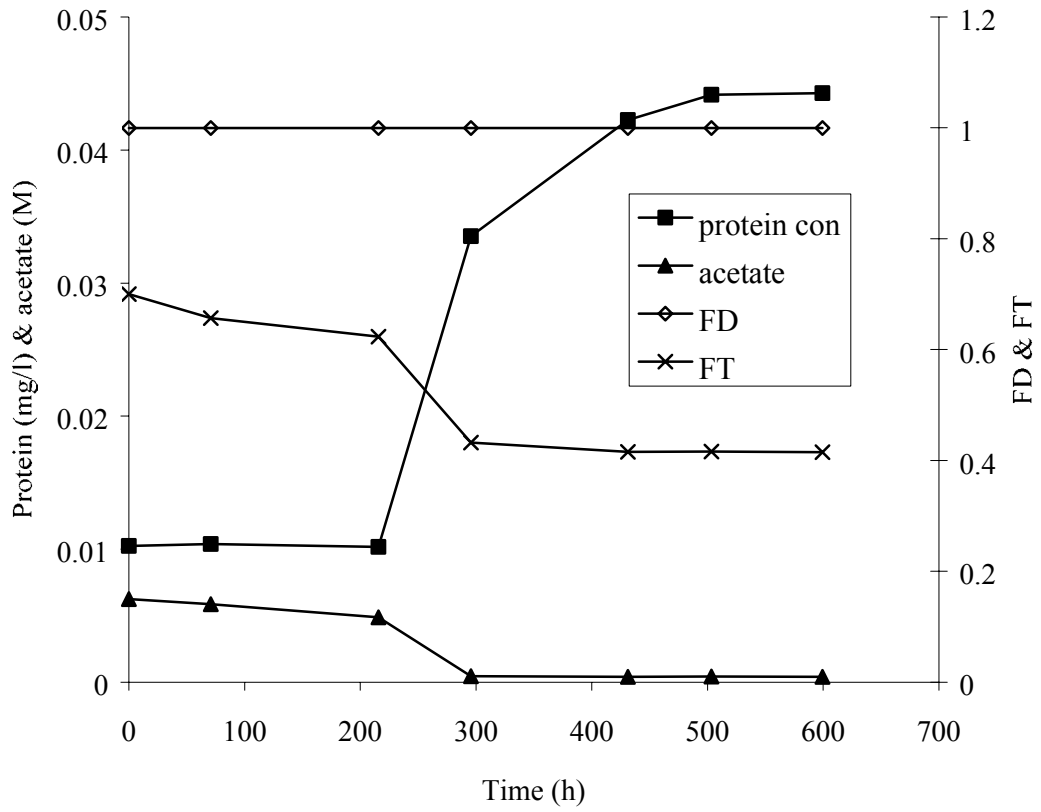


Figure 6.20  $F_D$ ,  $F_T$ , protein, and acetate concentrations under methanogenic conditions.

approached zero, as would be predicted by redox reaction stoichiometry (neglecting biomass synthesis), then the final acetate concentrations could have been determined by available Fe(III) concentrations.

Some important and shared trends were observed for the Mn(IV)-, nitrate-, and sulfate-reducing conditions, as shown in Figures 6.17-6.19. First, in all cases, the trend in the kinetic factor  $F_D$  was very similar to the trend in acetate concentrations. Under each condition, a rapid decrease in the acetate concentration was accompanied by a rapid drop in  $F_D$ , and was followed by a leveling off of the acetate. However,  $F_D$  continued to approach zero, albeit at a very low rate. Second, the thermodynamic factor  $F_T$  remained equal (or very close) to 1 throughout the duration of the three experiments. These results strongly suggest that under Mn(IV)-, nitrate-, and sulfate-reducing conditions, the kinetics of electron donor utilization play an important role in determining acetate thresholds. This is somewhat analogous to kinetic controls on  $S_{\min}$ , the minimum concentration that can sustain steady-state growth, as previously discussed.

In contrast, under methanogenic conditions, the thermodynamic factor  $F_T$  played a more important role in controlling the acetate threshold compared to  $F_D$  (Figure 6.20).  $F_T$  was less than 1 at the onset of the experiment and began decreasing at a relatively low rate immediately. At around 200 h, the rate of decline in  $F_T$  increased, which was associated with a sharp decrease in acetate.  $F_T$  eventually leveled off to approximately 0.4. Throughout this time,  $F_D$  remained equal to one. The reason why the acetate threshold was primarily controlled by thermodynamics is probably that the standard free energy release associated with the aceticlastic methanogenesis process is quite low,

especially in comparison to the free energy releases associated with the other TEAPs examined in this study. Therefore, as observed here, the thermodynamic factor  $F_T$  cannot be assumed to be equal to one and is very sensitive to changes in environmental conditions.

In summary, examination of the kinetic and thermodynamic factors  $F_D$  and  $F_T$  provided valuable insight into the mechanisms controlling acetate thresholds under a variety of TEA conditions that are commonly observed in contaminated groundwater plumes undergoing bioremediation. Based on these evaluations, it appears that acetate thresholds are primarily controlled by electron donor kinetics when the microorganisms can grow utilizing metabolic processes that are relatively favorable from an energetic standpoint. This includes Mn(IV)-, nitrate-, and sulfate-reducing conditions. However, if acetate metabolism is occurring via a form of metabolism such as aceticlastic methanogenesis that generates very little free energy, then acetate concentrations may be controlled by thermodynamic factors. The actual magnitude of kinetically-determined acetate thresholds probably is dependent on the value of  $K_D$  (or  $K_A$ ). As discussed above, according to the respiration rate model,  $K_D$  and  $K_A$  reflect the energy changes associated with the electron-donating and accepting reactions. Therefore, the kinetic factors also involve some thermodynamic elements. The levels of thermodynamically-controlled acetate threshold are probably related to the standard free energy release of the redox reactions. Based on Equation (5.13), the more free energy released, the higher the  $F_T$  value and the higher respiration rate. Thus, more acetate will be consumed before the net respiration rate goes down to zero.

## CHAPTER 7

### Conclusions

The main goal of the project was to evaluate the hypothesis that characteristic ranges of acetate threshold concentrations may exist for different predominant TEAPs, and, thus, may be useful as bioremediation “footprints”.

The threshold experimental results demonstrated that acetate thresholds for the different TEAPs increased in the order of Fe(III)<Mn(IV)  $\approx$  nitrate<sulfate<CO<sub>2</sub>. Acetate thresholds determined under Mn(IV)-, NO<sub>3</sub><sup>-</sup>-, and Fe(III)-reducing conditions appeared to be similar and more than an order of magnitude lower than those determined for less favorable TEAPs such as sulfate-reduction or methanogenesis.

The microbial respiration model provided valuable insight into the mechanisms controlling experimental-determined acetate thresholds. Acetate thresholds were primarily controlled by electron donor kinetics when the microorganisms utilize energetically favorable electron-acceptors, including Mn(IV), nitrate, and sulfate and were controlled by thermodynamic factors under less energetically-favorable conditions such as acetoclastic methanogenesis.

In conclusion, each TEAP appear to establish a characteristic range of acetate threshold concentrations, and the acetate thresholds are controlled kinetically or thermodynamically under different TEAPs. The results of the project suggest that acetate thresholds could be a potentially useful bioremediation indicator, although this must be verified under more complex field conditions.

## References

- Alberty, R.A. 1998. Calculation of standard transformed Gibbs energies and standard transformed enthalpies of biochemical reactants. *Arch. Biochem. Biophys.* 353,116-130.
- Alexander, M. 1999. *Biodegradation and Bioremediation*, Second Edition. Academic Press, San Diego.
- Aubert, C., E. Lojou, P. Bianco, M. Rousset, M. Durand, M. Bruschi and A. Dolla. 1998. The *Desulfuromonas acetoxidans* triheme cytochrome *c7* produced in *Desulfovibrio desulfuricans* retains this metal reductase activity. *Appl. Environ. Microbiol.* 64(4), 1308-1312.
- Bae, W. and B.E. Rittmann. 1996. A structured model of dual-limitation kinetics. *Biotechnol. Bioeng.* 49, 683-689.
- Balch, W.E. and R.S. Wolfe. 1976. New approach to the cultivation of methanogenic bacteria: 2-mercaptoethanesulfonic acid (HS-CoM)-dependent growth of *Methanobacterium ruminantium* in a pressurized atmosphere. *Appl. Environ. Microbiol.* 32(6), 781-791.
- Benjamin, M.M. 2002. *Water Chemistry*, First Edition. McGraw-Hill Companies, Inc., New York.
- Bondoux, G., P. Jandik, and W. R. Jones. 1992. New approach to the analysis of low levels of anions in water. *J.Chromatogr.* 602, 79-88.
- Brown, S.C., C.P.L. Grady and H.H. Tabak. 1990. Biodegradation kinetic of substituted phenolics: demonstration of a protocol based on electrolytic respirometry. *Wat. Res.* 24(7), 853-861.
- Bryant, M.P. 1972. Commentary on the Hungate technique for culture of anaerobic bacteria. *Am. J. Clin. Nutr.* 25, 1324-1328.
- Bryant, M.P. and D.R. Boone. 1987. Emended description of strain MST (DSM 800T), the type strain of *Methanosarcina barkeri*. *Int. J. Syst. Bacteriol.* 37, 169-170.
- Champine, J.E., B. Underhill, J.M. Johnson, W.W. Lilly, and S. Goodwin. 2000. Electron transfer in the dissimilatory iron-reducing bacterium *Geobacter metallireducens*. *Anaerobe.* 6, 187-196.
- Chapelle, F.H. 1997. Identifying redox conditions that favor the natural attenuation of chlorinated ethenes in contaminated groundwater systems. *Proceedings of Symposium on Natural Attenuation of Chlorinated Organics in Groundwater*. US EPA/540/R, 19-22.
- Chapelle, F.H., S.K. Haack, P. Adriaens, M.A. Henry, and P.M. Bradley. 1996.

- Comparison of  $E_h$  and  $H_2$  measurements for delineating redox processes in a contaminated aquifer. *Environ. Sci. Technol.* 30(12), 3565-3569.
- Chapelle, F.H., and D.R. Lovley. 1992. Competitive exclusion of sulfate reduction by FeIII-reducing bacteria: a mechanism for producing discrete zones of high-iron ground water. *Ground Water*. 30, 29-36.
- Chapelle, F.H., P.B. McMahon, N.M. Dubrovsky, R.F. Fuji, E.T. Oaksford, D.A. Vroblesky. 1995. Deducing the terminal electron accepting processes in hydrologically diverse groundwater systems. *Water Resour. Res.* 31, 359-371.
- Chapelle, F.H., D.A. Vroblesky, J.C. Woodward, and D.R. Lovley. 1997. Practical considerations for  $E_h$  and  $H_2$  measurements for delineating redox processes in a contaminated aquifer. *Environ. Sci. Technol.* 30(12), 3565-3569.
- Christensen, T.H., P.L. Bjerg, S.A. Banwart, R. Jakobsen, G. Heron, H.-J. Albrechtsen. 2000. Characterization of redox conditions in groundwater contaminant plumes. *J. Cont. Hydrol.* 45,165-241.
- Conrad, R. 1996. Soil microorganisms as controllers of atmospheric trace gases ( $H_2$ ,  $CO$ ,  $CH_4$ ,  $OCS$ ,  $N_2O$ , and  $NO$ ). *Microbiol. Rev.* 60, 609-640.
- Cooney, M.J., E. Roschi, I.W. Marison, C. Comminellis, and U. Von Stockar. 1996. Physiologic studies with the sulfate-reducing bacterium *Desulfovibrio desulfuricans*: Evaluation for use in a biofuel cell. *Enzyme Microb. Technol.* 18(5), 358-365.
- Cord-Ruwisch, R., Seitz, H. and Conrad, R. 1988. The capacity of hydrogenotrophic anaerobic bacteria to compete for traces of hydrogen depends on the redox potential of the terminal electron acceptor. *Arch. Microbiol.* 149, 350-357.
- Crawford, R.L. and D.L. Crawford. 1996. *Bioremediation: Principle and Application*. Cambridge University Press, New York.
- Daniels, L., R.S. Hanson and J.A. Phillips. 1994. Chapter 22. Chemical Analysis, p. 512-554, In: *Methods for General and Molecular Bacteriology*, P. Gerhardt, ed-in-chief. American Society for Microbiology, Washington, D.C.
- Deppenmeier, U. 2002. Redox-driven proton translocation in methanogenic Archaea. *Cel. Mol. Lif. Sci.* 59(9), 1513-1533.
- Dua, M., A. Singh, N. Sethunathan, A.K. Johri. 2002. Biotechnology and bioremediation: successes and limitations. *Appl. Microbiol. Biotechnol.* 59,143-152.
- Elferink, S. J. W. H. O., S. B. I. Luppens, C. L. M. Marcelis, and A. J. M. Stams. 1998. Kinetics of acetate oxidation by two sulfate reducers isolated from anaerobic granular sludge. *Appl. Environ. Microbio.* 64(6), 2301-2303.

- Esener, A.A., J.A. Roels and N.W.F. Kossen. 1983. Theory and applications of unstructured growth models: kinetic and energetic aspects. *Biotechnol. Bioeng.* 25, 2803-2841.
- Eweis, J.B, S.J. Ergas, D.Y. Chang, and E.D. Schroeder. 1998. *Bioremediation Principles*. McGraw-Hill Companies, Inc., New York.
- Fennell, D. E. 1998. Comparison of Alternative Hydrogen Donors for Anaerobic Reductive Dechlorination of Tetrachloroethene. Ph.D. Dissertation. Cornell University, Ithaca, NY.
- Fennell, D.E. and J.M. Gossett. 1998. Modeling the production of and competition for hydrogen in a dechlorinating culture. *Environ. Sci. Technol.* 32, 2450-2460.
- Ferguson, T.J. and R.A. Mah. 1983. Isolation and characterization of an H<sub>2</sub>-oxidizing thermophilic methanogen. *Appl. Environ. Microbiol.* 45, 265-274.
- Fukuzaki, S., N. Nishio, and S. Nagai. 1990. Kinetics of the methanogenic fermentation of acetate. *Appl. Environ. Microbiol.* 56(10), 3158-3163.
- Galli, R. and P.L. McCarty. 1989. Biotransformation of 1,1,1-trichloroethane, trichloromethane, and tetrachloromethane by a *Colstridium* sp. *Appl. Environ. Microbiol.* 55(4), 837-844.
- Galushko, S. A. and B. Schink. 2000. Oxidation of acetate through reactions of the citric acid cycle by *Geobacter sulfurreducens* in pure culture and in syntrophic coculture. *Arch. Microbiol.* 174, 314-321.
- Giraldo-Gomez, E., S. Goodwin and M. Switzenbaum. 1992. Influence of mass transfer limitations on determination of the half saturation constant for hydrogen uptake in a mixed-culture CH<sub>4</sub>-producing enrichment. *Biotechnol. Bioeng.* 40, 768-776.
- Grady, C.P.L., B.F. Smets, and D.S. Barbeau. 1996. Variability in kinetic parameter estimates: a review of possible causes and a proposed terminology. *Wat. Res.* 30(3), 742-748.
- Hansen, T. A. 1994. Metabolism of sulfate-reducing prokaryotes. *Antonie van Leeuwenhoek* 66, 165-185.
- Heiden, S., R. Hedderich, E. Setzke and P.K. Thauer. 1994. Purification of a two-subunit cytochrome-b-containing heterodisulfide reductase from methano-grown *Methanosarcina barkeri*. *Eur. J. Biochem.* 1221(2), 855-61.
- Ho, T., M.I. Scranton and G.T. Taylor. 2002. Acetate cycling in the water column of the Cariaco basin: seasonal and vertical variability and implication for carbon cycling.

Limnol. Oceanogr. 47, 1119-1128.

Hoehler, T.M., M.J. Alperin, D.B. Albert, and C.S. Martens. 1998. Thermodynamic control on hydrogen concentrations in anoxic sediment. *Geochim. Cosmochim. Acta.* 62(10), 1745-1756.

Hoh, C.Y. and R. Cord-Ruwisch. 1996. A practical kinetic model that considers end product inhibition in anaerobic digestion processes by including the equilibrium constant. *Biotechnol. Bioengin.* 51, 597-604.

Hoh, C. and R. Cord-Ruwisch. 1997. Experimental evidence for the need of thermodynamic considerations in modeling of anaerobic environmental bioprocesses. *Wat. Sci. Tech.* 36(10), 109-115.

Hopkins, B.T., M.J. McInerney, and V. Warikoo. 1995. Evidence for an anaerobic syntrophic benzoate degradation threshold and isolation of the syntrophic benzoate degrader. *Appl. Environ. Microbiol.* 61(2), 526-530.

Huang, J., J. Her, and C Jih. 1997. Kinetic of denitrification and denitrification in anoxic filters. *Biotechnol. Bioengin.* 59(1), 52-61.

Hungate, R.E. 1950. The anaerobic mesophilic cellulolytic bacteria. *Bacteriol. Rev.* 14, 1-49.

Hunter, K.S., Y Wang, P.V Cappellen. 1998. Kinetic modeling of microbially-driven redox chemistry of subsurface environments: coupling transport, microbial metabolism and geochemistry. *J. Hydrol.* 209, 53-80.

Jackson, B.E. and M.J. McInerney. 2002. Anaerobic microbial metabolism can proceed close to thermodynamic limits. *Nature.* 415, 454-456.

Jin, Q. and C.M. Bethke. 2002. Kinetics of electron transfer through the respiratory chain. *Biophysical J.* 83, 1797-1808.

Jin, Q. and C.M. Bethke. 2003. A new rate law describing microbial respiration. *Appl. Environ. Microbiol.* 69(4), 2340-2348.

King, G.M. 1991. Measurement of acetate concentrations in marine pore waters by using an enzymatic approach. *Appl. Environ. Microbiol.* 57, 3476-3481.

Kleerebezem, R., and A.J.M. Stams. 2000. Kinetics of syntrophic cultures: a theoretical treatise on butyrate fermentation. *Biotechnol. Bioengin.* 67(5), 528-543.

Kovárová-Kovar, K., and T. Egli. 1998. Growth kinetics of suspended microbial cells: From single-substrate-controlled growth to mixed-substrate kinetics. *Microbiol. Mol. Biol. Rev.* 62(3), 646-666.

- Liu, C., S. Kota, J.M. Zachara, J.K. Fredrickson, and C.K. Brinkman. 2001a. Kinetic analysis of the bacterial reduction of goethite. *Environ. Sci. Technol.* 35, 2482-2490.
- Liu, C., J.M. Zachara, Y.A. Gorby, J.E. Szecsody, and C.F. Brown. 2001b. Microbial reduction of Fe(III) and sorption/precipitation of Fe(II) on *Shewanella putrefaciens* strain CN32. *Environ. Sc. Technol.* 35, 1385-1393.
- Liu, C., Y.A. Gorby, J.M. Zachara, J.K. Fredrickson, and C.F. Brown. 2002. Reduction kinetics of Fe(III), Co(III), U(VI), Cr(VI), and Tc(VII) in Cultures of dissimilator metal-reducing bacteria. *Biotechnol. Bioengin.* 80(6), 637-649.
- Löffler, F.E., J.M. Tiedje, and R.A. Sanford. 1999. Fraction of electron consumed in electron acceptor reduction and hydrogen thresholds as indicators of halorespiratory physiology. *Appl. Environ. Microbiol.* 65(9), 4049-4056.
- Lovley, D. R. 1985. Minimum threshold for hydrogen metabolism in methanogenic bacteria. *Appl. Environ. Microbiol.* 49, 1530-1531.
- Lovley, D. R. 1991. Dissimilatory Fe(III) and Mn(IV) reduction. *Microbiol. Rev.* 55(2), 259-287.
- Lovley, D.R., and S. Goodwin. 1988. Hydrogen concentrations as an indicator of the predominant terminal electron-accepting reactions in aquatic sediments. *Geochim. Cosmochim. Acta* 52, 2993-3003.
- Lovley, D.R. and E.J.P. Phillips. 1987. Competitive mechanisms for inhibition of sulfate reduction and methane production in the zone of ferric iron reduction in sediments. *Appl. Environ. Microbiol.* 53, 2636-2641.
- Lovley, D.R., and E.J.P. Phillips. 1988. Novel mode of microbial energy metabolism: organic carbon oxidation coupled to dissimilatory reduction of iron or manganese. *Appl. Environ. Microbiol.* 54(6), 1472-1480.
- Lowry, O.H., N.J. Rosebrough, A.L. Farr, and R.J. Randall. 1951. Protein measurement with the folin phenol reagent. *J. Biol. Chem.* 193, 265-275.
- Ludvigsen, L., H.J. Albrechtsen, G. Heron, P.L. Bjerg, and T.H. Christensen. 1998. Anaerobic microbial redox processes in a landfill leachate contaminated aquifer (Grindsted, Denmark). *J. Cont. Hydrol.* 33, 273-291.
- Madsen, E.L. 1991. Determining *in situ* biodegradation: Facts and challenges. *Environ. Sci. Technol.* 25, 1661-1673.
- Magbanua, B.S., Y. Lu and C.P. L. Grady. 1998. A technique for obtaining representative biokinetic parameter values from replicate sets of parameter estimates. *Wat. Res.*, 32(3),

849-855.

McCarty, P. L. 1972. Energetics of organic matter degradation, p. 91-118. In R. Mitchell (ed.), *Water Pollution Microbiology*, vol. 1. Wiley-Interscience, New York.

McCarty, P.L. 1975. Stoichiometry of biological reactions. *Progress in Water Technol.* 7(1), 157-172.

McMahon, P.B., and F.H Chapelle. 1991. Microbial production of organic acids in aquitard sediments and its role in aquifer geochemistry. *Nature.* 349, 233-235.

Middleton, A. C. and A. W. Lawrence. 1977. Kinetics of microbial sulfate reduction. *J. WPCF*, 1659-1670

Miller, T.L. and M.J. Wolin. 1974. A serum bottle modification of the Hungate technique for cultivating obligate anaerobes. *Appl. Microbiol.* 27(5), 985-987.

Min, H. and S.H. Zinder. 1989. Kinetics of acetate utilization by two thermophilic acetotrophic methanogens: *Methanosarcina sp.* Strain CALS-1 and *Methanotherix sp.* Strain CALS-1. *Appl. Environ. Microbiol.* 55, 488-491.

Mitchell, P. 1961. Coupling of phosphorylation to electron and hydrogen transfer by a chemi-osmotic type of mechanism. *Nature.* 191, 144-148.

Myers, C.R., J.M. Myers. 1994. Ferric iron reduction-linked growth yields of *Shewanella putrefactans* MR-1. *J. Appl. Bacteriol.* 76(3), 253-258.

Myers, C.R. and K.H Nealon. 1988. Bacterial manganese reduction and growth with manganese oxide as the sole electron acceptor. *Science.* 240, 1319-1321.

National Research Council (NRC). 1993. *In situ* bioremediation: when does it work? B.E. Rittmann, Chairman, National Academy Press, Washington, DC.

Noguera, D.R., G.A. Brusseau, B.E. Rittmann and D.A. Stahl. 1998. Unified model describing the role of hydrogen in the growth of *Desulfovibrio vulgaris* under different environmental conditions. *Biotechnol. Bioengin.* 59(6), 732-746.

Oremland, R.S., J.S. Blum, A.B. Bindi, P.R. Dowdle, M. Herbel, and J.F. Stolz. 1999. Simultaneous reduction of nitrate and selenate by cell suspensions of selenium-respiring bacteria. *Appl. Environ. Microbiol.* 65(10), 4385-4392.

Oude Elferink, S.J.W.H., A. Visser, L. W. H. Pol and A. J. M. Stams. 1994. Sulfate reduction in methanogenic bioreactors. *FEMS Microbiol. Rev.* 15, 119-136.

Oude Elferink, S. J. W. H., S. B. I. Luppens, C. L. M. Marcelis, and A. J. M. Stams. 1998. Kinetics of acetate oxidation by two sulfate reducers isolated from anaerobic

- granular sludge. *Appl. Environ. Microbiol.* 64(6), 2301-2303.
- Panikov, N.S. 1995. *Microbial Growth Kinetics*. London: Chapman & Hall.
- Pfeiffer, T., S. Schuster, and S. Bonhoeffer. 2001. Cooperation and competition in the evolution of ATP-producing pathways. *Science*. 292, 504-507.
- Pirt, S.S. 1975. *Principles of Microbe and Cell Cultivation*. John Wiley Sons, New York.
- Postma, D. and R. Jakobsen. 1996. Redox zonation: equilibrium constraints on the Fe(III)/SO<sub>4</sub>-reduction interface. *Geochim. Cosmochim. Acta.* 60(17), 3169-3175.
- Price, N.C., R.A. Dwek, R.G. Ratcliffe and M.R. Wormald. 2001. *Principles and problems in physical chemistry for biochemists*. New York: Oxford University Press, Inc.
- Rittmann, B.E. and P.L. McCarty. 2001. *Environmental Biotechnology: Principles and Applications*. McGraw-Hill Companies, Inc., New York.
- Rittman, B.E., E. Seagren, B.A. Wrenn, A.J. Valocchi, C. Ray and L. Raskin. 1994. *In Situ Bioremediation*. 2<sup>nd</sup> ed. Noyes Publications, Park Ridge, NJ
- Robinson, J. A. and J. M. Tiedje. 1984. Competition between sulfate-reducing and methanogenic bacteria for H<sub>2</sub> under resting and growing conditions. *Arch. Microbiol.* 137, 26-32.
- Russell, J.B. and G.M. Cook. 1995. Energetics of bacterial growth: balance of anabolic and catabolic reactions. *Microbiol. Rev.* 59, 48-62.
- Schink, B. 1997. Energetic of syntrophic cooperation in methanogenic degradation. *Appl. Environ. Microbiol.* 61(2), 262-280.
- Seagren, E.A., and J.G. Becker. 1999. Organic acids as a bioremediation monitoring tool, P.343-348. *In* B.C. Alleman and A. Leeson (ed.), *Natural Attenuation of Chlorinated Solvents, Petroleum Hydrocarbons, and Other Organic Compounds*. Battelle Press, Columbus, OH.
- Seagren, E.A., and J.G. Becker. 2002. Review of natural attenuation of BTEX and MTBE in groundwater. *Practice Periodical of Hazardous, Toxic, and Radioactive Waste Management, ASAE.* 6(3), 156-172.
- Simon, J. 2002. Enzymology and bioenergetics of respiratory nitrite ammonification. *FEMS Microbiol. Rev.* 26:285-309.
- Simon, J., R. Gross, O. Einsle, P. M. H. Kroneck, A. Kröger, and O. Klimmek. 2000. A NapC/NirT-type cytochrome c (NrfH) is the mediator between the quinone pool and the cytochrome c nitrite reductase of *Wolinella succinogenes*. *Mol. Microbiol.* 35, 686-696.

- Smith, P.K., R.I. Krohn, G.T. Hermanson, A.K. Mallia, F.H. Gartner, M.D. Provenzano, E.K. Fujimoto, N.M. Goeke, B.J. Olson, and D.C. Klenk. 1985. Measurement of protein using bicinchoninic acid. *Anal. Biochem.* 150, 76-85.
- Snoeyink, V.L., and D. Jenkins. 1980. *Water Chemistry*. John Wiley & Sons, Inc., New York.
- Thauer, R.K., D. Möller-Zinkhan, and A.M. Spormann. 1989. Biochemistry of acetate catabolism in anaerobic chemotrophic bacteria. *Ann. Rev. Microbiol.* 43, 43-67.
- Thauer, R.K., K. Jungermann, and K. Decker. 1977. Energy conservation in chemotrophic anaerobic bacteria. *Bacteriol. Rev.* 41, 100-179.
- Van Spanning, R.J.M., A.P.N. de Boer, W.N.M. Reijnders, J.W.L. De Gier, C.O. Delorme, A.H. Stouthamer, H.V. Westerhoff, N. Harms, and J. van der Oost. 1995. Regulation of oxidative phosphorylation: the flexible respiratory network of *Paracoccus denitrificans*. *J. Bioenerg. Biomembr.* 27, 499-512.
- Warikoo, V., M. J. McInerney, J.A. Robinson and J.M. Suflita. 1996. Interspecies acetate transfer influences the extent of anaerobic benzoate degradation by syntrophic consortia. *Appl. Environ. Microbiol.* 62(1), 26-32.
- Watson, I.A., S.E. Oswald, K.U. Mayer, Y. Wu, and S.A. Banwart. 2003. Modeling kinetic processes controlling hydrogen and acetate concentrations in an aquifer-derived microcosm. *Environ. Sci. Technol.* 37, 3910-3919.
- Westermann, P., B.K. Ahring, and R.A. Mah. 1988. Threshold acetate concentrations for acetate catabolism by aceticlastic methanogenic bacteria. *Appl. Environ. Microbiol.* 55(2), 514-515.
- Westermann, P., B.K. Ahring, R.A. Mah. 1989. Acetate production by methanogenic bacteria. *Appl. Environ. Microbiol.* 55(9), 2257-2261.
- White, D. 1995. *The physiology and biochemistry of prokaryotes*. New York: Oxford University Press, Inc.
- Widdel, F. and N. Pfennig. 1977. A new anaerobic, sporing, acetate-oxidizing, sulfate-reducing bacterium, *Desulfotomaculum* (emend.) *acetoxidans*. *Arch. Microbiol.* 112, 119-122.
- Widdel, F. and N. Pfennig. 1981. Sporulation and nutritional characteristics of *Desulfotomaculum acetoxidans*. *Arch. Microbiol.* 129, 401-402.
- Wiechelmann, K.J., R.D. Braun, and J.D. Fitzpatrick. 1988. Investigation of the bicinchoninic acid protein assay-identification of the groups responsible for color

formation. *Anal. Biochem.* 175, 231-237.

Wolin, E.A., M.J. Wolin, and R.S. Wolfe. 1963. Formation of methane by bacterial extracts. *J. Biol. Chem.* 238, 2882-2886.

Wu, H. and M.I. Scranton. 1994. Cycling of some low molecular weight volatile fatty acids in a permanently anoxic estuarine basin. *Mar. Chem.* 47, 97-113.

Zeikus, J.G., R. Kerby and J.A. Krzycki. 1985. Single-carbon chemistry of acetogenic and methanogenic bacteria. *Science.* 227(4691), 1167-1173.

Zwolinski, M.D., R.F. Harris, and W.J. Hickey. 2000. Microbial consortia involved in the anaerobic degradation of hydrocarbons. *Biodegradation.* 11, 141-158.

## Appendix: Matlab Optimization Routine

### 1. T\_JB\_reg\_model.m

```
function dXdt = T_JB_reg_model(t, X)
% model JB1 with time-interpolated values of D, D+ and FT
global k Y KD KA
global d0 d1 d0p d1p a0 a1 a0m a1m f0 f1
% interpolate donor and acceptor concentrations from data
D = d0 + d1*X;
Dp = d0p + d1p*X;
A = a0 + a1*X;
Am = a0m + a1m*X;
if f0 == 0
    FT = 1;
else
    FT = 1 - f0 * (Dp*A/D)^f1;
end
% calculate Fd and Fa:
FD = D / (D + KD * Dp);
FA = A / (A + KA * Am);

% calculate growth rate
dXdt = Y * k * X * FD * FA * FT;
```

### 2. T\_JB1\_reg\_fit.m

```
%-----
% Fit Jin and Bethke model with FA = 1 to experimental data
%-----

format compact

global k Y KD KA

global t_fit X_fit D_fit Dp_fit A_fit Am_fit FT_fit

global d0 d1 d0p d1p a0 a1 a0m a1m f0 f1

global weights
```

```

num_experiments = 6;

filenames = [...

    'data_FeII50mM    '
    'data_FeII80mM    '
    'data_nitrate     '
    'data_Mn          '
    'data_Sulfate     '
    'data_Methanogenesis'];

%-----

% loop over the experimental data sets

%-----

for eid = 1:num_experiments

    %-----

    % load raw data

    %-----

    '-----'

    data_set = filenames(eid,:);

    eval(data_set);

    % extract experiment A, B or C: times, protein, acetate, acceptor

    t = Su_data(:,1);

    X = mean(Su_data(:,col_ids(1)+[0:num_replicates-1]),2);

    Xstd = std(Su_data(:,col_ids(1)+[0:num_replicates-1]),0,2);

```

```

D = mean(Su_data(:,col_ids(2)+[0:num_replicates-1]),2);
Dp = mean(Su_data(:,col_ids(3)+[0:num_replicates-1]),2);
A = mean(Su_data(:,col_ids(4)+[0:num_replicates-1]),2);
Am = mean(Su_data(:,col_ids(5)+[0:num_replicates-1]),2);
FT = ones(size(t));
if eid > 5
    FT = mean(Su_data(:,end-num_replicates+1:end),2);
end
% extract the portion of the data used for the FIT
pre_spike = find(t < spike_time);
t_fit = t(pre_spike);
X_fit = X(pre_spike,:);
Xstd_fit = Xstd(pre_spike,:);
D_fit = D(pre_spike,:);
Dp_fit = Dp(pre_spike,:);
A_fit = A(pre_spike,:);
Am_fit = Am(pre_spike,:);
FT_fit = FT(pre_spike,:);
num_rep = 1;
%-----
% perform static regressions, calculate Y
%-----
% D(X)

```

```

DrX = polyfit(X_fit,D_fit,1);
d0 = DrX(2); d1 = DrX(1);

% D+(X)

DprX = polyfit(X_fit,Dp_fit,1);
d0p = DprX(2); d1p = DprX(1);

% A(X)

ArX = polyfit(X_fit,A_fit,1);
a0 = ArX(2); a1 = ArX(1);

% A-(X)

AmrX = polyfit(X_fit,Am_fit,1);
a0m = AmrX(2); a1m = AmrX(1);

% FT(A,D,D+)

f0 = 0 ; f1 = 0;

if eid > 5

    FTrAD = polyfit(log(Dp_fit.*A_fit./D_fit),log(1-FT_fit),1);

    f0 = exp(FTrAD(2)) ; f1 = FTrAD(1);

end

%% FT_check = [1-f0*(Dp_fit.*A_fit./D_fit).^f1 FT_fit]'

% X(D) and Y

XrD = polyfit(D_fit,X_fit,1);

Y = -XrD(1);

%-----

% perform model fits

```

```

%-----
% set guesses for k and KD (KA is set to 0)

tlast = 3;

if eid > 5
    tlast = 4;
end

X0guess = X_fit(1);

kguess = log(X_fit(tlast)/X_fit(1)) / t_fit(tlast) / Y;

KDguess = 0.01;

KA = 0;

% set weights for optimization

weights = 1./Xstd_fit;

%weights = ones(size(Xstd_fit)); % un-comment to set weights to 1

% Optimize

options = optimset('LargeScale', 'on');

[parms, sse, residuals] = ...

    lsqnonlin('T_JB1_reg_fit_error',[kguess KDguess X0guess],[0 0 0],[Inf Inf
X_fit(end)],options);

% Show Results

Y

X0 = parms(3)

k = parms(1)

KD = parms(2)

```

```

KA

sse

%-----

% plot data and results

%-----

% 1- Protein: X(t)

%-----

figure(eid)

subplot(2,2,1)

colors = ['r.' ; 'g.' ; 'b.'];

for rid = 1:num_replicates

    Xsamp = Su_data(:,col_ids(1)+rid-1);

    plot(t,Xsamp,colors(rid,:))

    hold on

end

% Calculate and plot model predictions

options = odeset('RelTol',1e-6,'AbsTol',1e-9);

k = parms(1) ; KD = parms(2) ; KA = 0;

tm = linspace(0,t_fit(end),101);

[times, model_values] = ode23s('T_JB_reg_model',tm,X0,options);

plot(times,model_values,'k')

hold off

% add axis titles, etc...

```

```

xlabel('Time (h)')

ylabel('Protein (mg/l)')

title(data_set(6:end))

%-----

% 2- Donor: D(t)

%-----

subplot(2,2,3)

colors = ['r.' ; 'g.' ; 'b.'];

for rid = 1:num_replicates

    Xsamp = Su_data(:,col_ids(2)+rid-1);

    plot(t,Xsamp,colors(rid,:))

    hold on

end

Dmodel = d0 + d1*model_values;

plot(times,Dmodel,'k')

hold off

% add axis titles, etc...

xlabel('Time (h)')

ylabel('Donor (M)')

%-----

% 3- Acceptor-: A-(t)

%-----

subplot(2,2,4)

```

```

colors = ['r.' ; 'g.' ; 'b.'];

for rid = 1:num_replicates

    Xsamp = Su_data(:,col_ids(5)+rid-1);

    plot(t,Xsamp,colors(rid,:))

    hold on

end

Ammodel = a0m + a1m*model_values;

plot(times,Ammodel,'k')

hold off

% add axis titles, etc...

xlabel('Time (h)')

ylabel('Acceptor- (M)')

%-----

% 4- Regressions

%-----

subplot(4,4,3)

plot(X_fit,D_fit,'k.')

hold on

plot([X_fit(1) X_fit(end)],d0+d1*[X_fit(1) X_fit(end)],'b')

hold off

xlabel('X (mg/l)') ; ylabel('D (M)');

subplot(4,4,4)

plot(X_fit,Dp_fit,'k.')

```

```

hold on
plot([X_fit(1) X_fit(end)],d0p+d1p*[X_fit(1) X_fit(end)],'b')
hold off
xlabel('X (mg/l)' ); ylabel('D+ (M)');
subplot(4,4,7)
plot(X_fit,A_fit,'k.')
hold on
plot([X_fit(1) X_fit(end)],a0+a1*[X_fit(1) X_fit(end)],'b')
hold off
xlabel('X (mg/l)' ); ylabel('A (M)');
subplot(4,4,8)
plot(X_fit,Am_fit,'k.')
hold on
plot([X_fit(1) X_fit(end)],a0m+a1m*[X_fit(1) X_fit(end)],'b')
hold off
xlabel('X (mg/l)' ); ylabel('A- (M)');
end

```

### 3. T\_JB1\_reg\_fit\_error.m

```

function ferror = T_JB1_reg_fit_error(parms)
global k Y KD KA
global t_fit X_fit D_fit Dp_fit A_fit Am_fit FT_fit
global weights

```

```

k = parms(1);
KD = parms(2);
X0 = parms(3);
options = odeset('RelTol',1e-6,'AbsTol',1e-9);
[times, model_values] = ode23s('T_JB_reg_model',t_fit,X0,options);
ferror = weights .* (model_values - X_fit);

```

#### 4. data\_FeII50mM.m

%50 mMF(II)-reduction threshold

%TimeFe(II) (mM) (M)	Acetate (M)		Protein (mg/l)		Acetate (mM)		Fe(II) (M)		Fe(III)	
	A	B	A	B	A	B	A	B	A	B

Su\_data = [...

0	0.13	0.11	3.326	1.446	8.3281	9.2517	0.00013		0.00011	0.05
	0.05	0.0083281	0.0092517	0.043	0.043					
29.5	1.16	2.15	6.317	5.831	8.1322	9.1199	0.00116		0.00215	
	0.04897		0.04796		0.0081322	0.0091199			0.043337345	
	0.043231301									
45	7.61	7.97	10.933	11.176	7.0515	8.9126	0.00761		0.00797	
	0.04252		0.04214		0.0070515	0.0089126			0.045125208	
	0.043574249									
57	31.96		27.57	16.467	18.263	0.5854	0.5907	0.03196		0.02757
	0.01817		0.02254		0.0005854	0.0005907			0.055822439	
	0.057341634									
69	30.69		31.91	16.766	18.563	0.5717	0.5567	0.03069		0.03191
	0.01944		0.0182	0.0005717	0.0005567	0.055845104			0.057397883	
103	32.05		30.26	20.958	17.964	0.0571	0.0697	0.03205		0.03026
	0.01808		0.01985		0.0000571	0.0000697			0.056696436	

```

0.058203554

295    34.38    34.65 18.534 20.219 0.0076 0.0054 0.03438    0.03465
      0.01575    0.01546    0.0000076    0.0000054    0.056778326
      0.058309929

358.75 34.91 35.09 18.955 19.798 0.0055 0.0055 0.03491    0.03509
      0.01522    0.01502    0.0000055    0.0000055    0.0567818
      0.058309764

382    34.74    36.08 19.798 18.113 0.1201 0.1084 0.03474    0.03608
      0.01539    0.01403    0.0001201    0.0001084    0.056592211
      0.05813953

430    36.08    37.69 23.247 24.041 0.205 0.01611    0.03608
      0.03769    0.01405    0.01242    0.000205    0.00001611
      0.056451756 0.058292211

582.5 36.88 36.71 23.81 24.503 0.007 0.0072 0.03688    0.03671
      0.01325    0.0134 0.000007    0.0000072    0.056779319 0.058306951

846    37.24    37.06 23.823 24.674 0.0068 0.007 0.03724    0.03706
      0.01289    0.01305    0.0000068    0.000007    0.05677965
      0.058307282

```

];

% number of replicates

num\_replicates = 2;

% columns for X, D, D+, A and A- data

col\_ids = [4, 12, 14, 10, 8];

% spike time

spike\_time = 382;

### 5. data\_FeII80mM.m

%80 mMF(II)-reduction threshold

%TimeFe(II) (mM) (M)	Protein (mg/l) Acetate (M)	Acetate (mM) HCO3- (M)	Fe(II) (M)	Fe(III)
-------------------------	-------------------------------	---------------------------	------------	---------

%(h)	C	D	C	D	C	D	C	D	C	D
C		D	C	D						

Su\_data = [...

0	0.20	0.25	3.9	3.33	8.0269	8.9042	0.0002	0.000246195	0.05
0.05		0.0080269		0.0089042	0.043	0.043			
29.5	1.97	1.07	7.53	9.48	7.5717	8.5001	0.001969561	0.001074306	
	0.048230439	0.049171889		0.0075717	0.0085001	0.04376632			
	0.043681782								
45	10.03		11.01	15.55	16.28	4.3903	5.0443	0.010026858	0.011011638
	0.040173142	0.039234557		0.0043903	0.0050443	0.049029488			
	0.049398906								
57	44.58		44.14	25.15	23.35	0.4394	0.4713	0.044583706	0.044136079
	0.005616294	0.006110116		0.0004394	0.0004713	0.055565683			
	0.056964276								
69	48.04		46.36	36.23	33.83	0.1302	0.1139	0.04804	0.04636
	0.00216	0.003886195		0.0001302	0.0001139	0.05607721			
	0.057555543								
103	45.12		44.94	36.53	33.53	0.0427	0.0513	0.04512	0.04494
	0.00508	0.005306195		0.0000427	0.0000513	0.056221966			
	0.057659105								
295	47.27		48.43	36.65	36.23	0.0039	0.0032	0.04727	0.04843
	0.00293	0.001816195		0.0000039	0.0000032	0.056286155			
	0.05773868								
358.75	48.25	49.15	37.49	34.54	0.004	0.0027	0.04825	0.04915	
	0.00195	0.001096195		0.000004	0.0000027	0.05628599			
	0.057739507								
382	50.85		50.22	37.07	36.64	0.107	0.1106	0.05085	0.05022
	-0.00065	2.61952E-05		0.000107	0.0001106	0.056115591	0.057561002		
430	50.76		50.85	41.61	41.38	0.0513	0.076	0.05076	0.05085
	-0.00056	-0.000603805		0.0000513	0.000076	0.056207739	0.057618243		
582.5	51.66	50.31	41.84	41.61	0.0024	0.0056	0.05166	0.05031	-
	0.00146	-6.38048E-05		0.0000024	0.0000056	0.056288637	0.057734709		

```

846      51.57      48.61 41.69 42.26 0.0025 0.0055 0.05157      0.04861
-0.00137      0.001636195      0.0000025 0.0000055      0.056288471 0.057734875

```

```
];
```

```
Su_data(:,10:11) = Su_data(:,10:11) + 0.03 - 0.0002;
```

```
% number of replicates
```

```
num_replicates = 2;
```

```
% columns for X, D, D+, A and A- data
```

```
col_ids = [4, 12, 14, 10, 8];
```

```
% spike time
```

```
spike_time = 382;
```

## 6. data\_Mn.m

```
%Mn-reduction
```

%TimeProtein (mg/l)	Acetate (mM)			Acetate (M)			Mn(IV) (M)				
	Mn(II) (M) (based on acetate)			Mn(IV) (M)			Mn(IV) (M)				
HCO3- (M)	A	B	C	A	B	C	A	B	C	A	B
% (h)	A	B	C	A	B	C	A	B	C	A	B
C	A	B	C	A	B	C	A	B	C	A	B

```
Su_data = [...
```

```

0      1.012      0.723 0.868 6.1996 6.1048 6.1957 0.0061996      0.0061048
      0.0061957      0.00      0.00      0.00      0.05      0.05      0.05      0.043
0.043      0.043

```

```

12.5   1.943 1.701 1.944 6.0329 6.0101 5.9985 0.0060329      0.0060101
      0.0059985      0.0006668      0.0003788      0.0007888      0.0493332
      0.0496212      0.0492112      0.043289038 0.043169924 0.043339496

```

```

34.5   6.803 6.074 5.102 2.8348 2.0132 2.6757 0.0028348      0.0020132
      0.0026757      0.0134592      0.0163664      0.01408      0.0365408
      0.0336336      0.03592      0.048579834      0.04978222 0.04883659

```

60	10.479	11.377	9.581	1.0062	0.9584	0.9623	0.0010062	0.0009584
	0.0009623	0.0207736		0.0205856		0.0209336		0.0292264
	0.0294144	0.0290664		0.05160499		0.051527235		0.051671164
100.5	10.180	11.677	10.778	0.4831	0.4831	0.4809	0.0004831	0.0004831
	0.0004809	0.022866		0.0224868		0.0228592		0.027134
	0.0275132	0.0271408		0.052470383		0.05231355		0.052467571
180.5	9.796	11.499	11.073	0.0575	0.0516	0.0552	0.0000575	0.0000516
	0.0000552	0.0245684		0.0242128		0.024562		0.0254316
	0.0257872	0.025438		0.053174477		0.053027405		0.05317183
217	10.531	11.794	10.531	0.0147	0.0088	0.0111	0.0000147	0.0000088
	0.0000111	0.0247396		0.024384		0.0247384		0.0252604
	0.025616	0.0252616		0.053245284		0.053098211		0.053244787
265	10.531	10.952	9.688	0.0109	0.0104	0.0106	0.00001089	0.0000104
	0.0000106	0.02475484		0.0243776		0.0247404		0.02524516
	0.0256224	0.0252596		0.053251587		0.053095564		0.053245614
339	10.110	11.373	10.110	0.0090	0.0107	0.0104	0.000009	0.0000107
	0.0000104	0.0247624		0.0243764		0.0247412		0.0252376
	0.0256236	0.0252588		0.053254713		0.053095068		0.053245945
363.25	11.373	12.216	10.952	0.2429	0.2377	0.2431	0.0002429	0.0002377
	0.0002431	0.0238268		0.0234684		0.0238104		0.0261732
	0.0265316	0.0261896		0.052867759		0.052719529		0.052860977
432.75	13.176	12.252	13.176	0.0482	0.0477	0.0470	0.00004821	0.0000477
	0.000047	0.02460556		0.0242284		0.0245948		0.02539444
	0.0257716	0.0254052		0.053189846		0.053033857		0.053185396
564	13.176	12.483	12.252	0.0100	0.0096	0.0114	0.00001001	0.0000096
	0.0000114	0.02475836		0.0243808		0.0247372		0.02524164
	0.0256192	0.0252628		0.053253042		0.053096888		0.053244291
780	13.046	12.479	13.330	0.0102	0.0094	0.0111	0.0000102	0.0000094
	0.0000111	0.0247576		0.0243816		0.0247384		0.0252424
	0.0256184	0.0252616		0.053252728		0.053097219		0.053244787

];

% number of replicates

num\_replicates = 3;

% columns for X, D, D+, A and A- data

col\_ids = [2, 8, 17, 14, 11];

% spike time

spike\_time = 363.25;

### 7. data\_nitrate.m

%Nitrate-reduction

%TimeProtein (mg/l)	NH <sub>4</sub> <sup>+</sup> (M)			Acetate (mM)		Acetate (M)		HCO <sub>3</sub> <sup>-</sup> (M)	
NO <sub>3</sub> <sup>-</sup> (M)	A	B	C	A	B	A	B	A	B

%(h)	A	B	C	A	B	A	B	A	B
------	---	---	---	---	---	---	---	---	---

Su\_data = [...

0	0.486	0.729	0.486	5.2265	6.2317	0.005227	0.006232
	0.02	0.02	0.00000	0.00000	0.043	0.04300	

9	1.497	2.395	2.096	0.6213	0.5903	0.000621	0.000590
	0.0153948	0.0143586	0.00461	0.00564	0.050631897		
	0.052346141						

22.75	9.281	9.581	9.281	0.0903	0.0953	0.000090	0.000095
	0.0148638	0.0138636	0.00514	0.00614	0.05151036		
	0.053165047						

35.5	9.880	9.281	9.581	0.0781	0.0773	0.000078	0.000077
	0.0148516	0.0138456	0.00515	0.00615	0.051530543		
	0.053194826						

58.25	10.180	9.281	9.581	0.0712	0.0883	0.000071	0.000088
	0.0148447	0.0138566	0.00516	0.00614	0.051541959		
	0.053176628						

64.5	10.479	9.880	10.180	0.0874	0.0609	0.000087	0.000061
	0.0148609	0.0138292	0.00514	0.00617	0.051515158		
	0.053221957						

156	10.221	9.370	9.796	0.0772	0.0786	0.000077	0.000079
	0.0148507	0.0138469	0.00515	0.00615	0.051532032		

```

0.053192675
276    10.647    9.370 10.221 0.0077 0.0141    0.000008    0.000014
      0.0147812    0.0137824    0.00522    0.00622    0.05164701
      0.053299381
302.25 10.531 9.267 9.688 0.0070 0.0133    0.000007    0.000013
      0.0147805    0.0137816    0.00522    0.00622    0.051648168
      0.053300704
326    10.531    9.688 9.688 0.0300 0.0246    0.000030    0.000025
      0.0148035    0.0137929    0.00520    0.00621    0.051610118
      0.05328201
396    9.709    11.327 12.714 0.0308 0.0233    0.000031    0.000023
      0.0148043    0.0137916    0.00520    0.00621    0.051608795
      0.053284095
525    10.171    11.327 12.252 0.0329 0.0254    0.000033    0.000025
      0.0148064    0.0137937    0.00519    0.00621    0.05160532
      0.053280687

```

];

% number of replicates

num\_replicates = 2;

% columns for X, D, D+, A and A- data

col\_ids = [2, 7, 13, 9, 11];

% spike time

spike\_time = 326;

### 8. data\_Sulfate.m

%Sulfate-reduction

```

%TimeProtein (mg/l)          Acetate (mM)          Acetate (M)
                        SO42- (M)          HS- (M)
HCO3- (M)

```

```

%(h)  A      B      C      A      B      C      A      B      C      A      B
C      A      B      C      A      B      C

```

```
Su_data = [...
```

```

0      3.593      4.192 5.090 8.3595 8.0824 8.0899 0.0083595      0.0080824
      0.0080899      0.02      0.02      0.02      0.00      0.00      0.00      0.043
0.043      0.043

```

```

258.75 4.634 6.318 7.582 5.4166 5.4403 5.4345 0.0054166      0.0054403
      0.0054345      0.0170571      0.0173579      0.0173446      0.0029429
      0.0026421      0.0026554      0.047881861      0.047384231      0.047406234

```

```

329      18.534      19.377 18.534 1.8992 1.5771 1.5083 0.0018992      0.0015771
      0.0015083      0.0135397      0.0134947      0.0134184      0.0064603
      0.0065053      0.0065816      0.053700893      0.053775339      0.053901567

```

```

449      22.422      23.810 22.191 0.7056 0.6993 0.6797 0.0007056      0.0006993
      0.0006797      0.0123461      0.0126169      0.0125898      0.0076539
      0.0073831      0.0074102      0.055675533      0.055227533      0.055272366

```

```

582      23.810      25.196 22.653 0.6051 0.5759 0.5769 0.0006051      0.0005759
      0.0005769      0.0122456      0.0124935      0.012487      0.0077544
      0.0075065      0.007513      0.055841795      0.05543168      0.055442434

```

```

629      22.654      25.428 21.960 0.5682 0.5838 0.5844 0.0005682      0.0005838
      0.0005844      0.0122087      0.0125014      0.0124945      0.0077913
      0.0074986      0.0075055      0.055902841      0.055418611      0.055430026

```

```

693      22.989      25.223 25.862 0.4476 0.4193 0.4223 0.0004476      0.0004193
      0.0004223      0.0120881      0.0123369      0.0123324      0.0079119
      0.0076631      0.0076676      0.056102356      0.055690753      0.055698197

```

```

760.5 25.862 24.266 24.585 0.3936 0.4117 0.4109 0.0003936      0.0004117
      0.0004109      0.0120341      0.0123293      0.012321      0.0079659
      0.0076707      0.007679      0.056191692      0.055703326      0.055717057

```

```
];
```

```
% number of replicates
```

```
num_replicates = 3;
```

```
% columns for X, D, D+, A and A- data
```

```
col_ids = [2, 8, 17, 11, 14];
```

```
% spike time: no spike
```

```
spike_time = 1e9;
```

### 9. data\_Methanogenesis.m

```
%Methanogenesis
```

```
%TimeProtein (mg/l)          Acetate (mM)          Methane (mM)
                               Acetate (M)          Methane (M)
                               HCO3- (M)          ?G35 (kJ/mol)
FT
%(h)  A      B      C      A      B      C      A      B      C      A      B      C      A      B
C      A      B      C      A      B      C      A      B      C      A      B      C      A      B
A      B      C
```

```
Su_data = [...
```

```
0      9.267      10.110 11.373 6.5758 6.5694 5.5800 0.66890      0.66620
      0.66840      0.0065758      0.0065694      0.00558      0.0006689
      0.0006662      0.0006684      0.043      0.043      0.043      -
38.44674658 -38.45461412 -38.02796954 0.70244      0.70255      0.69629

70.75 8.846 10.531 11.794 6.4021 5.7589 5.4185 1.82090      1.83610
      1.80460      0.0064021      0.0057589      0.0054185      0.0018209
      0.0018361      0.0018046      0.043300619 0.044354112 0.043280435 -
35.79463579 -35.44049372 -35.39151437 0.66130      0.65539      0.65456

215.75 9.709 9.477 11.327 5.0241 4.6112 4.9822 2.98320      3.13500
      3.16850      0.0050241      0.0046112      0.0049822      0.0029832
      0.003135      0.0031685      0.045580321 0.046252817 0.044002231 -
33.77746565 -33.39307666 -33.69189422 0.62624      0.61916      0.62467

295.75 29.589 33.749 37.217 0.4426 0.4625 0.4349 6.43380      7.14970
      5.93620      0.0004426      0.0004625      0.0004349      0.0064338
      0.0071497      0.0059362      0.053159753 0.053116244 0.051525084 -
25.19047175 -25.03494515 -25.43175366 0.43155      0.42722      0.43821

431.25 40.868 45.657 40.230 0.3726 0.4210 0.4129 6.53610      7.66700
      7.87170      0.0003726      0.000421      0.0004129      0.0065361
      0.007667      0.0078717      0.053275558 0.0531849      0.05156148 -
```

```

24.7034117   -24.61181083   -24.57395426  0.41787   0.41526
      0.41418

503.25 42.465 47.573 42.465 0.3967 0.4223 0.4596 6.86050   7.92970
      8.46600      0.0003967      0.0004223      0.0004596      0.0068605
      0.0079297      0.008466      0.053235688  0.053182749  0.051484222 -
24.74179972 -24.53350139 -24.66584281  0.41896      0.41302      0.41680

599.25 42.784 46.934 43.103 0.3996 0.4245 0.4383 6.95650   7.99810
      8.43940      0.0003996      0.0004245      0.0004383      0.0069565
      0.0079981      0.0084394      0.053230891  0.053179109  0.051519459 -
24.72508984 -24.5249846   -24.55057972   0.41849      0.41278
      0.41351

```

```
];
```

```
% number of replicates
```

```
num_replicates = 3;
```

```
% columns for X, D, D+, A and A- data
```

```
col_ids = [2, 11, 17, 17, 14];
```

```
% spike time: no spike
```

```
spike_time = 1e9;
```